

DIAMONDS AND THEIR MINERAL INCLUSIONS
FROM THE SLOAN DIATREMES OF THE
COLORADO-WYOMING STATE LINE
KIMBERLITE DISTRICT, NORTH AMERICA

VOLUME I

TEXT

by

MARSHALL LORRENCE OTTER

THESIS SUBMITTED IN FULFILMENT
OF THE REQUIREMENTS FOR THE DEGREE OF
DOCTOR OF PHILOSOPHY

UNIVERSITY OF CAPE TOWN

OCTOBER, 1989

The copyright of this thesis vests in the author. No quotation from it or information derived from it is to be published without full acknowledgement of the source. The thesis is to be used for private study or non-commercial research purposes only.

Published by the University of Cape Town (UCT) in terms of the non-exclusive license granted to UCT by the author.

DECLARATION

I hereby declare that the work presented in this thesis is my own, except where otherwise stated in the text.

Marshall L. Otter
October, 1989

ABSTRACT

The Sloan diamonds were investigated for their physical characteristics, inclusion mineralogy and composition, and carbon isotope composition. The relationships between these features are described and interpreted with respect to diamond genesis.

The physical characteristics investigated include crystal state, crystal regularity, primary morphology, resorption morphology, primary and secondary size/mass, colour, surface features and inclusion content. Significant relationships between these characteristics were found. The proportion of an individual crystal, lost during resorption, decreases with increasing diamond size. Larger crystals and diamonds displaying brown colours appear to have been more susceptible to breakage relative to smaller crystals and diamonds of other colours, respectively. Brown colours were more common on smaller diamonds relative to larger stones and, further, were more common on single crystal forms relative to twinned/aggregate crystals. Variation in diamond physical characteristics between the various kimberlite phases in the Sloan 1 & 2 complex has been documented. The Sloan 2 phase is characterized by larger and less resorbed diamonds relative to those in other kimberlite phases in the diatreme. In addition, corrosion sculpture is much more common on Sloan 2 diamonds.

The primary inclusions recovered from 100 Sloan diamonds fall into the broadly defined eclogitic and peridotitic parageneses found worldwide. At Sloan, the eclogitic minerals predominate (Ecl./Ecl.+Per ratio = 0.78). The paragenetic division of the inclusions is also reflected by differences in the physical characteristics of their diamond hosts. The peridotitic diamonds are largely twinned or aggregate crystals and do not exceed .02 carat in mass whereas the eclogitic diamonds are larger (up to .35 carat) and occur mostly as single crystal octahedra.

The peridotitic minerals are olivine (16 diamonds), orthopyroxene (4), Cr-rich pyrope (2), Cr-rich diopside (1) and ferro-periclase (1). These belong to the lherzolitic sub-paragenesis and show close affinities to those minerals found in "infertile" garnet peridotites at the Sloan locality as well as to the diamondiferous peridotite from the Schaffer locality. The olivines are mostly Fo 92 and, except for two, have significant chrome contents (.08 - .14 wt.% Cr₂O₃). The orthopyroxenes have unusually high calcium concentrations ranging from 1.0 to 1.4 wt.% CaO. The Cr-rich pyropes are calcium saturated and the Cr-rich diopside is unusual with .20 wt.% K₂O. Calculated equilibration conditions for the peridotitic inclusions range between 1224 and 1469 °C and 56-83 kbar, suggesting a deeper origin for peridotitic diamonds from Sloan relative to those from other localities. The ferro-periclase indicates highly reducing conditions during peridotitic diamond crystallization.

The eclogitic minerals are pyrope-almandine (32 diamonds), sulphide (23), omphacitic clinopyroxene (19), rutile (12), coesite (3), K-feldspar (2) and kyanite (1). A zircon was recovered from one diamond and, based on its host diamond carbon isotope composition, is believed to belong to the

eclogitic paragenesis. Compositionally, the eclogitic minerals are typical of those found in diamonds worldwide. The pyrope-almandine garnets are chrome-poor ($\leq .15$ wt.% Cr_2O_3), contain trace levels of sodium (.12 - .28 wt.% Na_2O) and exhibit a wide range in Mg/Mg+Fe (.36 - .66). The omphacitic clinopyroxenes are enriched in both the jadeite component (18 - 57 mol.%) and in potassium (.10 - 1.2 wt.% K_2O). Equilibration temperatures calculated for five eclogitic garnet/clinopyroxene pairs range from 1088 to 1114°C. Disequilibrium assemblages occur in two eclogitic diamonds and, in one stone, eclogitic pyrope-almandine was found coexisting with olivine. Based on U-Th-Pb isotope analysis, the zircon inclusion, and, therefore, the eclogitic diamonds are believed to have crystallized during the Proterozoic.

A wide range of carbon isotope compositions ($\delta^{13}\text{C} = -3.8$ to -29.4 ‰) was found for the Sloan diamonds. This represents the largest range found for diamonds from a single locality. Three diamond groups are defined based largely on their carbon isotope composition: Group I = -3.8 to -5.9 ‰ (vs. PDB); Group II = -8.5 to -12.8 ‰; and Group III = -12.5 to -29.4 ‰. Group I is comprised entirely of diamonds belonging to the peridotitic paragenesis, as defined based on inclusion composition. Groups II and III are comprised largely of eclogitic diamonds. Notable exceptions are the two diamonds with Cr-poor olivine inclusions, one of which coexisted with pyrope-almandine. The Group II diamonds crystallized in a Mg-rich environment relative to those represented by Group III, whereas the Group III diamonds apparently crystallized in two, compositionally distinct (Mn-rich and Mn-poor) environments as reflected by garnet and clinopyroxene compositions. The eclogitic diamonds in Groups II and III differ in size; those in the former range up to .35 carat in mass, whereas those in Group III do not exceed .07 carat. Significant heterogeneity in $\delta^{13}\text{C}$ composition within individual Group III diamonds was found, but those in Groups I and II are relatively homogeneous.

Based on these observations, at least three, compositionally distinct diamond crystallization environments beneath the North American continent were sampled by the Sloan kimberlites. Based on carbon isotope modelling, it is shown that both Group I and Group II diamonds could possibly have crystallized in a closed system by Rayleigh fractionation of relatively homogeneous carbon reservoirs. Possible sources for the Group I diamonds have $\delta^{13}\text{C}$ compositions between -4 and -5 ‰ which is similar to that inferred to be primordial carbon. Possible sources for the Group II diamonds have $\delta^{13}\text{C}$ compositions between -9 and -10 ‰ which could represent a source carbon produced by the mixing of the Group I and Group III carbon sources. According to the modelling, Group II diamonds also could have crystallized by equilibrium crystallization of slightly heterogeneous CO_2 reservoir having predominantly a primordial ($\delta^{13}\text{C} = \sim -6$ ‰) carbon isotope signature. Group III diamonds must have crystallized from a very heterogeneous and highly ^{13}C depleted carbon reservoir, a source which likely represents crustal carbon which was recycled into the mantle via subduction.

VOLUME I
TABLE OF CONTENTS

<u>CHAPTER</u>	<u>PAGE</u>
1. <u>INTRODUCTION</u>	1
2. <u>GEOLOGY OF THE SLOAN KIMBERLITE OCCURRENCE</u>	4
2.1 COLORADO-WYOMING KIMBERLITE PROVINCE	4
2.2 THE SLOAN KIMBERLITE OCCURRENCES	8
3. <u>PHYSICAL CHARACTERISTICS OF THE SLOAN DIAMONDS</u>	11
3.1 OVERVIEW	11
3.2 SAMPLING	12
3.3 METHODS	17
3.4 CRYSTAL STATE	18
3.5 CRYSTAL REGULARITY	19
3.6 MORPHOLOGY	21
3.6.1 Primary Morphology	21
3.6.2 Resorption Morphology	23
3.7 SIZE/MASS	29
3.7.1 Sieve Class	29
3.7.2 Primary Mass	31
3.8 COLOUR	33
3.9 SURFACE FEATURES	37
3.9.1 Xenolithic Features	37
3.9.2 Deformation Features	40
3.9.3 Other Surface Features	41
3.10 MINERAL INCLUSION CONTENT - VISUAL ASSESSMENT.....	43
3.10.1 Secondary Inclusions	44
3.10.2 Primary Inclusions	44
3.11 RELATIONSHIPS	46
3.11.1 Variation in Crystal State	46
3.11.2 Variation in Resorption Morphology	47
3.11.3 Variation in Primary Morphology	48
3.11.4 Variation in Colour	49

<u>CHAPTER</u>	<u>PAGE</u>
3. <u>PHYSICAL CHARACTERISTICS OF THE SLOAN DIAMONDS (cont.)</u>	
3.12 DISCUSSION	50
3.12.1 Crystallization	50
3.12.2 Residence in the Mantle	56
3.12.3 Plastic Deformation	57
3.12.4 Resorption	58
3.12.5 Crystal Breakage	60
3.12.6 Late Stage Etching	61
4. <u>MINERAL INCLUSIONS IN SLOAN DIAMONDS</u>	62
4.1 OVERVIEW	62
4.2 METHODS	65
4.3 INCLUSION CLASSIFICATION	68
4.3.1 Primary/Secondary Division	71
4.3.2 Paragenetic Division	73
4.4 PERIDOTITIC INCLUSION COMPOSITION	75
4.4.1 Olivine	75
4.4.2 Orthopyroxene	77
4.4.3 Garnet	78
4.4.4 Clinopyroxene	78
4.4.5 Ferro-Periclase	79
4.4.6 Thermobarometry	81
4.4.7 Paragenesis	86
4.5 ECLOGITIC INCLUSION COMPOSITION	87
4.5.1 Garnet	88
4.5.2 Clinopyroxene	90
4.5.3 Coesite	93
4.5.4 K-Feldspar	94
4.5.5 Kyanite	94
4.5.6 Rutile	95
4.5.7 Sulphide	96
4.5.8 Thermobarometry	97
4.5.9 Paragenesis	99
4.6 OTHER MINERAL INCLUSIONS	100
4.6.1 Zircon	101
4.6.2 Possibly Primary Clinopyroxene	103
4.6.3 Other Possibly Primary Inclusions	104
4.6.4 Possible Contaminants	105
4.6.5 Secondary Inclusions	108
4.7 RELATIONSHIPS	108
4.8 DISCUSSION	109

<u>CHAPTER</u>	<u>PAGE</u>
5. <u>CARBON ISOTOPE COMPOSITION OF SLOAN DIAMONDS</u>	118
5.1 OVERVIEW	118
5.1.1 Terminology	118
5.1.2 Previous Work	121
5.2 METHODS	125
5.3 RESULTS	127
5.4 RELATIONSHIPS	129
5.5 MODELLING	133
5.5.1 Equilibrium Crystallization	135
5.5.2 Fractional Crystallization	136
5.6 DISCUSSION	138
6. <u>SUMMARY AND CONCLUSIONS</u>	145
<u>ACKNOWLEDGEMENTS</u>	154
<u>REFERENCES</u>	157

VOLUME II
TABLE OF CONTENTS

	PAGE
<u>TABLES</u>	1
<u>FIGURES</u>	44
<u>APPENDICES</u>	176
APPENDIX I	
DIAMOND DESCRIPTION SCHEME	176
APPENDIX II	
PHYSICAL CHARACTERISTICS OF THE SLOAN DIAMONDS	
- REPRESENTATIVE SAMPLE ..	187
APPENDIX III	
PHYSICAL CHARACTERISTICS OF THE SLOAN DIAMONDS	
- SELECTED SAMPLE ..	220
APPENDIX IV	
INCLUSION DESCRIPTION SCHEME	223
APPENDIX V	
ANALYTICAL CONDITIONS FOR MICROPROBE ANALYSES	227
APPENDIX VI	
INCLUSION AND XENOLITH MINERAL ANALYSES	234
APPENDIX VII	
OTHER CHARACTERISTICS OF THE SLOAN DIAMONDS	
- SELECTED SAMPLE	255

1. INTRODUCTION

Natural diamonds are believed to have grown within their stability field in the Earth's upper mantle (Kennedy and Nordlie, 1968). Thermobarometric work on minerals included in diamond (see Boyd et al., 1985) supports this premise. A further assumption, that the strongly bonded structure of diamond can retain information on its growth environment, is supported by the ancient isotopic signatures found for both diamonds (Ozima et al., 1983) and their mineral inclusions (Richardson et al., 1984). Diamonds, therefore, not only provide a window into the upper mantle, possibly to depths of >450 km (Moore and Gurney, 1985), but they also appear to be time capsules preserving information on the Earth's early evolution.

Some features of diamond are altered by processes experienced subsequent to growth, either during their residence in the mantle or during transport and residence in the kimberlite (or lamproite) or even during alluvial transport upon erosion from their source (Harris et al., 1975; Chrenko et al., 1977; Robinson, 1979a). Diamonds, therefore, also record information on events affecting them subsequent to their growth.

Based on the above, investigations of diamond can be divided generally into those concerned with their growth environment and those concerned with environments encountered

subsequent to growth. This division, which is usually only tacitly acknowledged in the literature, is emphasized in this thesis in the belief that it clarifies the problems being investigated and will maximize the information obtained.

In this study, diamonds and their mineral inclusions from the Sloan diatremes in the Colorado-Wyoming State Line kimberlite district have been investigated. This represents the first detailed study of diamonds from a North American locality following on preliminary studies of State Line diamonds (McCallum et al., 1979) and their inclusions (Meyer and McCallum, 1986).

Three aspects of the Sloan diamonds were investigated: their physical characteristics, their mineral inclusion composition and their carbon isotope composition. The physical characterization of the Sloan diamonds was accomplished using a description scheme which recognizes both primary and secondary characteristics. However, without other information (e.g. primary inclusion compositions), the information derived from the physical characterization of the Sloan diamonds is more pertinent to defining the events they experienced subsequent to growth, especially in the kimberlite itself.

The most significant portion of this study has been devoted to defining the paragenetic subpopulations of diamond in the Sloan kimberlites. This is accomplished by exploring relationships between inclusion composition, carbon isotope composition and primary physical features on inclusion-bearing and xenolith diamonds. The paragenetic subgroups found at Sloan are compared to those found in diamonds worldwide. Furthermore, since many diamonds worldwide are believed to

have been derived from the disaggregation of peridotitic and eclogitic host assemblages, the inclusion mineral compositions have been compared to those in xenoliths, especially the diamondiferous variety, from the State Line kimberlite district. The significance of these observations is discussed with particular focus on diamond genesis and mantle evolution, on both regional and worldwide scales.

2. GEOLOGY OF THE SLOAN KIMBERLITE OCCURRENCE

2.1 COLORADO-WYOMING KIMBERLITE PROVINCE

Kimberlite was first recognized in the Colorado-Wyoming kimberlite province in 1964 by M.E. McCallum and D.H. Egger. Since then, more than 100 kimberlite bodies have been discovered (Hausel et al., 1985), the majority occurring in the Iron Mountain and State Line districts (Figure 2.1).

The kimberlite intruded a Proterozoic mobile belt which consists of older (1.8-1.7 Ga) metamorphic terrane discordantly intruded by 1.4 Ga old granitic rocks (Peterman et al., 1968). The metamorphic rocks are believed to be a result of collision between island arcs and the Archaean, Wyoming Province craton in the north (Karlstrom and Houston, 1984). Subsequent continental accretion occurred between 1.7 and 1.1 Ga (Condie, 1982), as evidenced by the existence of at least two other broad, supracrustal rock belts to the south (Figure 2.2).

The kimberlite emplacement was proposed to be late Silurian-early Devonian, based on Ordovician and Silurian sedimentary xenoliths in the diatremes (Chronic et al., 1969). The Devonian emplacement age subsequently has been confirmed using other dating techniques (Naesar and McCallum, 1977; Smith, 1979; Larson and Amini, 1981). The kimberlite occurrences define a rough north-south trend on the eastern

flank of the Front range in Colorado and the Laramie range in Wyoming (Figure 2.1). Their emplacement is thought to have been controlled by a deep-seated fracture system that later dominated the structural evolution of the Front and Laramie ranges (McCallum et al., 1975).

The kimberlite occurs in diatremes, as small plugs, or as blows, dykes and sills. The largest diatremes are Schaffer 13 and the Sloan 1 & 2 complex. Diatremes and plugs predominate in the State Line district whereas the Iron Mountain district occurrences are mostly dykes, some of which can be traced for 1.5 km (Smith et al., 1979). Both breccia (TKB) and massive porphyritic kimberlite varieties occur. The former predominates in diatremes and plugs, whereas the massive variety is common in dykes. These features are believed to reflect different levels in the intrusive system; the Iron Mountain dyke network representing the root zones of the deeply eroded, diatreme breccias (Smith et al., 1979). The kimberlite typically is intensely serpentized, commonly is carbonatized, and locally is silicified and/or fenitized (Eggler and McCallum, 1973; McCallum et al., 1975; 1977; Smith et al., 1979).

Besides sedimentary xenoliths of early Paleozoic age, a number of lower crustal and upper mantle xenoliths have been recovered from the Colorado-Wyoming kimberlite occurrences. Granulites, eclogites, a range of pyroxenites and peridotites as well as megacrysts have been described in the literature. A diamondiferous peridotite (McCallum and Eggler, 1976) and a diamond-graphite eclogite (Collins, 1982) also have been found in the State Line area. Figure 2.3 is a schematic cross-section of the lithosphere beneath the State Line area which

was originally presented by Egglar et al. (1979) and has been redrawn by this author based on the discussion of Egglar et al. (1987). It is based on P-T equilibration data on xenoliths and is included as an aid to understanding present thinking on the structure of the Devonian upper mantle of the State Line region.

Granulites (two-pyroxene granulites, two-pyroxene garnet granulites, clinopyroxene-garnet granulites) and gabbro norites are interpreted to represent lower crust (Bradley and McCallum, 1984). Megacrysts are divided into chrome-poor and chrome-rich varieties (Egglar et al., 1979). Both are interpreted to have crystallized from alkaline magmas similar to the kimberlite magma itself.

Bimineralic eclogites with or without accessory rutile, corundum, kyanite, sphene, sanidine, quartz and graphite are described by Ater (1982) and Ater et al. (1984). These workers divide the eclogites into peraluminous (kyanite-bearing) and metaluminous (kyanite-free) varieties. On this basis, the diamond-graphite eclogite from Sloan, as described by McCandless and Collins (1989), belongs to the metaluminous group, but based on mineral composition and thermobarometric data, the diamond-bearing xenolith is distinct from all other eclogites described so far in the State Line area. Ater et al. (1984) suggest that the non-diamondiferous eclogites may represent subducted oceanic crust which has undergone partial melting and recrystallization. The origin of the diamondiferous eclogite remains speculative.

Egglar et al. (1987) group the peridotites and pyroxenites into "infertile" and "enriched" rock types. Enriched rocks have higher whole rock sodium and calcium

concentrations and minerals with relatively low $Mg/(Mg+Fe)$ and $Cr/(Cr+Al)$ values. The infertile rocks include garnet, spinel-garnet and spinel peridotites which are interpreted to be residua from a Precambrian melting event involving the entire lithosphere. The enriched group of ultramafics include peridotites and websterites which represent infertile lithosphere which was subsequently enriched at shallow depths by "igneous processes" (Eggler et al., 1987). The websterites are believed to comprise a network of dykes, veins and layers that cut the shallower spinel-bearing infertile peridotite and were bordered by zones of enriched peridotite (see inset, Figure 2.3). The high ratio of enriched to infertile rocks found in the kimberlites is believed to be a consequence of the kimberlite exploiting preexisting conduits of enriched material rather than reflecting relative abundances at depth. Important to this study are the infertile garnet peridotites which were previously termed "Group I" peridotites by Kirkley (1980). These rocks equilibrated in the diamond stability field and include the diamondiferous garnet peridotite described by McCallum and Eggler (1976).

It is noted that the different xenolith types vary in composition from locality to locality. Accordingly, in this work, the minerals from Sloan diamonds are compared primarily to minerals in xenolithic material from the Sloan diatremes. As it happens, most of the xenoliths recovered from the State Line kimberlites were derived from the Sloan 2 phase of the Sloan 1 & 2 complex.

Diamond first was reported in the State Line area in 1975 when, during the routine thin section preparation of a serpentized garnet peridotite from the Schaffer 3

kimberlite, deep scratches were noticed on the grinding plate (McCallum and Egger, 1976). This was only the second authenticated occurrence of "in situ" diamonds in North America, the first being from the "kimberlite" (recently reclassified as lamproite (Scott Smith and Skinner, 1984)) at Murfreesboro, Arkansas where diamonds were discovered in 1906 (Miser and Ross, 1922). Subsequently, about twenty kimberlites, all in the State Line district, have proven to be diamondiferous (McCallum et al., 1977; 1979; Carlson and Marsh, 1989). The Iron Mountain kimberlites are barren.

The 78 diamonds described by McCallum et al. (1979), as well as those noted in the two diamondiferous xenoliths, are mostly < 2 mm in size. The largest diamond reported from the State Line area to date was found at Chicken Park and weighs ~2.6 carats (M.E. McCallum, pers. comm., 1989). Diamond grades reported from the region range from approximately 0.01 carat/tonne at Schaffer and Aultman (Lincoln, 1983), to 0.2 carat/tonne at Sloan (Gold, 1984; Shaver, 1988), and to a maximum average of ~0.4 carat/tonne at George Creek (K. Hilton, pers. comm., 1989).

2.2 THE SLOAN KIMBERLITE OCCURRENCES

The Sloan group of kimberlite bodies occur in the State Line district approximately 65 kilometres northwest of Fort Collins, Colorado (Figure 2.1). Six outcrops have been found and are designated Sloan 1-6. The relative positions and approximate areal extent of the main bodies (Sloan 1,2,5 and 6) are shown in Figure 2.4. The Sloan 3 and 4 occurrences (not plotted) outcrop as small dykes or blows and are situated

respectively to the west and east of the major bodies. Kimberlite emplacement apparently was fault controlled with pronounced joint sets in the host granites and gneisses being responsible for variations in surface plan (McCallum and Egger, 1971).

Based on outcrops, the closely spaced Sloan 1 and Sloan 2 pipes originally were mapped as two separate bodies. This seemed reasonable considering the striking contrast in xenolithic material between the two pipes. The Sloan 2 diatreme is characterized by the absence of Paleozoic sedimentary xenoliths and the mantle xenoliths are much more abundant and better preserved relative to those from Sloan 1. Notwithstanding this, McCallum (1976) argued that the two bodies were emplaced in a single event and that the observed differences could be explained if the Sloan 2 pipe had failed to penetrate the surface during eruption. Recent mapping during prospecting operations has at least confirmed subsurface continuity between the two kimberlite bodies (Shaver, 1988). In this dissertation, the body is referred to as the "Sloan 1 & 2 complex" with "Sloan 2" representing a separate kimberlite phase within the complex.

The diamonds for this study were obtained mostly from the Sloan 1 & 2 complex, although four diamonds came from the Sloan 5 and Sloan 6 diatremes. The major kimberlite phases of these pipes, as mapped by K. Shaver, are shown in Figures 2.5 and 2.6. They are recognized on the basis of differences in their macrocrystic and groundmass mineralogy, xenolith type and abundance, as well as on alteration features (Table 2.1). The nine kimberlite phases, originally recognized in the Sloan 1 & 2 complex, have subsequently been reclassified into six

phases (DK 1-6) which are believed to better represent the major structural and petrographic provinces within the pipe. The "brown porphyry" kimberlite (DK 6) was described as cross-cutting other kimberlite phases in the Sloan 1 & 2 complex, but no other relative age information between the various kimberlite phases has been documented.

3. PHYSICAL CHARACTERISTICS OF THE SLOAN DIAMONDS

3.1 OVERVIEW

A diamond can be described according to physical characteristics (e.g. mass, morphology, colour), chemical characteristics (e.g. carbon isotope composition, trace element content), mineral inclusion characteristics (e.g. paragenesis), as well as by other characteristics such as electrical conductivity. Such features can be separated into two broad genetic categories: primary and secondary characteristics. Primary characteristics are those which the diamond acquired during crystallization and these relate to aspects of the diamond growth environment. Secondary features result from processes active on primary forms subsequent to diamond formation. All characteristics which can be seen or measured on individual diamonds, in essence, are secondary features. Primary features can only be inferred based on present knowledge. That some primary characteristics can be recognized is a consequence of processes experienced since growth.

In this chapter, the physical characteristics of diamonds recovered from both kimberlite and xenoliths from Sloan are investigated as a prelude to the study of their mineral inclusion and carbon isotope composition. As it is important to determine primary characteristics, especially in studies of

mineral inclusions, a significant proportion of the discussion is devoted to defining which primary characteristics it is possible to determine. The characteristics described are crystal state, crystal regularity, morphology, size/mass, colour, surface features and inclusion content. The description scheme used was developed during the course of this study (Appendix I). It is essentially a combination of those devised by Harris et al. (1975) and Robinson (1979a), with emphasis on distinguishing between primary and secondary characteristics. This includes a semi-quantitative calculation of primary mass using a method devised by D.N. Robinson (pers. comm., 1984) at the Anglo American Research Laboratory.

Where appropriate, the results of this investigation are compared to those of previous studies of the physical characteristics of diamonds, especially diamonds from the State Line area (McCallum and Egger, 1976; McCallum et al., 1979; Collins, 1982; McCandless and Collins, 1989).

3.2 SAMPLING

More than 22,000 diamonds weighing approximately 300 carats were recovered by the Superior Oil Company during testing operations on the Sloan kimberlite diatremes between 1980 and 1983 (Table 3.1). The diamonds were derived from numerous test pits (Figures 3.1 and 3.2), each representing about 50 tonnes of kimberlite. The exposures allowed detailed surficial mapping of the kimberlite bodies and, therefore, the kimberlite phase from which each 50 tonne sample was derived is documented. The bulk samples were processed for

macrodiamonds (>.5 mm) by various methods including a sortex, grease tables and a jig.

The diamond parcel was provided for study in individual packets which were catalogued by test pit (and therefore kimberlite phase) and recovery method (Table 3.1). In addition, an assessment of diamond recovery efficiency for each pit was provided. The latter is based on the percentage recovery of seed diamonds planted in the bulk sample just prior to processing through the plant.

The characterization of the Sloan diamonds - the aim of this thesis - was accomplished based on three samples of the total test population which are termed the "Sieved", "Representative" and "Selected" samples (Table 3.2). All of the diamonds in the Sieved and Representative samples and most of those in the Selected sample were recovered from the Sloan 1 & 2 complex (Figure 3.1). The Selected sample also includes three diamonds from the Sloan 5 diatreme and one diamond from the Sloan 6 diatreme (Figure 3.2). These samples are presented in flow diagram form in Figure 3.3 as a means of considering what each subsample represents.

Of initial interest is whether or not the entire Sloan diamond population (i.e. all the diamonds in the kimberlite) is representative of the diamond reservoir in the Devonian upper mantle through which the Sloan kimberlites erupted. Already a possible bias has been mentioned with respect to xenolith abundances (Section 2.1) where the high proportion of "enriched" peridotite xenoliths relative to "infertile" peridotite xenoliths is thought to be due to selective sampling by the kimberlite rather than representing the relative volume of these rock types at depth (Egglar et al.,

1987). Although the enriched peridotites are apparently not related to the diamond-bearing mantle, a similar bias may extend to the diamond subpopulations at Sloan. It is therefore emphasized that the Sloan diamond population (and samples derived from it) may not be representative of the entire diamond population in the upper mantle through which the kimberlite passed.

Does the test production sample represent the entire Sloan diamond population? Assuming the test pits were positioned in a relatively random and unbiased fashion, the characteristics of the test production sample may reflect those of the total Sloan diamond population. However, a complicating factor is the presence of more than one kimberlite phase. Previous studies have noted differences in diamond characteristics between kimberlite phases as well as with depth in single pipes (Harris et al., 1975; 1979). Here it is not possible to consider variation with depth, but differences between kimberlite phases can be documented since each test pit was from a known phase (Figure 3.1). Therefore, before the test production sample can be considered as a whole, each kimberlite phase is first considered individually.

Finally, the actual numbers of diamonds described from each kimberlite phase must be considered. Harris et al. (1975) found that, in order to obtain reproducible results, at least 500 stones from each sieve class in a particular sample were needed. Even if all of the diamonds recovered from Sloan were considered, this constraint would not be fulfilled and the samples finally described in this study should be considered with this limitation in mind.

The Sieved and Representative diamond samples were investigated in order to assess the overall physical character of the Sloan 1 & 2 complex diamond population and to document variation within the complex. The samples are discussed in total; as Sloan 1, Sloan 2 and Dyke kimberlite body subsamples; and as DK 1-4 kimberlite phase subsamples within the Sloan 1 kimberlite body.

The Sieved sample comprises the diamonds from all "high" recovery test pits in the Sloan 1 & 2 complex, as well as those from test pit 40 in the Dyke kimberlite body. As the name implies, the diamonds in the Sieved sample were sieved as a means of assessing the size distribution of the Sloan diamond populations.

The Representative sample is a subsample of the Sieved sample on which a more detailed examination of physical characteristics was conducted. The sample consists of between 200 and 500 diamonds from each of the DK 1-6 kimberlite phases (Table 3.2). All of the diamonds from the selected pits were described except in the case of Pit 47 (DK 4) which was quartered before sampling.

The Selected sample was derived from the total test production parcel during an initial search for diamonds with recoverable mineral inclusions. Some of the Selected sample diamonds also occur in the Sieved and Representative samples. The sample is comprised of 100 inclusion-bearing production diamonds and three "xenolithic" diamonds. The latter, which did not have recoverable mineral inclusions, were found in contact with either eclogitic garnet or clinopyroxene (Figures 3.4 - 3.6) and, based on the garnet and clinopyroxene compositions, these are believed to be fragments of.

diamoniferous eclogites. These diamond "eclogites" as well as one described by Collins (1982) are all from the Sloan 2 kimberlite which has provided most of the xenoliths recovered from the Sloan locality. Inferences drawn based on the Selected sample are limited because the sample is statistically minute. In addition, the inclusion-bearing and/or xenolithic diamonds as such may not be representative of the Sloan diamonds in general. Nonetheless, this sample represents the bulk of the inclusion-bearing and/or xenolithic diamonds recovered from Sloan and it is important to describe their physical characteristics.

Finally, a description of the diamond sample numbering system is required. Each diamond in the Representative and Selected samples has been uniquely numbered and the numbering system reflects the consecutive arrival of four parcels of the total parcel which was provided for study in stages starting in 1983 (see Appendix I, Table A). Diamond numbers SL 1 to 29 were selected for study by J.J. Gurney during his visit to the Sloan locality in 1983. A further 23 inclusion-bearing diamonds (SL 1-1 to 1-23) and later 100 more (SL A1 to A100) were selected from the parcel by A. Daley of Superior Oil and provided for study. The bulk of the Sloan diamonds comprising the Sieved and Representative sample were provided as a unit in 1986 and these were numbered in sequence for each test pit. For instance, there are x diamonds from test pit 5 which are numbered from SL5-1 to 5-x. Not all of the inclusion-bearing diamonds provided for study are included in the Selected sample because inclusions were not recovered from them. Only the Selected sample diamonds (or fragments) and a small number

of the Representative sample diamonds were not recombined in their test pit packets subsequent to their description.

3.3 METHODS

A preliminary visual inspection of each diamond was conducted using a stereoscopic microscope (6-240 X magnification) with both transmitted and reflected light. Photomicrographs of selected diamonds were taken using a standard 35 mm SLR camera mounted on a stereoscopic or a petrographic microscope and with 200 ASA colour slide film.

A number of crystals were selected for scanning electron microscope (SEM) documentation. After cleaning in 30% HF and distilled H₂O they were mounted on aluminium specimen stubs using colloidal silver solution for adhesive. A thin (~20 nm) gold-palladium coat was applied to maximize conductivity. Whole crystal and detail photographs were taken using Cambridge Stereoscan S180 and S200 scanning electron microscopes. The bulk of the work was accomplished at 5 kV. Once the SEM work was completed, the Au-Pd coat was removed by soaking the diamonds overnight in aqua regia with subsequent ultrasonic cleaning.

The physical characteristics of the Sloan diamonds were described according to the description scheme outlined in Appendix I and the data collected is tabulated in Appendices II (Representative sample) and III (Selected sample). Not all of the characteristics in the description scheme were described and/or are discussed in this study.

The Sieved and Representative sample diamonds were sieved using Pierres diamond sieves. Whole sieve classes and

selected single crystals were weighed to the nearest mg in order to determine average mass for each sieve class (Appendix I, Table B). The diamonds in the Selected sample were individually weighed, but only a few were sieved before being cracked for inclusion recovery (Appendix III).

Diamond colour was described against an opaque white background using a fibre optics reflected light source. Inclusion content was assessed using both transmitted and reflected light

3.4 CRYSTAL STATE

Crystal state refers to whether the diamond is broken or not. The Sloan diamonds were described simply as "whole", "broken" or "unknown". No attempt was made at separating crystals into "chipped" or "fragment" categories. Most of the diamonds classified as "unknown" are highly resorbed crystals with irregular shapes. In such cases, it is difficult to decide whether the diamond is unbroken, or whether it is a broken crystal which had experienced extreme resorption subsequent to breakage.

The crystal state data obtained on the Sloan diamonds (Appendices II and III) are summarized in Table 3.3. More than 50% of the diamonds in the total Representative sample were described as broken crystals, whereas about 40% were described as whole crystals. Approximately 6% of the diamonds could not be confirmed as either whole or broken. Similar relative proportions of whole, broken and unknown diamonds are found in the Sloan 1, Sloan 2 and Dyke subsamples and in most of the individual kimberlite phase subsamples. The DK 1

kimberlite phase subsample is unique in having a higher proportion of whole crystals relative to broken crystals and the highest proportion of diamonds in the unknown category.

A much higher proportion of the diamonds in the Selected sample are whole crystals. This is almost certainly a sampling bias since these diamonds were chosen on the basis of primary inclusion content which is difficult to assess in broken or fractured diamonds.

These apparent trends are also reflected by "whole to broken crystal ratios" calculated for the sample and the various subsamples (Table 3.3). This ratio which ignores the "unknown" category diamonds, is a convenient way of considering the crystal state character of diamond parcels.

Finally, it was difficult to ascertain the crystal state of the xenolithic diamonds even when the attached mineral matter was removed. The irregular surfaces on xenolith diamonds SL 56-6 (Figure 3.4c,d) and SL 56-8 (Figure 3.6d) may not have resulted from breakage and these samples are therefore classified as unknown. Xenolith diamond SL 56-7 which exhibits similarly irregular surfaces (Figure 3.5c) is fractured on one side (Figure 3.5d) and could therefore be classified as broken.

3.5 CRYSTAL REGULARITY

Crystal regularity refers to a deviation, if any, from the regular or equidimensional form. This "distortion" is not related to diamond "deformation" (see Section 3.9.2), but rather is a function of inequalities in facial development during crystallization. Harris et al. (1975) divide diamonds

into "regular" and "distorted" groups by visually assessing the degree to which the crystal is misshapen. In a similar fashion, Robinson (1979a) divides diamonds into "nearly equidimensional", "slightly distorted", "flat", "elongate" and "irregular" classes.

In general, most diamonds are distorted to some degree and the system of Harris et al. (1975) seems inadequate. However, the distinctions in Robinson's scheme cannot be precisely defined. Therefore, the Sloan diamonds (single crystal forms only) were described as "nearly equidimensional", "distorted" and, only in exceptional cases as "flattened" (Appendices II and III). The latter are rare at Sloan and are not considered separately in this discussion. Otherwise, broken crystals for which it was difficult to ascertain the crystal's primary regularity were classified as "unknown", and twinned or aggregate crystals were left "unclassified". As such, this feature cannot be considered very easily in any quantitative fashion and the data obtained must be considered within this limitation.

Very few (<5 %) of the Sloan diamonds (single crystal forms) were described as nearly equidimensional (Table 3.4). Most are distorted to some degree. However, some interesting shapes were encountered (Figure 3.7) and such individual cases are probably more useful to discerning growth conditions than generalized data obtained on large samples. The high percentage of diamonds in the Selected sample classified as nearly equidimensional (Table 3.4) is again probably a result of biased sampling.

Xenolith diamonds SL 56-6 (Figure 3.4) and SL 56-8 (Figure 3.6) are twinned or aggregate forms and, therefore,

were left unclassified. Xenolith diamond SL 56-7 (Figure 3.5) may also be a twin, but because of the uncertainty is classified as an unknown with respect to crystal regularity.

3.6 MORPHOLOGY

Diamonds with pristine, unresorbed or unbroken morphologies are relatively rare in nature (Robinson, 1979a). Nevertheless, based on remnant crystal faces and certain surface features (see Section 3.9.3), the primary growth morphology of most diamonds can be delineated. Here, the primary growth forms of the Sloan diamonds and their secondary resorption morphologies are considered separately.

3.6.1 Primary Morphology

The more common primary growth forms of diamond are octahedra, cubo-octahedra, cubes, macles and aggregates of these crystal morphologies (Harris et al., 1975). Examples of Sloan diamonds inferred as having these primary forms are exhibited in Figures 3.8 (octahedra), 3.9 (cubes and cubo-octahedra), 3.10 (macles), and 3.11 (aggregates). In this study, the octahedra were sometimes described as "complex". As the term suggests, such crystals were complexly formed: sometimes resembling aggregates, but with each of the apparently aggregated crystals having grown in the same crystallographic orientation (Figure 3.8q-v). The category was created because of the high incidence of such crystals in the Sloan parcel. It is a subjective category and is perhaps more akin to the discussion of crystal regularity. The "pseudo-rhombic dodecahedral" habit, observed as being

relatively common for xenolithic diamonds (Robinson, 1979a,b; Robinson et al., 1984), was sometimes distinguished (Figure 3.8w,x). Such cases essentially are stepped octahedra and in this study such crystals also were classified as complex octahedra. Diamond SL 52-7 (Figure 3.7) is a spectacular example of such a pseudo-rhombic dodecahedral form. Macles, defined according to Whitelock (1973), include contact twins only. The aggregates are divided into "simple" and "polycrystalline" categories. In general, if the number of crystals in the aggregate could be easily counted, it was termed a simple aggregate. When the primary morphology could not be discerned it was classified as "unknown".

A large proportion of the Sloan diamonds in both the Representative and the Selected samples, as well as in all the subsamples therein, are inferred to have crystallized as single crystal octahedra (including complex forms) (Table 3.5). Subordinate but significant proportions of simple aggregates and macles also are found. Cube forms, including cubo-octahedra (Figure 3.9) and polycrystalline aggregates occur but together constitute less than 4% of the total Representative sample (Table 3.5). A reassessment of data reported by McCallum et al. (1979) on 78 diamonds from the Colorado-Wyoming State Line area shows similar relative abundances of the primary forms (Table 3.5), although the percentage of twins is increased at the expense of single crystal octahedra and no cube forms were found.

Note that the DK 2 kimberlite phase, which has a relatively low proportion of single crystal octahedra, also has the highest proportion of "unknown" diamonds. The Sloan 2 phase exhibits the opposite relationship. In general, as the

proportion of unknown category diamonds increases, the proportion of octahedra as well as other forms decreases (Table 3.5). This suggests that the relative proportion of the various primary forms within the unknown category is similar to those of the sample in general, which suggests that, overall, the data can be considered without unknown category diamonds. Based on this assumption, the ratio of primary single crystals (octa, cubo-octa, cube) to twinned forms (macle, simple and polycrystalline aggregate), which ignores the unknown category diamonds, is calculated for the various subsamples (Table 3.5). These ratios are relatively constant at around 3 for most of the kimberlite phases, the exception being the Dyke phase which has a ratio of 4.

Xenolith diamond SL 56-6 is a macle (Figure 3.4a,b) and SL 56-8 a simple aggregate (Figure 3.6c). Xenolith diamond SL 56-7 (Figure 3.5) may be a twinned/aggregate crystal or a complex octahedron and, therefore, was classified as having an unknown primary morphology.

3.6.2 Resorption Morphology

The term "resorption" is used in this thesis to describe a process which, subsequent to growth, diminishes the primary size and alters the primary morphology of the diamond, whether it be by oxidation, graphitization or some other mechanism (not including breakage). The resorption of the octahedral form of diamond generally produces the rounded dodecahedral or, more correctly, the tetrahexahedroidal morphology (Robinson, 1979a). Transitional forms have caused confusion in the formulation of diamond classification schemes. Two methods for dealing with the problem have evolved. Milashev

(1965) and McCallum et al. (1979) classify diamonds having more than 75% {111} faces as "octahedra" whereas those with more than 75% {110} faces are termed "dodecahedra". Crystals having shapes in between are termed "intermediate" or "transitional". Whitelock (1973) and Harris et al. (1975) prefer to use the 50% rule which assigns crystals to either the "octahedra" or "dodecahedra" classes based simply on the predominant crystal face present. Additional categories such as "flattened dodecahedra" and "spheres" have also been used. These classification schemes are largely qualitative since the class a crystal is finally assigned to is based on arbitrary cut off points and includes a range of resorption forms.

As one of the aims of this study is to delineate the primary growth features of the Sloan diamonds, it is important to quantify, if possible, the relationship between the original crystal and its present day resorbed counterpart. Robinson (1979a) considered mass loss due to resorption and determined that the conversion of a regular octahedron to a tetrahexahedroid involves a minimum mass (and volume) loss of 45%. Since unresorbed diamonds have lost 0% mass, it should be a simple matter to derive percentage resorption, or alternatively, percentage preservation figures for transitional forms. Realizing this, D.N. Robinson (pers. comm., 1984) devised a scheme by which the transitional forms could be semi-quantitatively classified according to the amount of resorption/preservation. Figure 3.12 shows Robinson's (op cit.) five resorption/preservation categories and their approximate average preservation values. Similar to the earlier schemes, it is based on the proportion of the diamond surface showing octahedral crystal faces. Besides

being important for qualitatively characterizing diamond populations and sub-populations, this scheme provides a means of quantifying diamond preservation in a given occurrence. Robinson (pers. comm., 1984) notes, however, that since his Category 1 diamonds have such a large range of preservation values (1 - 55%), that are impossible to discriminate, populations with a significant proportion of Category 1 diamonds cannot be compared to other suites on a quantitative basis. The importance of this method, from the viewpoint of this study, is that it allows at least a semi-quantitative calculation of primary mass for single crystals (see Section 3.7.2).

Robinson (op cit.) prefers to emphasize the semi-quantitative aspect of his system because of a number of inherent problems with its application. The major problem is that natural diamonds are seldom the ideal forms required by the scheme. The progressive resorption of natural octahedra from Category 5 resorption forms to Category 1 forms are illustrated for Sloan diamonds in Figure 3.8a-k. Distortion, a common feature of diamonds, will certainly cause error in the measurement (Figure 3.8f,k). Also, strictly speaking, macles and aggregates should be classified on different scales (Figures 3.10g,h and 3.11h respectively). In his preliminary study, Robinson (op cit.) included them and found no changes in the final figures. Other errors can be attributed to human judgement. For instance, some diamonds exhibit pseudohemimorphic morphologies where one portion of the crystal appears to be more resorbed than the rest of the stone. Extreme examples of this morphology, such as those in Figure 3.8l-p, are believed to have resulted from partial

protection during resorption, possibly in a xenolith (Robinson et al., 1989). Whether a diamond has been partially protected or not may sometimes be difficult to establish since it is dependent on the original size of the faces on the diamond. In this study, diamonds which appear to have been protected during resorption are defined as having "non-uniform" resorption morphologies. In these cases, both categories were recorded and then averaged. The aim is to estimate in a semi-quantitative fashion the proportion of the diamond remaining subsequent to resorption. In questionable cases, the diamond should be classified as "unknown".

With these limitations in mind, the resorption morphology data on the Sloan diamonds, summarized in Table 3.6 can now be discussed. When considered in total (Figure 3.13) the diamonds in the Representative sample span the range in resorption categories, but the highest proportion occurs in Category 1. The diamonds in the Selected sample, on the other hand, (Figure 3.13) are better preserved with the bulk occurring in Category 4. This again is probably a reflection of biased sampling.

The diamonds described from the Sloan 2 kimberlite body are, on the whole, better preserved relative to those in the Sloan 1 and Dyke kimberlite bodies (Figure 3.14). As can be seen, Sloan 2 has significantly higher proportions of Category 5, 4 and 3 diamonds and a much lower percentage of Category 1 diamonds relative to the Sloan 1 and Dyke kimberlite phases. In Figure 3.15, it appears that both the DK 1 and DK 2 phases have a lower percentage of Category 1 diamonds relative to the DK 3 and DK 4 phases. Note, however, the higher percentage of

unknown resorption category diamonds in DK 2, which may be significant.

These relationships are perhaps more easily digested when the data are translated into percentage preservation figures for each subsample (Table 3.6). For this calculation, the data are first normalized without the "unknown" category diamonds. The resulting proportions in each resorption category, when multiplied by the average percent preservation value for that category (Figure 3.12), produce values which when added together represent the proportion of diamond material preserved in the sample. An example of this calculation is presented as a footnote in Table 3.6. It is noted that these are maximum values since many of the Category 1 diamonds which are calculated at 55% preservation have probably lost more material. Even so, the calculated preservation values on the Sloan diamonds (Table 3.6) still reflect the previous observations that: 1) the Selected sample diamonds are better preserved than those in the Representative sample; 2) the Sloan 2 diamonds are better preserved than Sloan 1 and Dyke phase diamonds; and 3) there are similarities between the diamonds in DK 1 and DK 2 and between the diamonds in DK 3 and DK 4.

The preservation values calculated for whole crystals only (Table 3.6), are consistently higher than those calculated for combined whole and broken subsamples. This is probably because a greater proportion of Category 1 diamonds, relative to those in other categories, are broken (Figures 3.13 - 3.15). This exhibits the inherent problem of classifying broken crystals when their whole character cannot be determined. However, the revised preservation values,

which are based on whole diamonds only, do not change the previous conclusions.

In general, approximately 25% of the Sloan diamond bulk was apparently lost during resorption. Note that the actual amount (mass or volume) of material lost during resorption from individual diamonds in each resorption category varies with the diamond's size. Larger diamonds in, for example, resorption Category 3 (75% average preservation) must have lost more material than the smaller diamonds in that category. The actual amount of material lost during the resorption of the Sloan diamonds is considered in Section 3.7.2, whereas the relationship between preservation and diamond size is considered in Section 3.11.2.

The resorption morphology of the three xenolith diamonds is difficult to determine as it is not clear that the irregular surfaces (Figures 3.4 - 3.6) result from resorption. Assuming "resorption" is responsible, all three exhibit some sharp edges and appear to have been non-uniformly resorbed. In particular, Diamond SL 56-8 (Figure 3.6) appears to be a classic case of non-uniform resorption. However, the amount of diamond remaining is impossible to ascertain and therefore the sample is classified as unknown. Diamond SL 56-7 (Figure 3.5) also is classified as unknown for similar reasons. Diamond SL 56-6 (Figure 3.4) appears to have been at least 90 % preserved and therefore is classified in Category 5.

Finally, note that the lowest proportion of diamonds exhibiting non-uniform resorption occur in the Sloan 2 kimberlite body (Table 3.6).

3.7 SIZE/MASS

Diamonds can be weighed and their size reported in mass units, usually "carats" (1 carat = 200 mg). However, in studies of large numbers of diamonds, it is not viable to individually weigh each diamond and most studies separate their samples using special diamond sieves with circular apertures of known diameters. In such studies diamond mass is reported, only approximately, as the average mass for each sieve class. Although, not ideal, the practice is continued in this study, at least for the Sieved and Representative samples. The Selected sample diamonds were individually weighed but only a few were sieved before they were broken and, therefore they are not considered with respect to sieve class. The approximate correspondence between sieve class or aperture diameter and diamond mass is listed in Appendix I - Table B. Note that the Pierres sieve classes (+00 and +0), (+1 and +2) and (+3 and +4) are combined in order to standardize the aperture diameter interval at .2 mm for plots.

Because of resorption and/or breakage, the sieve or mass data collected is best thought of as the diamond's secondary size. In this section, the secondary diamond size, as determined either by sieving or weighing, is first discussed and then the determination of primary mass is discussed.

3.7.1 Sieve Class

The sieve class data obtained for the Sloan diamonds are summarized in Table 3.7, and the total Sieved and Representative sample data are plotted with respect to sieve aperture diameter along with the State Line sample size data

in Figure 3.16. In general, most of the Sloan diamonds are very small with less than 5% exceeding ~2 mm in size (~.07 carat). The largest diamond recovered from the Sloan kimberlite occurrence, which does not occur in the samples defined in this study, weighs 1.24 carats (Shaver, 1988).

For further discussion, the size data are combined into -3, +3 -9 and +9 sieve classes as summarized in Table 3.8. These combined sieve classes correspond to diamond masses of approximately <.02, .02 - .07 and >.07 carat respectively. This allows a comparison of the Sieved and Representative sample sieve data with the Selected sample mass data (Figure 3.17). As can be seen, the Selected sample has a higher percentage of larger diamonds (>.02 carat) compared to the Sieved and Representative samples. This is, again, attributed to sampling bias.

Less obvious is a similar relationship between the Sieved and Representative samples. Both Figures 3.16 and 3.17 show that the Representative sample has a higher percentage of the larger diamonds relative to the Sieved sample. The trend is also apparent for the Sloan 1 and Sloan 2 subsamples (Figure 3.18). (Note that the Dyke subsamples in both the Sieved and Representative samples are one and the same.) The proportions of larger and smaller diamonds in the DK1 and DK4 subsamples, on the other hand, are relatively consistent between the Sieved and Representative samples (Figure 3.19). The increase in the proportions of larger stones in the DK2, DK3 and Sloan 2 subsamples between the Sieved and Representative samples is probably due to sampling bias which suggests that the latter may not be as representative as its name implies.

The relative proportions of diamond sizes between the Sloan 1 and Sloan 2 subsamples, however, is consistent between the Sieved and Representative samples (Figure 3.18). In both samples, a smaller proportion of -3 sieve class diamonds are found in the Sloan 2 body relative to the Sloan 1 and Dyke bodies. This is evident in the Representative sample even though the DK 2 and DK 3 subsamples are enriched in the larger diamonds relative to the Sieved sample. The higher proportion of large diamonds in the Sloan 2 subsample is, therefore, considered to be significant. Based on the Sieved sample size data (Figure 3.19), the diamond size distributions in the DK 1-4 phases are not believed to be significantly different.

The xenolithic diamonds (SL 56-6, SL 56-7 and SL 56-8), which are from the Sloan 2 kimberlite body, occur in the larger size classes and have secondary masses of .04, .11 and .13 carat respectively (see Appendix III).

3.7.2 Primary Mass

The primary mass of individual diamonds is estimated, for whole crystals only, by simply dividing the crystal's secondary mass by its resorption category average preservation value (Figure 3.12). For instance, diamond SL 52-62 from sieve class +0 (approximate mass = .010 ct) and with a Category 3 resorption morphology (approximate preservation of 75%) would theoretically have had a primary mass of $.010 \text{ ct.} \div .75 = .013 \text{ carat}$. Again, this is only a semi-quantitative calculation especially considering the use of average mass and preservation values. Nonetheless, it is suggested that the values calculated at least acknowledge the loss of diamond mass (and volume) due to resorption. Such loss may be

significant when relating diamond size to other primary characteristics and should always be considered when investigating resorbed diamond populations.

The primary mass values calculated for individual whole diamonds in the Representative and Selected samples are listed in Appendices II and III respectively. The Representative sample data are combined into mass categories, $<.02$, $.02 - .07$ and $>.07$ carat (which can be related to combined sieve class data as discussed previously) and plotted for the various subsamples in Figures 3.20 - 3.22. Of interest here is whether the distinctions noted between the Sloan 1 and Sloan 2 phases with respect to their secondary size distribution are found for the primary distributions.

Note that, because resorption diminishes the primary size of the diamond, a calculation of primary mass should increase the proportions of diamonds in the larger size classes at the expense of the proportions in the smaller size classes. This is evident in Figures 3.20 - 3.22. The largest changes occur in the Sloan 2 subsample (Figure 3.21) and in the DK 2 subsample (Figure 3.22), where nearly 10% of the smaller diamonds in the resorbed samples would originally have occurred in the larger size classes. With these adjustments, the apparent enrichment of larger diamonds in the Sloan 2 subsample over the Sloan 1 subsample is still observed. In Figure 3.21, it is evident that even before resorption, the Sloan 2 kimberlite body subsample was significantly enriched in larger diamonds relative to the Sloan 1 and Dyke kimberlite body subsamples.

As a point of interest, the largest diamond in the Representative sample (SL 21-263), weighing 1.22 carats, has a

category 4 resorption morphology and weighed nearly 1.5 carats prior to the resorption event. The largest diamond recovered from Sloan (1.24 carats) has a Category 2 resorption morphology and must have originally weighed nearly 2 carats. Two other large diamonds found at Sloan, which have category 1 resorption morphologies, probably exceeded 2 carats in original mass.

3.8 COLOUR

Diamond in its purest form is colourless. Most diamond colour is believed to be caused by impurities which absorb electromagnetic radiation in the visible light spectrum. Impurities also absorb radiation in the ultra-violet and infra-red portions of the spectrum and variations in colour, UV and IR absorption have been correlated with specific lattice impurities. Diamond is "typed" based on the presence or absence of lattice impurities and, in the following, diamond colour is discussed along with diamond type as a means of considering the causes, as well as the primary or secondary nature, of the various diamond colours observed.

Diamonds are divided into two basic types. The more common "Type I" diamond is rich in nitrogen impurity whereas the rarer "Type II" diamond is essentially devoid of nitrogen ((Robertson et al., 1934; Kaiser and Bond, 1959; Lightowers and Deane, 1964). The two types are further subdivided and distinguishing properties of the various subtypes are tabulated in Table 3.9. Type I diamond is subdivided into Type Ia and Type Ib varieties based mostly on differences in the form of the nitrogen impurity. The nitrogen in Type Ib

diamond occurs as single substitutional atoms that are known to give Type Ib diamond an amber to orange hue (Bruton, 1970). Synthetic diamonds are usually of Type Ib material. Experimental work has shown that, given time and the proper temperature conditions, single substitutional nitrogen can aggregate (Chrenko et al., 1977; Brozel et al., 1978; Evans, 1978; Evans and Qi, 1982). Diamonds containing aggregated nitrogen are classified as Type Ia. Subdivisions within this group are based on the extent of aggregation. The nitrogen in Type IaA diamonds occurs mostly as substitutional pairs whereas in Type IaB diamonds the nitrogen occurs as larger aggregates including N₃ centres and platelets. Such aggregation causes the loss of the Type Ib amber colour and Type Ia diamonds occur in various colours usually ranging from yellow to colourless. Absorption caused by the N₃ centres in Type IaB diamonds can produce a strong yellow coloration (Loubser and Wright, 1973).

Type IIa diamond, normally colourless, is probably just a purer form of Type IaA diamond (Bibby, 1982). Type IIb diamonds are distinctive in that they are natural semi-conductors, a property attributed to the presence of single substitutional boron atoms in the diamond lattice (Lightowers and Collins, 1975). The characteristic blue colour of Type IIb diamond is due to absorption of long wavelength radiation by boron (Chrenko, 1971).

Lattice impurities are not responsible for all diamond colours. Although some aggregates of nitrogen may be responsible for brown coloration (Harris et al., 1975), brown colours may also be caused by graphite exsolution along glide planes (Urusovskaya and Orlov, 1964). In support of the

latter, Robinson (1979a) and Robinson et al. (1989) note that brown diamonds commonly show textures indicative of plastic deformation (see Section 3.9.2). Such textures also are common on pink diamonds suggesting that deformation can be responsible for the pink coloration (Gurney, 1989). Green coloration may occur due to an overabundance of single substitutional nitrogen atoms (Orlov, 1973), but most green coloration is associated with surficial alpha-particle radiation damage, most commonly from U and Th released into ground water (Vance et al., 1973). Finally, sub-microscopic inclusions are responsible for some diamond colours. Grey or black coloration has been noted in diamonds having numerous small black inclusions.

Based on these considerations, the primary or secondary nature of diamond colour may be difficult to assess. Brown, pink and green diamonds may not be exhibiting their primary colours and, since diamond colour may change during nitrogen aggregation, colourless and yellow diamonds also may not be exhibiting their primary colours. Type Ib diamonds exhibiting amber colours may reflect only short periods of mantle residence before eruption since the process of nitrogen aggregation is probably irreversible under ambient mantle conditions (Brozel et al., 1978). The amber colour, therefore, may reflect the diamonds growth state. Grey coloration which has been correlated with other primary diamond characteristics (Robinson et al., 1989) and blue coloration may also be primary diamond colours.

The colours documented on the Sloan diamonds are summarized in Table 3.10. The Sloan diamonds were classified broadly into colourless, grey, brown, yellow, amber, green,

pink and other categories. Within the broad divisions were classified various hues (ie. light brown, yellow brown - Appendices II and III), but these distinctions are highly subjective and the data are difficult to handle. Such hues are, therefore, not considered in detail here.

In general, 60 - 70 % of the Sloan diamonds are brown, whereas a quarter exhibit grey colours (Table 3.10). Less than 10% of the diamonds were classified as colourless. This is in contrast to the State Line sample studied by McCallum et al. (1979), in which over 60% were classified as colourless, approximately 10% as grey and 14% as brown.

Yellow diamonds which are relatively common in southern African localities (Harris et al., 1975; 1979) are rare at Sloan. Only one diamond in the sample population exhibited the pristine yellow coloration which characterizes "Cape" diamonds. Amber diamonds also are rare and only seven diamonds in the sample were classified a "pristine amber" as opposed to "brown amber". Pale green and pink colours are rare in Sloan diamonds.

It may be significant that kimberlite phases DK 1 and DK 4 show an increase in grey diamonds at the expense of brown stones (Table 3.10).

A few diamonds exhibit non-uniform coloration (Appendices II and III) which, in some cases, is a marked colour change across a boundary, but in most cases is a patchy discoloration. Such non-uniform coloration is inevitably associated with fracturing and with secondary inclusion material and is apparently caused by associated reflections within the crystal.

Two of the xenolithic diamonds are light grey, whereas the other is grey-brown in colour (Appendix III).

3.9 SURFACE FEATURES

The surface features observed on the Sloan diamonds (Appendices II and III) are discussed in three subsections: Xenolithic Features; Deformation Features; and Other Features. The latter are mostly textures related to resorption.

3.9.1 Xenolithic Features

Surface features which are more common on diamonds from xenoliths, or which may otherwise imply a xenolithic association, are discussed here. The percentages of Sloan diamonds in the Representative and Selected samples exhibiting the various xenolithic features described are shown in Table 3.11. Robinson (1979a) and Robinson et al. (1984) observed that pseudo-rhombic-dodecahedral crystal faces are more common on xenolithic diamonds than on production diamonds at Orapa. Surface textures associated with this morphology such as serrate laminae, knob-like asperities and graphite coatings, therefore, are included in this section.

Sloan diamonds exhibiting serrate laminae and knob-like asperities are shown in Figure 3.23a-h. These features also occur on Diamond SL 52-7 (Figure 3.7) in association with the pseudo-rhombic dodecahedral form. The xenolith diamonds found in this study provide additional support of a xenolithic association for these features. Diamond SL 56-8 exhibits serrate laminae and all three xenolith diamonds exhibit knob-like asperities and associated graphite (Figures 3.4 - 3.6).

The graphite does not occur as a coating, but is more massive and sometimes intimately interlaced (intergrown?) with the irregular and fractured diamond surfaces.

It is noted that the definition of some of these features is somewhat vague and therefore their recognition and genetic interpretation suffers. For instance, serrate laminae, which may be caused by resorption at the edges of a finely layered crystal, also occur in connection with imbricate triangular plates which, although resorbed, are still a growth structure. In other words, similar structures may result from more than one process.

The most common of these features present on Sloan production diamonds is serrate laminae, with approximately 12% of the diamonds exhibiting this feature (Table 3.11). Knob-like asperities and graphite coats are less common, occurring on ~5% of the stones. Graphite coats also are a common feature on the State Line diamonds studied by McCallum et al. (1979), although knob-like asperities were not described.

Diamonds may be partially protected during resorption and this is most convincingly evidenced by diamonds exhibiting non-uniform resorption (Figure 3.81-p). Such protection is believed to be provided by xenoliths hosting the diamonds. Non-uniform resorption might also take the form of channelling as shown in Figure 3.23i-k. These features, called "etch channels" by Orlov (1973), appear to have been cut or eroded possibly by a resorbing medium which was channelled within the confines of adjacent xenolith minerals. Surface fractures, usually along cleavage, which have been enhanced or widened during resorption are not considered to be resorption channels. Approximately 4% of the Sloan diamonds exhibit what

are interpreted to be resorption channels. Xenolith diamonds SL 56-6 and SL 56-8 also exhibit such channels (see Figure 3.4d) which are filled with graphite.

Sharp, unresorbed edges and smooth faces occurring on some diamonds (Figure 3.23k,l) suggest that the diamond must have been totally shielded and therefore may indicate a xenolithic association. Only about 1% of the Sloan diamonds exhibit such features.

Finally, large pyramidal or hexagonal pits occurring on unbroken surfaces of ~1% of the Sloan diamonds (Figure 3.23m,n) may represent formerly intergrown xenolith minerals. Alternatively, the pyramidal pits may represent an interpenetrant diamond. Large inclusions are ruled out as the diamonds are otherwise whole and exhibit insufficient resorption to have previously enclosed such a large grain. It is envisaged that during diamond growth, other minerals may sometimes grow syngenetically with the diamond without becoming totally overgrown. Complex crystals with embayed morphologies may also form in a similar manner (see Figure 3.8v).

The various "xenolithic" features described here commonly occur together on a single diamond and it is perhaps more relevant to tally the number of diamonds exhibiting such features. On this account, approximately 20% of the Representative sample diamonds exhibit one or more xenolithic surface textures, whereas 25% exhibit xenolithic features and/or non-uniform resorption (Table 3.11).

3.9.2 Deformation Features

Glide plane dislocations indicating plastic deformation are enhanced by resorption and appear as lamination lines parallel to cleavage on tetrahexahedroidal surfaces (Urusovskaya and Orlov, 1964; Robinson, 1979a). The offset is minute and is generally not expressed on octahedral faces except rarely as linear arrays of trigonal etch pits. Based on this evidence, resorption must post-date plastic deformation.

It is not clear from the literature whether plastic deformation alters, to any significant degree, the original shape of the crystal. However, considering its lack of expression on octahedral faces, it would seem that it does not. Plastic deformation, therefore, can be easily documented only on resorbed diamonds.

According to Harris et al. (1979) and Robinson et al (1989), diamonds exhibiting plastic deformation features are common in all major kimberlites studied. Robinson et al. (1989) and Harris et al. (1984) report that, at some localities, up to 30% of the stones in certain sieve classes are plastically deformed. They do not state whether this figure applies to only resorbed stones or the whole population, but the difficulty in observing plastic deformation on unresorbed diamonds, especially with only a hand lens or binocular microscope, might support the former. Hence, the figures reported for the samples investigated might be lower limits, with their values dependent on the degree of preservation in each population. D.N. Robinson (pers. comm., 1984) believes that higher proportions (up to 65%) of the diamonds studied are plastically deformed.

Lamination lines (Figure 3.23o,p), which are generally not well developed on Sloan diamonds, were noted on only 2.0% of the diamonds in the total Representative sample (Table 3.12). Only one diamond in the sample population has what may possibly be described as a linear array of trigonal etch pits.

3.9.3 Other Surface Features

Other surface features described on the Sloan diamonds, and discussed in this section, can be broadly divided into growth, resorption, late-stage etching, breakage and surface discoloration features (Table 3.13). These were described largely according to the definitions of Robinson (1979a).

Triangular plates (Figures 3.7a,b and 3.24a) were commonly observed on the octahedral faces of the Sloan diamonds (Table 3.13). These features are ascribed to growth (Robinson, 1979a), although on the Sloan diamonds they most often have rounded corners and edges due to resorption. All three xenolithic diamonds exhibit triangular growth plates (Figures 3.4 - 3.6) and these features also were described by McCallum et al. (1979) on diamonds in the State Line sample population.

Shield-shaped laminae (Figure 3.24b), also relatively common on Sloan diamonds (Table 3.13), result from resorption and reveal the internal layering of the diamond crystal. Apart from differing in outline, they are usually thinner than triangular growth plates. Terraces (Figure 3.24c), as described by Robinson (1979a), often occur in association with both rounded triangular growth plates and shield-shaped laminae.

The most common resorption textures noted on the Sloan diamonds are negatively-oriented trigonal etch pits (Figure 3.24c,d) which occur exclusively on octahedral faces. They especially are common on Sloan 2 and Dyke kimberlite diamonds (Table 3.13). Negatively-oriented tetragonal etch pits were only rarely encountered (Table 3.13). Most occur on resorbed cubic faces (Figure 3.9b,d,f), but the feature was also noted on breakage surfaces parallel to the cubic {100} crystal plane (Figure 3.24e). No positively-oriented tetragonal etch pits were identified. Crescentic steps, a rather subjective category, were documented predominantly on cubic diamonds (Figure 3.9c). Hexagonal etch pits also were noted on some Sloan diamonds (Figure 3.24f).

Elongate hillocks (Figure 3.24g,h) were documented on some diamonds. Only prominent cases were noted, however, and more diamonds probably exhibit this feature than is reflected in Table 3.13. Finally, the herringbone pattern (Figure 3.10h), which results from resorption causing enhancement across the twin line on macles, was evident on a large proportion of resorbed macles (compare Tables 3.5 and 3.13). This feature often aided in identifying the primary macle form.

Corrosion sculpture (Figure 3.25a-d), which occurs only on tetrahedral surfaces and therefore postdates most resorption (Robinson, 1979a; Robinson et al., 1989), was found only rarely on Sloan 1 and Dyke diamonds, but commonly on Sloan 2 diamonds (Table 3.13). This constitutes the most striking difference in physical characteristics between diamonds from different kimberlite phases. Frosting (Figures 3.8a and 3.24f), also a late-stage etch feature, was noted

only rarely, but is apparently not more common on diamonds from the Sloan 2 kimberlite phase relative to other phases (Table 3.13).

Diamond breakage along cleavage planes was noted on a number of crystals (Table 3.13) and in many cases is associated with large pits on the breakage surfaces (Figure 3.25e-g). The latter are believed to represent large inclusions that facilitated breakage of the host diamond due to internal strain developed by differential expansion during emplacement. Similar pits also were documented on non-cleavage breakage surfaces and in all, ~20% of the broken diamonds have such pits (Table 3.13).

Some broken crystals exhibit resorption on the broken surfaces (Figures 3.25e-h). This feature may be more common than the values in Table 3.13 suggest since many of the diamonds classified as having an unknown crystal state (see Section 3.4) may be broken crystals with highly resorbed breakage surfaces.

Bright green spots (Figure 3.26) were noted on some diamond surfaces and also are associated with fractures within diamonds. These are believed to be areas of localized radiation damage caused, after eruption of the kimberlite, by alpha-particles emitted from included radioactive material or adjacent radioactive materials in the kimberlite.

3.10 MINERAL INCLUSION CONTENT - VISUAL ASSESSMENT

The following is an assessment of the mineral inclusion content of the Sloan diamonds based on a visual examination of the Representative sample diamonds. Both primary and

secondary inclusions are considered. In general, discrete inclusions, unassociated with fractures to the diamond surface, were considered to be primary, whereas those associated with fractures were described as secondary (See Section 4.3). The compositional characteristics of mineral inclusions in Sloan diamonds are comprehensively discussed with respect to the Selected sample in Chapter 4.

3.10.1 Secondary Inclusions

The description of secondary mineral inclusions was limited to an assessment of their presence or absence which essentially reflects the presence or absence of fractures in the diamonds. Secondary inclusions comprise material that apparently was introduced along fractures, as well as the alteration products of primary inclusions (Figure 3.27). Between 50-75% of the Sloan diamonds contain secondary inclusion material (Table 3.14).

3.10.2 Primary Inclusions

The transparency, colour and form of primary inclusions were considered in an effort to discern their mineralogy and paragenesis. Pristine primary inclusions are preserved in over half of the Sloan diamonds (Table 3.14). The large majority of such inclusions are black to dark brown, opaque crystals (Table 3.14) and more than half of these have rosette structures (Figure 3.28a-d) which commonly form in relation to sulphide (Harris and Gurney, 1979b).

Less than 5% of the Representative sample diamonds have discernable transparent primary inclusions (Table 3.14). Most of the transparent inclusions are colourless and can not, with

confidence, be assigned to a paragenesis. Orange garnets, probably of eclogitic affinity, are the next most common transparent inclusion (Figure 3.29) and only one diamond in the Representative sample contained a purple, peridotitic garnet inclusion (Figure 3.30) (identity confirmed by subsequent removal and analysis (see Section 4.4.3)). Amber, pale green and brown inclusions were also documented.

Bimineralic, transparent inclusions were seen in two diamonds of the Representative sample. An orange and pale green inclusion, recovered intact from diamond SL 5-4 (Figure 3.31), is essentially an eclogite (see Section 4.5).

The most common coexisting inclusion phases are "sulphide" rosettes and discrete opaque inclusions (Table 3.15) suggesting that some, if not most, of the inclusions described as discrete opaque inclusions are in fact sulphides although this has not been confirmed. Coexisting, colourless and opaque minerals (rosetted and discrete), and coexisting pale orange and rosetted opaque crystals also are relatively common (Table 3.15).

Less than 2% of the Representative Sample diamonds could be classified with respect to their paragenesis (Table 3.14). Although a higher percentage of "eclogitic" relative to "peridotitic" inclusions were identified, it is possible that many of the colourless crystals as well as the opaque inclusions are peridotitic. It is, therefore, not possible based on this visual examination to confirm the predominance of eclogitic over peridotitic inclusions in the Sloan diamond population in general.

One diamond in the Representative sample (SL 52-7) has what can be termed a "cloud" (Figure 3.7e). More translucent

than opaque, the wispy brown cloud occurs in the centre of the crystal and is elongate in its apparent growth direction. The cloud's composition has yet to be determined.

3.11 RELATIONSHIPS

Relationships (or the lack thereof) between the physical characteristics investigated on the Representative sample diamonds are described in this section. The relationships are discussed with respect to crystal breakage, secondary morphology, primary morphology and colour. Variation of these features with size is discussed within these categories.

3.11.1 Variation in Crystal State

The proportion of broken diamonds is found to vary with diamond size and diamond colour as indicated by variations in the whole to broken crystal ratio calculated for diamonds grouped together based on these features.

An increase in the proportion of broken diamonds as diamond size increases is indicated by the whole to broken crystal ratios listed in Table 3.16. In general, a lower proportion of diamonds in the -3 sieve classes are broken relative to those in the +3 -9 sieve class, except in the DK 4 and Dyke subsamples. The ratios calculated for the +9 sieve classes are not considered reliable due to the small number of samples. The ratios calculated for the +3 -9 sieve classes for the individual DK 1-4 kimberlite phases as well as the Dyke kimberlite body may also be suspect on this account.

Whole to broken crystal ratios calculated for the colourless, grey and brown diamond subsamples are listed in

Table 3.17. In general, these ratios are lower for brown diamonds relative to grey and colourless diamonds suggesting that brown diamonds are more susceptible to breakage. A similar relationship was noted for diamonds at Kao (Whitelock, 1973). The DK 4 kimberlite phase again deviates from this general trend. The ratios calculated for colourless diamonds are suspect because of small sample numbers.

3.11.2 Variation in Resorption Morphology

The proportion of material lost from individual diamonds during resorption varies with diamond size. This relationship has previously been considered by plotting the ratio of octahedra to dodecahedra for each sieve class (Whitelock, 1973). Here, however, the relationship can be described in a more quantitative fashion using Robinson's (pers. comm., 1984) resorption class preservation values (Figure 3.12). The percent preservation for the diamonds in each sieve class is determined, for whole crystals only, simply by dividing the total present mass in each sieve class by the total calculated primary mass and multiplying by 100. The results of this calculation are tabulated in Table 3.18 and plotted in Figures 3.32 and 3.33. Except for the diamonds in the DK 2 kimberlite phase (Figure 3.33), smaller diamonds tend to be more resorbed relative to larger diamonds as has been noted at other localities (Whitelock, 1973; Harris et al., 1975). The same trend is found when considering combined sieve classes (Table 3.19). The small number of samples in the +9 sieve class do not allow a rigorous treatment for larger diamonds.

3.11.3 Variation in Primary Morphology

The relative proportions of primary forms, as indicated by the single to twinned crystal ratio, vary systematically with diamond colour, but the relationship is not clear for diamond size.

The single to twinned crystal ratio is generally lower for the grey diamond subsamples relative to the brown diamond subsamples (Table 3.20), reflecting a greater tendency for brown diamonds to occur as single crystal forms. The data on colourless crystals may not be reliable due to the small numbers of diamonds involved.

The variation of the single to twinned crystal ratio with secondary size (ie. combined sieve class) is tabulated in Table 3.21. The figures suggest that there are more twins in the larger sieve classes in the Sloan 1 (except in the DK 4 phase) and Dyke kimberlite body subsamples, but that the opposite is true in the Sloan 2 kimberlite body subsample. Again, the ratios calculated for the +9 sieve class are probably not representative due to the small sample numbers involved.

When primary morphology is related to primary mass (Table 3.22), which is perhaps more appropriate, the trends are not as strong. Although similar variation in the single to twinned crystal ratio is found for the Sloan 2 and Dyke bodies, there is no variation with mass for the Sloan 1 sample, nor for the Representative sample as a whole. It is not known the extent to which this variation (or lack thereof) is due to small sample numbers.

3.11.4 Variation in Colour

Figure 3.34 shows that the proportion of grey diamonds in the total Representative sample, as well as in the Sloan 1, Sloan 2 and Dyke kimberlite body subsamples, increases at the expense of brown diamonds with increasing diamond size (plotted as combined sieve class). Similar trends are also found for diamonds in each of the DK 1-4 kimberlite phase samples (not plotted). Because of small sample numbers, the trend for colourless crystals with diamond size is not as well constrained. When related to primary mass (Figure 3.35), similar trends are exhibited. An increase of brown diamonds with decreasing size has been noted at other localities (Harris et al., 1975; 1979; 1984).

Robinson (1979a) and Robinson et al. (1989) show that at the southern African localities investigated, a higher proportion of brown diamonds exhibit surficial lamination lines than do diamonds of other colours. Because only a small number of the diamonds investigated in this study exhibit lamination lines (Table 3.12), the relationship is difficult to ascertain for Sloan diamonds. Considering the total Representative sample only, the percentage of diamonds of each colour class which exhibit lamination lines does not appear to vary significantly with colour as is shown below:

Percentage of n with Lamination Lines

Total*	Colourless	Grey	Brown
n=1816	n=150	n=463	n=1196
2.0	2.0	1.7	1.9

*Includes 1 Yellow, 1 Amber and 1 Pink diamond

3.12 DISCUSSION

Based on observations on the physical characteristics of diamonds from southern African kimberlites, Robinson et al. (1989) established a general sequence of events affecting diamonds: crystallization; residence in the mantle; plastic deformation; resorption; crystal breakage and late-stage etching. This provides a convenient framework in which the significance of the data collected on the Sloan diamonds, including relationships between different characteristics (summarized in Table 3.23) and variation between kimberlite phases (summarized in Table 3.24) can be discussed.

3.12.1 Crystallization

The primary physical characteristics described and relationships between them are pertinent in this discussion of the diamond growth environment(s) represented by the Sloan diamond population. Also considered, is the relationship between xenolithic diamonds and their host rock. Of initial importance, however, is the occurrence of both eclogitic and peridotitic minerals in the Sloan diamonds which suggests that at least two crystallization environments are represented at Sloan. It is therefore stressed that any conclusions drawn based only on physical characteristics and without corresponding paragenetic data, are necessarily generalized.

The Sloan diamonds grew mostly as single crystal octahedra although a significant proportion are macles and aggregates. Cubo-octahedra and cube forms are relatively rare at Sloan, as is the case at most localities worldwide (Whitelock, 1973; Harris et al., 1975; 1979; 1984; 1986; Hall

and Smith, 1984). In synthetic systems, cube forms result from growth at lower temperatures relative to those required for the growth of octahedra (Bovenkerk, 1961). However, most natural cube forms are believed to have resulted from "abnormal" fibrous growth (as opposed to "normal" spiral growth) under conditions of higher carbon-supersaturation relative to that in which single crystal octahedra grow (Lang, 1979; Sunagawa, 1984). The cuboid forms associated with polycrystalline and coated diamonds from Zaire and Sierra Leone appear to have grown under such conditions (Gurney, 1989). The cubic faces observed on Sloan diamonds most often occur in combination with octahedral faces forming combined cubo-octahedral forms (Figure 3.9). Some of these crystals may represent octahedral overgrowth on cubic forms, the latter having been exposed by resorption. Whether the cubic layers formed by fibrous growth or whether they resulted from growth at slightly depressed temperatures is not known.

The reasons for the growth of macles or simple aggregates are not well understood. Harris and Gurney (1979a) note that inclusions commonly occur at the twin plane of macle crystals and this suggests that macles form due to diamond nucleation occurring on other mineral grains. This, however, does not explain the occurrence of inclusion-free macles, which at Sloan, comprise about 20% of the macle population. Alternatively, macles may simply form more often due to an increase in nucleation density, a parameter which, in synthetic systems, has been shown to increase with pressure (Wakatsuki, 1984).

The relative abundance of single and twinned crystal forms found at Sloan matches those found at most localities

(Harris et al., 1975; 1979; 1984). At some localities, however, the relative abundances observed are "abnormal". At Orapa and Jwaneng, a very high proportion of twinned or aggregate crystal forms were found by Harris et al. (1986). The relative abundance of single to twinned forms, which in this study has been expressed as the ratio of single to twinned crystals, may relate to the growth environment(s) sampled by the kimberlite. This ratio, therefore, is perhaps a useful index for characterizing the diamond populations at different localities. However, without corresponding paragenetic information, it is difficult, if not impossible, to relate this information to the actual growth environment(s) sampled by the kimberlite.

The small variation in the single/twinned crystal ratio between the various kimberlite phases at Sloan (Table 3.5) may not be meaningful because of small sample numbers involved. It is considered unlikely that it relates to variation in diamond morphology at depth.

The diamonds from the State Line area, in general, are small relative to diamonds found elsewhere and this certainly is a reflection of the crystallization environments sampled. This could relate to the diamond growth rate, the duration of the crystallization event and/or simply the availability of carbon for diamond precipitation. Again, because of the presence of at least two diamond populations, which may have different size distributions, inferences made based on the Sloan diamond size distribution cannot be justified.

The higher proportion of larger crystals in the Sloan 2 kimberlite body relative to the Sloan 1 and Dyke phase kimberlite bodies may be real since it is evident in both the

Sieved and Representative samples (Figure 3.18). It is apparently not solely a function of the better preservation of Sloan 2 diamonds (Table 3.6) since the relationship also is evident with respect to primary mass (Figure 3.21). It is possible that the relationship is a function of sampling at depth. The Sloan 2 kimberlite phase, for instance, could represent a different eruptive phase which may have sampled a source that was not sampled by other phases migrating upward along the same conduit (M.E. McCallum, pers. comm., 1989). The relationship could also be a kinetic effect where larger crystals were, for some reason, concentrated in the Sloan 2 portion of the pipe during eruption. As far as this investigator is aware, variation in diamond size (esp. primary size) between kimberlite phases in a single locality has not been documented elsewhere.

The variation of colour with primary morphology (Table 3.21) and with primary mass (Figure 3.35) suggests that the colours observed are related to the growth environment. The slightly higher single/twinned crystal ratios found for brown relative to those determined for grey and colourless crystals (Table 3.21) suggests that, in general, the grey and colourless diamonds formed under different physical and chemical conditions relative to brown diamonds. Impurity type and concentration may be responsible for this variation. The increase of brown diamonds with decreasing diamond size (secondary size) has been observed at other localities (Harris et al., 1975; 1979; 1984), but has not been considered with respect to primary size. The trend has never been adequately explained, but may also be a consequence of differences in impurity content.

Although smaller diamonds tend to be brown, and brown diamonds tend to be twinned crystals, there is no strong correlation between primary morphology and mass. A plausible explanation is that much of this observed variation in primary characteristics results from disproportionate contributions from the two paragenetic crystallization environments sampled by the kimberlite.

Finally, the association between diamonds and xenoliths is considered. The occurrence of xenolithic diamonds in the State Line district is proven. Diamond-bearing xenoliths are rare worldwide, but both a diamond peridotite (McCallum and Egger, 1976) and a diamond-graphite eclogite (Collins, 1982; McCandless and Collins, 1989) as well as the three diamondiferous "xenoliths" described in this study have been found in the area. The occurrence of xenolithic surface textures and/or non-uniform resorption morphologies on ~25% of the Sloan diamonds, suggests that many of the Sloan diamonds, if not all, were derived from disaggregated xenoliths.

Some of the surface features deemed to be "xenolithic", appear to be growth structures. The "intergrowth pit" described in this study is one of those features, but other features (e.g. serrate laminae, knob-like asperities, graphite coats) shown by Robinson (1979a) and Robinson et al. (1984) to be more common on xenolithic diamonds, may also be primary. Robinson (1979a) noted that serrate laminae were commonly associated with trigonal etch pits and suggested that serrate laminae, as well as associated graphite coats and knob-like asperities, also result from resorption. Serrate laminae on Sloan diamonds usually appeared to be a growth structure rather than a feature which was caused by resorption (see

Figure 3.7). McCandless and Collins (1989) state that the graphite in the diamond-graphite eclogite (TP 121), has forms similar to those found for primary graphite in the eclogites described by Robinson et al. (1984). The graphite associated with the xenolithic diamonds described in this study was interspersed with the fragmented diamond surface and it appeared that the diamond and graphite are intergrown. The graphite, therefore, may represent the final stages of carbon precipitation during xenolith crystallization. Knob-like asperities also may result from such metastable growth. Their less common occurrence on production diamonds might be expected since such irregular protrusions would be prime targets during resorption.

The pseudo-rhombic dodecahedral crystals found in this study commonly are relatively unresorbed (Figure 3.7) and it is clear that the form is primary. In this respect, it is pertinent to consider crystal regularity. A low proportion of regularly shaped diamonds is a feature observed at all kimberlite localities so far studied. The processes responsible for such growth distortion have not been adequately addressed in the literature. Sunagawa (1984) suggests that virtually all diamond growth occurs from solution. One might expect a large number of regular crystals if they were allowed to grow uninhibited. The lack of regular crystals, therefore, suggests that diamonds are inhibited during growth. The former, it is envisaged, might occur if xenolith minerals (and inclusion) minerals are crystallizing simultaneously. Even with diamond's incredibly high form energy (Harris and Gurney, 1979a), it seems possible that the direction of crystal growth could, in some instances, be

influenced by surrounding crystals. The "complex" octahedral form defined in this thesis may result from such growth.

3.12.2 Residence in the Mantle

It is difficult to estimate the time between Sloan diamond crystallization and eruption to the surface. This problem has, recently, been considered in relation to diamond type (Harris, 1987). As is discussed in Section 3.8, diamond type, besides being a function of impurity (especially nitrogen) concentration, is defined based on aggregation state of the nitrogen. The extent of such aggregation is believed to increase with time (Brozel et al., 1978; Evans and Qi, 1982), but this has not been quantitatively calibrated. The colour differences present in the Sloan diamonds may relate to nitrogen aggregation. On this basis, the occurrence of a few amber diamonds, for which the colour is inferred to reflect single substitutional N atoms, may indicate that some diamonds grew just prior to kimberlite eruption.

The lack of yellow diamonds at Sloan is notable since yellow diamonds are relatively common elsewhere (Harris et al., 1975; 1979; 1984). As certain forms of nitrogen are believed to give diamond this colour (Table 3.9), the lack of yellow diamonds at Sloan may reflect differences in nitrogen concentration and/or aggregation state which may relate to the time of residence in the mantle. The increase of brown diamonds with decreasing diamond size may also relate to impurity content and residence time.

3.12.3 Plastic Deformation

Although not a common feature, the occurrence of lamination lines on a small proportion of Sloan diamonds suggests that at least a portion of the Sloan diamond population was plastically deformed. However, considering the poor development of lamination lines and the virtual absence of other deformation textures such as linear arrays of trigonal etch pits on octahedral faces, the deformation of Sloan diamonds was not severe. As has been established in previous studies (Robinson, 1979a; Robinson et al., 1984), diamond deformation must have predated resorption since lamination lines are glide planes enhanced by resorption.

Evans (1976) estimates that natural diamond deformation occurs at approximately 1300 °C and at 50 kbar. Some investigators believe that diamond deformation occurs during the same event which forms sheared peridotites (Robinson, 1978; Harris et al., 1984; Robinson et al., 1989). No diamonds have been found in association with such rocks, however.

Orlov (1973) reports that "clear signs of plastic deformation" occur on diamonds from xenoliths (of unspecified type), which are themselves highly fragmented and altered. He also notes the occurrence of shattered diamonds in these nodules. He takes this as evidence for diamond deformation occurring during xenolith disaggregation which is presumably related to the kimberlite eruption. Note that there is some question of the reliability of deformation observations on xenolithic diamonds since such diamonds tend to be well preserved, which hinders the recognition of deformational features.

The occurrence of deformed diamonds in undeformed xenoliths has been reported. Robinson (1979a) found "tentative direct evidence" of plastic deformation in one diamond from eclogite, but cites the occurrence of brown diamonds, the colour of which some investigators believe may be caused by deformation, in eclogite xenoliths as further evidence for deformation. Robinson et al. (1989) show that a large proportion of diamonds having colours other than brown, are deformed, as was also observed for Sloan diamonds. The presence of brown diamonds is therefore not necessarily an indication of deformation.

At present there is no consensus as to the cause and timing of diamond deformation. Although it is clear that deformation predates resorption, there is no clear evidence of the length of time between deformation and resorption. It seems possible, however, that diamond deformation may occur soon after crystallization and possibly due to stresses occurring within the confines of coprecipitating host rock material.

3.12.4 Resorption

Robinson (1979a) comprehensively discusses the experimental work from which the environmental conditions probably responsible for the more commonly observed resorption features of diamond have been inferred. In general, oxidation is considered to be responsible for most resorption features. Specific features can be related to temperature and the type of oxidant. Fused kimberlite (Frank and Puttick, 1958), and water and carbon dioxide (Evans and Sauter, 1961; Phaal, 1965) produce negatively-oriented etch pits (trigonal and

tetragonal) at temperatures greater than 950 °C. Positively oriented etch pits will form in oxygen at lower temperatures (between 450 - 1000 °C; Evans and Sauter, 1961). At higher temperatures and high oxygen pressures, water will produce positive features up to approximately 1100 °C (Harris and Vance, 1974; Harris, 1975). Hexagonal etch pits are a result of the combined growth of positive and negative pits at intermediate temperatures (Evans and Sauter, 1961; Phaal, 1965). In general, most of the Sloan diamonds seem to have experienced some resorption and according to the experimental evidence discussed above, the resorption probably occurred at high temperatures (>900°C) and by oxidation in the presence of fluids rich in H₂O or CO₂. The occurrence of diamonds displaying resorbed breakage surfaces suggests that diamond resorption as a process is occurring during the kimberlite eruption since, as discussed in the next section, breakage is likely a late-stage process.

In general, the larger diamonds at Sloan are better preserved (Table 3.19). The fact that large diamonds having Category 1 resorption morphologies are present suggests that resorption was sufficiently strong or of sufficient duration to resorb significant amounts of material. The presence of small diamonds is therefore significant. The survival of small diamonds may be a consequence of a number of factors including: a reduced rate of chemical attack due possibly to a non-uniform distribution of the resorbing medium; or a reduced exposure to the resorbing medium possibly because of protection. Unresorbed diamonds, exhibiting smooth-faces and sharp-edges, were either wholly encased during resorption or, alternatively, could have crystallized after resorption

ceased. The occurrence of diamonds displaying non-uniform resorption indicates that they were partially protected during resorption. Robinson (1979a) shows that xenolithic diamonds in general tend to be better preserved relative to production diamonds which suggests that such protection may be provided by host xenoliths.

The diamonds in the Sloan 2 kimberlite body are better preserved relative to those in other kimberlite phases at Sloan. As discussed previously, the amount of preservation in various portions of the Sloan pipe may be dependent on a number of factors. However, the general relationship between percent preservation and size suggests, since Sloan 2 diamonds are larger, that, in fact, the effect is largely a function of diamond size. In other words, though the difference in diamond sizes between Sloan 1 and 2 is apparently not a result of better preservation, it is still feasible that the better preservation of the Sloan 2 diamonds is a result of their larger sizes.

3.12.5 Crystal Breakage

Robinson et al. (1989) report that more than 50% of the diamond crystals at most southern African kimberlite localities are broken and the Sloan diamonds do not deviate from this trend.

Whether a diamond is susceptible to breakage depends on the processes responsible for diamond breakage. Certainly, some diamond breakage occurs as a result of decompression during eruption either due to differential expansion between included phases and the diamond host or because of inherent weaknesses in the crystal structure. At Sloan, breakage due

to the former is indicated by inclusion pits on some, albeit only a small proportion of the broken diamond surfaces, whereas the greater susceptibility of brown diamonds to breakage suggests that brown diamonds are intrinsically weak, possibly because of high impurity content.

Some diamonds may break as a result of impact, either during eruption or during the diamond recovery process. At Sloan, the observed increase in broken diamonds with increasing size may be due to the greater probability of larger diamonds being involved in such collisions.

Some breakage must have occurred before resorption (but not necessarily corrosion) ceased, as evidenced by the occurrence of resorbed breakage surfaces (Figure 3.25e-h).

3.12.6 Late Stage Etching

The virtual absence of corrosion sculpture on Sloan 1 and Dyke kimberlite body diamonds and its relatively common occurrence on Sloan 2 diamonds is intriguing. According to Robinson et al. (1984), such corrosion is particularly common on diamonds from hypabyssal kimberlite in diatreme root zones. They suggest that the texture develops mainly after the kimberlite has been emplaced. The more common occurrence of this feature on Sloan 2 diamonds is consistent with the blind diatreme hypothesis of McCallum (1976), since such an environment may provide the proper physical and chemical conditions (slower cooling ?) for corrosion sculpture formation.

4. MINERAL INCLUSIONS IN THE SLOAN DIAMONDS

4.1 OVERVIEW

The early visual identification and misidentification of minerals in diamond is reviewed by Harris (1968). The first instrumental identification was accomplished by Mitchell and Giardini (1953) who, using X-ray diffraction techniques, confirmed olivine as an inclusion in diamond. Meyer (1968) and Meyer and Boyd (1969) reported the first electron microprobe analyses of minerals recovered from diamond. Early studies of inclusions using XRD and microprobe techniques are reviewed by Meyer and Tsai (1976), Sobolev (1974) and Harris and Gurney (1979a). Recent work on large numbers of inclusion-bearing diamonds from single well-defined localities is discussed in reviews by Meyer (1987) and Gurney (1989).

Of particular interest here is the observation, first made by Meyer and Boyd (1969), that primary minerals included in diamond occur in two broad parageneses termed peridotitic (P-type) and eclogitic (E-type). Both paragenetic groups have been found in diamonds at every locality studied worldwide. This is intriguing because the two groups apparently represent two distinct growth environments of diamond. This assumption is based on compositional differences between associated mineral inclusions, but also is supported by isotopic model ages derived from inclusions of both paragenetic types (Table

4.1). Based on present data, most P-type diamonds (i.e. diamonds with P-type inclusions) appear to have formed in the Archaean (Richardson et al., 1984), whereas E-type diamonds appear to have crystallized at various times during the Proterozoic (Richardson, 1986; Smith et al., 1989a).

Based on variations in inclusion composition, as well as on correlative variations in the carbon isotope composition of the diamond host, subdivisions within the two broad paragenetic groups have been documented at some localities. The extent to which such subgroups represent distinct diamond crystallization events, however, is not as well constrained. Smith et al. (1989b) and Richardson (1989) have recently reported on single P-type diopside inclusions, from two southern African localities, which they suggest are Proterozoic in age. In the light of this, it is important to mention that Archaean model ages for P-type diamonds, as discussed earlier, were determined on sub-calcic garnet inclusions of harzburgitic affinity which crystallized in the absence of clinopyroxene. The harzburgitic and lherzolitic subgroups of peridotitic diamonds, in general, may represent different crystallization events in time.

The temporal relationships of E-type diamonds appear to be more complicated. Smith et al. (1989b) report a wide range of Sm-Nd model ages (2.4 - 1.4 Ga, as well as one obviously spurious age of 7.5 Ga) for single E-type garnets from six large diamonds from the Finsch mine. These are interpreted to be evidence for a multi-stage origin for these garnets, suggesting that model ages derived from composited samples may be meaningless. It may be significant that some of the eclogitic garnet inclusions analyzed by Smith et al. (1989b),

are compositionally distinct relative to most of those previously reported from Finsch diamonds (see Gurney et al., 1979). It is possible that the compositionally distinct subgroups of E-type diamonds found at various localities also represent distinct crystallization events in time.

It should be mentioned that, although extremely unusual, single diamond crystals containing both the P-type and E-type minerals have been discovered (Prinz et al., 1975; Hall and Smith, 1984; Moore and Gurney, 1989). Finally, it is noted that some diamond growth may occur in close association with kimberlite magma possibly near the time of emplacement, as has been recently suggested for coated diamonds from Zaire (Navon et al., 1988) and for so-called microdiamonds (Haggerty, 1986).

Thus, not only are both P- and E-type diamonds present in every locality so far studied, but subgroups within the two broad categories of diamond, which in themselves may represent distinct crystallization events, occur at many localities. Although there are general compositional similarities between subgroups, each locality appears to be unique and no regional trends have been found. A complicated picture is emerging where diamond crystallization has apparently occurred in relatively small, localized events throughout much of geologic time. It is important, therefore, to delineate the diamond subpopulations present at each individual locality.

In this chapter, the chemical compositions of mineral inclusions and xenolith minerals associated with the Selected sample of Sloan diamonds are discussed. The inclusions, recovered from 100 Sloan diamonds, are first classified with respect to their primary or secondary character. Most of

those classified as primary can be divided, based on mineralogy, composition and coexisting phases, into the major peridotitic and eclogitic paragenetic groups found worldwide. The major element compositions of the inclusions are then presented by mineral phase within these broad groups, and compared to similar minerals recovered from diamonds worldwide. The compositions of inclusion minerals are also compared to those of corresponding phases in xenoliths from the Sloan locality. In this respect, particular attention is paid to the mineral compositions of diamondiferous xenoliths found in the State Line kimberlite district as they are probable source rocks for at least some of the Sloan diamonds. Relationships between inclusion and xenolith mineral composition and host diamond physical characteristics, especially primary characteristics, are then described. Based on these observations, possible paragenetic diamond subpopulations at Sloan are defined. Comparisons with the paragenetic subpopulations found at other localities allow speculation on diamond genesis as well as on the composition and evolution of the upper mantle beneath North America.

4.2 METHODS

The procedures used in sampling the 103 inclusion-bearing and/or the xenolith diamonds comprising the Selected sample are discussed in Chapter 3. Here, the methods of inclusion recovery, the preparation of the inclusion and xenolith minerals for microprobe analysis and the microprobe analytical conditions are described.

Before cracking the diamonds for inclusion removal, they were soaked overnight in 30% HF in order to dissolve any surface impurities which might be mistaken for inclusion material during the recovery process. The cleaned diamond crystals were then re-inspected to refine initial observations on their physical characteristics. At this point, the diamond mass was determined to the nearest .005 carat (1 mg) using a Sartorius 2004-MP6 balance. The mass and other physical features recorded for this Selected sample of 103 diamonds are listed in Appendix III and discussed in Chapter 3.

It is pertinent here to emphasize the importance of documenting, in as much detail as possible, the inclusion characteristics just prior to cracking the diamond. This is especially important when working with fractured diamonds as it minimizes the chances of misidentifying secondary inclusions or, even worse, external contaminants as primary inclusions. Because of just such problems encountered in this study, an Inclusion Description Scheme has been developed (Appendix IV) which, when used during inclusion recovery, should maximize the recognition of primary minerals as discussed in Section 4.3.

The mineral inclusions were removed by breaking the diamonds in a specially devised diamond cracker (Figure 4.1). This tool was designed with a screw-on cap so that the shattered diamond would be confined inside. Unfortunately, problems were encountered with the microscopic inclusion fragments getting lodged and lost in the gap between the cap and the cracker body. It was found that breaking the diamond in the capless body, inverted onto a large glass slide (Figure 4.2), was more successful. The shattered diamond and

inclusion fragments fall onto the glass slide which can then be inspected with a microscope using both reflected and transmitted light. A polarizer is advantageous especially for identifying colourless birefringent minerals which resemble diamond fragments in unpolarized light.

Inclusion crystals and fragments were picked using a fine dentist's probe with a wetted tip, and mounted in a drop of "Petropox" epoxy glue on a standard 280x480 mm glass probe slide (one inclusion fragment per slide). Although "Petropox" requires curing for 10 minutes at 120°C, it was chosen for this operation because of its low viscosity and long life at room temperature. Once the epoxy had cured, the inclusion minerals were exposed by hand, using well worn 600 grit silicon carbide sandpaper. In view of the possible discovery of moissanite as an inclusion in diamond in this project, it is emphasized that before this step, the inclusions recovered were totally enclosed in epoxy. Any contaminant, therefore must have been introduced prior to this step. Final polishing for microprobe analysis was done by hand on a paper polishing disk using 3 micron diamond paste.

Mineral grains from the three diamondiferous eclogites recovered during this study were hand separated from the diamond and, like the inclusion minerals, mounted in "Petropox" epoxy glue on standard 280x480 mm glass probe slides. The diamond fragments remaining from inclusion and xenolith mineral recovery were saved in glass vials for carbon isotope determination (this study), as well as for possible UV-IR absorption, helium isotope and other future work.

Before analysis, the polished grain mounts were carbon coated (approx. 25 angstroms thick) using a Varian

evaporation-type vacuum coater. Major element analyses of inclusion and xenolith grains were carried out on a fully automated Cameca/Camebax Microbeam electron microprobe. The analytical conditions, standards used and relevant counting statistics for the various minerals analyzed are listed in Appendix V.

Where possible, at least three spots per mineral grain were analyzed and, if the replicate analysis agreed within statistical limits, they were averaged. Analyses of multiple grains of one mineral species from the same diamond were likewise combined if similar within statistical error. Only two cases of similar minerals with significantly different compositions were found in single diamonds. The averaged inclusion and xenolith mineral analyses are listed in Appendix VI.

4.3 INCLUSION CLASSIFICATION

The classification of minerals included in diamond is accomplished on two interdependent levels. Because it is important to determine the relative timing of inclusion formation, they must first be classified as either primary or secondary with respect to the diamond growth environment. Once this is done, the inclusions can be further classified according to their paragenesis and composition.

The division of inclusions into primary and secondary groups is based on both physical and compositional criteria. In general, isolated crystals which are unassociated with fractures to the diamond surface are considered primary. Secondary or "epigenetic" inclusions form when fluids invade

fractures in diamond thereby replacing or altering a primary mineral, or crystallizing secondary minerals in the void created by the fracture. Morphology, colour and compositional homogeneity should also be considered when distinguishing primary and secondary inclusions.

Based on morphological and epitaxial relationships between inclusions and their diamond host, a further subdivision of primary inclusions into "protogenetic" and "syngenetic" types has been suggested (Meyer and Tsai, 1976; Meyer, 1987). Most investigators agree that inclusions with imposed cubo-octahedral morphologies and/or an epitaxial relationship with their diamond host must have nucleated on growing diamond surfaces and, therefore, are syngenetic with diamond (Meyer and Tsai, 1976; Robinson, 1978; Harris and Gurney, 1979a). Conversely, randomly oriented mineral inclusions with non-cubic morphologies consistent with their own crystal structure may have formed previous to diamond overgrowth (Robinson, 1978; Harris and Gurney, 1979a). Meyer (1987) suggests that irregularly shaped inclusions might also be protogenetic. Inclusions that can unambiguously be considered protogenetic are extremely rare (Harris and Gurney, 1979a) and compositional differences between syngenetic and protogenetic inclusions have so far not been reported. Nevertheless, it is important to record the features pertinent to such a division.

The classification of the Sloan diamonds as primary or secondary was based on the following considerations:

- I. Description Before Diamond Breaking
 - A. Association with fractures to the diamond surface
 - B. Morphology -- shape/crystal faces
 - C. Colour -- pristine/discoloured/surface alteration

- II. Description After Diamond Breaking
 - A. Morphology -- shape/crystal faces
 - B. Colour -- pristine/discoloured/surface alteration
- III. Mineralogy and Composition
 - A. Homogeneous/Inhomogeneous
 - B. Reported previously in diamond
 - C. Otherwise associated with mantle xenoliths
 - D. High pressure and temperature phase

These parameters have been incorporated into an Inclusion Description Scheme (Appendix IV) which, when used during the inclusion recovery process, assists in determining the primary or secondary nature of the inclusion, a sometimes difficult decision.

Once the relative time of formation between the inclusion and its host has been determined, the inclusions can be further classified according to their mineral paragenesis. As outlined in Section 4.1, previous work has shown that primary inclusions can be divided on the basis of mineralogy, composition and coexisting phases into peridotitic and eclogitic groups. This is obviously a feature related to the primary growth environment and since the minerals of these two suites do not normally coexist in the same diamond, it is a useful way to categorize, not only the inclusion, but the diamond host as well. Based on the uncertainty of their origin, secondary minerals are largely ignored in the literature and have not been classified into paragenetic groups.

Table 4.2 lists, in their appropriate categories, the minerals that have previously been reported as inclusions in diamond. The application of the two interdependent classification schemes to the Sloan inclusions will provide

opportunity for further discussion on the minerals and their classification.

4.3.1 Primary/Secondary Division

The minerals recovered from the Sloan diamonds are listed by diamond number in Appendix VII. Table 4.3 summarizes this data and groups the inclusions into primary, possibly primary and secondary categories. The possibly primary division was adopted in this study in order to accommodate inclusions which may be primary, but which do not meet the requirements set out previously.

All of the minerals reported as primary were visually confirmed as being unassociated with fractures to the diamond surface in at least one Sloan diamond. Some of the primary inclusions have cubo-octahedral morphologies with planar or slightly curved crystal faces (see Figure 3.29), but, more commonly, faces show extreme curvature which gives the inclusions an irregular, rounded appearance. No non-cubic minerals were documented as having morphologies of their own crystal class. Primary inclusions show no discoloration or surface alteration and generally are compositionally homogeneous. The exception is sulphide inclusions which, in many cases, show inhomogeneity due to exsolution.

Some of the primary inclusions reflected in the abundance figures were either not seen before diamond cracking or appeared to be associated with fractures to the surface. Such questionable cases were classified as primary only if the mineral had been seen without fractures in another Sloan diamond and exhibited other primary features. Some of the rutiles, for instance, were classified as primary based on

their morphology even though they were associated with penetrative fractures, exhibited discolouration and/or were slightly inhomogeneous.

The high pressure form of SiO_2 , coesite (Coes, 1953), has previously been reported in diamond (Sobolev et al., 1976b; Sobolev, 1984a; Gurney et al., 1984a; Hall and Smith, 1984). Eight Sloan diamonds released SiO_2 inclusions, but only three could convincingly be considered primary coesite (see Section 4.5.3). The rest are classified as possibly primary SiO_2 . They may be quartz pseudomorphs after coesite or, alternatively, may be secondary quartz, a common alteration product in State Line xenoliths (McCallum et al., 1977). Magnetite and ilmenite also have been reported as primary inclusions (Prinz et al., 1975; Meyer and Svisero, 1975; Sobolev et al., 1976a; Mvuemba Ntanda et al., 1982), but they were not confirmed as primary inclusions in this sample of Sloan diamonds. Finally, moissanite and corundum were recovered but their occurrence may be contamination as discussed in Section 4.6.4

Most of the secondary inclusions recovered are angular fragments, although some are pseudomorphs, usually after primary, cubo-octahedral inclusions (see Figure 3.27). Discoloration and surface alteration are common and the majority of secondary inclusions are highly altered, hydrous phases.

It is emphasized that it is very important that secondary phases are not reported as primary inclusions. In this study, only inclusions with the highest credentials are classified as primary. It is hoped that in using these constraints, all

minerals reported as primary were, indeed, formed either before or simultaneously to diamond crystallization.

4.3.2 Paragenetic Division

On the basis of the four minerals, garnet, clinopyroxene, olivine and orthopyroxene, 61 of the 89 diamonds from which primary inclusions were recovered can be classified as peridotitic or eclogitic (Table 4.4a). This classification can be refined by taking into account the observations of previous studies. For instance, rutile, coesite, K-feldspar and kyanite have previously been considered to be eclogitic (Sobolev, 1974; Meyer, 1987). In this study, none of these minerals coexist with peridotitic minerals, but in some cases occur with eclogitic garnets and clinopyroxenes (Table 4.5). They are therefore classified as eclogitic. Ferro-periclase has previously been found associated with highly magnesian orthopyroxene in diamonds (Scott Smith et al., 1984; Rickard et al., 1989), and is therefore classified as peridotitic.

As might be expected, not every diamond could be unequivocally classified as eclogitic or peridotitic. The clinopyroxenes in diamonds SL A11, SL A28 and SL A32 are unlike other clinopyroxenes found in diamond and, therefore, are left unclassified. Zircon has previously been classified as peridotitic (Mvuemba Ntanda et al., 1982), but this could not be confirmed in this study.

One Sloan diamond, SL A57, released an olivine (Fo 92.2) and a typical eclogitic garnet. Diamonds containing minerals of mixed paragenesis have been reported in three other instances. Prinz et al. (1975) found olivine (Fo 92.6) coexisting with omphacitic clinopyroxene, rutile and SiO₂ in a

diamond from an unknown African locality. Hall and Smith (1984) report the occurrence of olivine (Fo 91), pyrope-almandine garnet and Na-rich clinopyroxene in an Argyle diamond. Moore and Gurney (1989) recovered an olivine (Fo 94.9) and an eclogitic garnet from a Monastery mine diamond. In the latter, the garnet is an ultra-high pressure form with pyroxene solid solution (see Moore and Gurney, 1985).

Sloan diamond SL A57 was a simple aggregate, consisting of two intergrown octahedra, which exhibited non-uniform resorption. It is possible that the garnet and olivine occurred in opposing octahedra which may have grown in two separate crystallization events. Unfortunately, the positions of the two inclusions were not adequately described before breakage. The Monastery diamond was a single crystal tetrahedron (R.O. Moore, pers. comm., 1986).

Table 4.4b is a refined classification based on the above considerations. It shows that the dominant inclusion type at Sloan, excluding sulphides, is eclogitic. Even the sulphides, commonly considered to fall into both inclusion suites (Harris and Gurney, 1979b; Yefimova et al., 1983), show strong affinities to the eclogitic inclusions at Sloan. On the basis of coexisting phases, ten of the 23 diamonds from which sulphide was recovered can be classified as eclogitic (Table 4.4b). No sulphides were recovered from diamonds containing peridotitic minerals although "sulphide" rosette features were visually identified in at least three of these stones. Based on these considerations, as well as on compositional constraints (see Section 4.5.7), it is assumed that all of the Sloan diamonds which released sulphides are eclogitic.

If all of the sulphides are classified as eclogitic (Table 4.4c), the Sloan diamonds have an eclogitic/(eclogitic + peridotitic) ratio of approximately 0.78. Thus, the Sloan kimberlites are added to the growing list of localities with predominantly eclogitic diamonds. Other localities include: Argyle, Ellendale 5 & 9, Monastery, Orapa and Premier (Hall and Smith, 1984; Moore and Gurney, 1989; Gurney et al., 1984a; 1986).

4.4 PERIDOTITIC INCLUSION COMPOSITION

The peridotitic minerals recovered from Sloan diamonds are olivine, orthopyroxene, chrome-rich pyrope, chrome-rich diopside and ferro-periclase. The compositions of each mineral phase are considered separately and compared to similar minerals found in diamonds worldwide, as well as to corresponding minerals in xenoliths from the Sloan kimberlite occurrence. The mineral compositions of the diamondiferous peridotite from the Schaffer locality are also considered. Thermobarometric information derived from the inclusions is then discussed and finally, aspects of their paragenesis relative to worldwide trends are considered.

4.4.1 Olivine

Colourless olivine inclusions were recovered from 16 diamonds. The crystals range from 20 to 200 microns in maximum dimension and commonly exhibit irregular, curved-faced morphologies (see Figure 3.30). Olivine was found coexisting with orthopyroxene (2 diamonds), chrome-rich pyrope (2) and,

in one unusual association in diamond SL A57, pyrope-almandine (Table 4.5).

The olivines range from Fo 91.3 to 92.7 with the average of 91.9 falling below the worldwide median of approximately 93 (Figure 4.3). The calcium concentrations in the olivine inclusions are generally high relative to other occurrences, with values ranging up to .24 wt.% CaO. Nickel concentrations (.20 - .37 wt.% NiO) are similar to those reported for olivine inclusions elsewhere, but occur at the lower end of the range. Except for two olivines, chrome concentrations range from .08 to .14 wt.% Cr₂O₃, which is high for terrestrial olivines, but is characteristic of inclusion olivines worldwide (Meyer, 1987). Although reported here as the trivalent oxide, chrome in olivine inclusions from diamond may be present in the divalent state according to the observations of Burns (1975) and Hervig et al. (1980).

The chrome contents of the olivines from diamonds SL A11 and SL A57, the latter which coexisted with pyrope-almandine, were below the analytical detection limits of $.02 \pm .02$ wt.% Cr₂O₃ (for 30 second peak and background counts). Interestingly, these two Cr-poor olivines are slightly enriched in magnesium relative to the rest of the olivines from Sloan diamonds. In the case of a mixed paragenesis found in a Monastery diamond (Moore and Gurney, 1989), the olivine that coexisted with a high pressure "group B" pyrope-almandine also is substantially enriched in magnesium (Fo 94.9) relative to the other olivines recovered from Monastery diamonds. The olivine (Fo 91) found coexisting with omphacite in the Argyle diamond (Hall and Smith, 1984) is apparently not significantly different from those in associated diamonds.

No unaltered olivine was present in the diamond peridotite found in the Schaffer pipe, but when compared to peridotitic xenoliths from the Sloan kimberlite, the olivines in Sloan diamonds show compositional affinities to those from "infertile" garnet peridotites (as classified by Egger et al., 1987) with respect to forsterite and chrome content (Figure 4.4) and calcium content.

4.4.2 Orthopyroxene

Like olivine, orthopyroxene usually appears colourless in diamond. It was found in four Sloan diamonds and coexisted with olivine in diamonds SL A34 and SL A64 (Table 4.5).

All four inclusions have Mg/(Mg+Fe) ratios of approximately 93 (Figure 4.5), similar to most orthopyroxenes recovered from diamond worldwide (but unlike the "websteritic" orthopyroxenes found in Orapa diamonds - Gurney et al., 1984a) (Figure 4.6). The Sloan group are distinguished by unusually high calcium concentrations (1.0 - 1.4 wt.% CaO) relative to those found in diamonds worldwide. Otherwise, they have typical chrome (.41 -.48 wt.% Cr₂O₃) and aluminium (.49 -.93 wt.% Al₂O₃) concentrations.

The orthopyroxene inclusions also show compositional affinities to the orthopyroxenes from "infertile" garnet peridotites from the Sloan kimberlite (Egger et al., 1987) having similar Mg/(Mg+Fe) ratios, but slightly higher calcium concentrations (Figure 4.7). No unaltered orthopyroxene was present in the diamond peridotite from the Schaffer pipe.

4.4.3 Garnet

Chrome-rich pyropes were recovered from Sloan diamonds, SL A12 and SL 27-6 and, in both diamonds the garnets coexisted with olivine (Table 4.5). In diamond SL A12, the garnet was present as an elongate, transparent, pale-blue crystal with a maximum dimension of 250 microns. Because of its light colour and isotropic character, it was nearly mistaken for a diamond fragment during recovery. The identification of the chrome-rich pyrope in diamond SL 27-6 was not difficult as it exhibited a bright purple colour (Figure 3.30), which is characteristic of peridotitic garnets in diamond worldwide.

Compositionally, both garnets are calcium-saturated (Figure 4.6) and plot near the lherzolite trend (Sobolev, 1974) in calcium-chrome space (Figure 4.8). Note, however, that they show chrome enrichment relative to all other lherzolitic garnets from diamond.

When plotted with Sloan ultramafic xenolith garnets (Figures 4.7 and 4.9), the inclusion garnets most closely resemble those from "infertile" garnet peridotites (Eggler et al., 1987). Note that the chrome-rich pyrope inclusions plot near the garnet from the diamondiferous peridotite nodule from the Schaffer pipe as described by McCallum and Eggler (1976).

4.4.4 Clinopyroxene

Chrome-rich diopside was recovered from Sloan diamond SL A78. Two pale green crystals were documented and recovered, the largest being approximately 100 microns in maximum dimension.

The clinopyroxene composition is similar to other chrome-rich diopsides found in diamond (Figure 4.6) having a high

Mg/(Mg+Fe) ratio (92.9), high chrome content (1.29 wt.% Cr₂O₃) and a low aluminium (.99 wt.% Al₂O₃). It is unusual in having a high potassium concentration (.20 wt.% K₂O). Similar potassium-rich chrome-rich diopsides were recovered from Koffiefontein diamonds (Rickard et al., 1989).

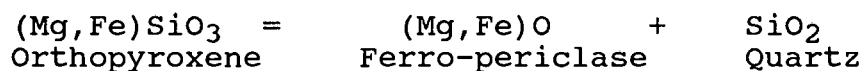
When compared to clinopyroxenes from Sloan ultramafic xenoliths (Figure 4.7) the inclusion obviously groups with the clinopyroxenes from "infertile" garnet peridotites (Eggler et al., 1987).

4.4.5 Ferro-Periclase

Ferro-periclase (78.7 wt.% MgO, 19.4 wt.% FeO) was recovered from Sloan diamond SL A100. The single crystal is oblate with a maximum dimension of 60 microns and exhibits curved crystal faces of unknown symmetry. The mineral is isotropic and dark orange to brown in colour.

The occurrence of this mineral in diamond is rare. After burning an Arkansas diamond in air at 850°C, Newton et al. (1977) found "finely polycrystalline, light tan ash" which they identified as being predominantly periclase with minor magnetite. They concluded that it was probably a secondary product of combustion, possibly after magnesite. Other minerals recovered from the same diamond were olivine, chrome-rich diopside and ortho-clinopyroxene. Moore et al. (1986) and Rickard et al. (1989) report on ferro-periclase recovered from four Koffiefontein diamonds, one of which coexisted with orthopyroxene, implying a peridotitic association. A further occurrence of the mineral is reported from two diamonds in the Orroroo kimberlites in Australia (Scott Smith et al., 1984). These authors prefer to call the mineral "magnesian-wustite".

Another Orroroo diamond released orthopyroxene. The possibly coincidental association with orthopyroxene suggests that the ferro-periclase may form, as suggested by Cardoso (1980), according to the breakdown reaction:



Scott Smith et al. (1984) reject such a mechanism since mantle enstatites of typical compositions ($\text{Mg}/\text{Mg}+\text{Fe} \sim .93$) would not produce ferro-periclases with the observed composition ($\text{Mg}/\text{Mg}+\text{Fe} \sim .86$). Both Cardoso (1980) and Scott Smith et al. (1984) consider as unlikely a possible secondary origin for the mineral, since the breakdown or alteration reaction would have to be very precise to produce it in more than one diamond from such small samples. The recovery of ferro-periclase from the Sloan diamond supports a primary origin.

Magnesio-wustite is considered to be a major constituent of the Earth's lower mantle (Yagi et al., 1979). Its occurrence as a primary mineral in diamond carries with it important implications for the origin of both diamonds and kimberlites. Experimental work involving magnesio-wustite is largely concerned with iron-magnesium fractionation models for the primitive Earth (Mao et al., 1979). Pressures typically considered are in excess of 100 kbar. For the magnesio-wustite and enstatite coexisting in the Koffiefontein diamond to have crystallized in equilibrium, pressures greater than 200 kbar are possible (Yagi et al., 1979). However, other factors such as oxygen-fugacity affect the stability of magnesio-wustite. Without more specific experimental evidence and further evidence of coexisting minerals, it is perhaps

premature to consider, in too much detail, the implications of its occurrence in diamond. It may, however, imply deeper depths of origin for at least some diamonds and kimberlites as is also surmised from pyroxene solid solution in eclogitic garnet inclusions from Monastery mine diamonds (Moore and Gurney, 1985).

4.4.6 Thermobarometry

Experimental studies on simple mineral systems have shown that coexisting minerals in equilibrium with each other will exchange cations in a systematic fashion in response to variations in temperature and/or pressure. Based on these observations as well as on theoretical considerations, various "geothermometers" and "geobarometers" have been developed which have been used to calculate equilibration temperatures and pressures from compositions of minerals in natural systems. However, care must be taken when applying these methods, as they have been developed usually from limited data on specific systems over limited temperature and/or pressure ranges. Seldom do the conditions, under which the various "thermobarometers" were formulated, correspond exactly to the assemblages being investigated. Ultimately, the investigator must decide which thermobarometer is most appropriate to use for the samples under investigation and then judge the extent to which the data are meaningful. A more detailed account of general problems in applying thermobarometric methods is beyond the scope of this study. Comprehensive discussions, especially with respect to mantle assemblages, have been presented by Carswell and Gibb (1980; 1987); Finnerty and Boyd (1984; 1987) and Bell (1985).

The legitimate application of thermobarometers to inclusions in diamond is hindered by two problems. The first involves the question of whether or not it is correct to consider two (or more) inclusions isolated from each other within the same diamond as representing an equilibrium assemblage. This assumption has generally found acceptance for three reasons: (1) multiple inclusions of the same mineral in a single diamond are usually compositionally equivalent; (2) different phases from individual diamonds from single localities yield compatible arrays of tie lines; and (3) temperatures calculated for coexisting phases in single diamonds from single localities generally define reasonable, internally consistent trends (see for instance Gurney et al., 1984 a&b; 1986).

Delineating trends is dependent on obtaining a reasonable number of data points and the second problem, therefore, is that minerals which can be used for thermobarometric calculations, especially coexisting pairs, are rare in diamond. The rare occurrence of multiple phase assemblages within single diamonds further limits the choice of thermobarometers.

Because of the last constraint, most of the temperatures reported for peridotitic inclusions from diamond have been calculated from either olivine/garnet pairs using the method of O'Neill and Wood (1979;1980), or from rare chrome-rich diopsides using the diopside solvus of Lindsley and Dixon (1976). Most pressures have been estimated from orthopyroxene compositions using the barometers of MacGregor (1974) and/or Nickel and Green (1985). Each of these methods has, in one way or another, been applied to the peridotitic inclusions

from Sloan diamonds and the assumptions required and the limitations of each method will be discussed with respect to the specific cases.

An initial estimate of temperature for a Sloan peridotitic diamond was derived from the chrome-rich diopside in diamond SL A78 using the diopside solvus determined by Lindsley and Dixon (1976). The temperature was calculated using the program TEMPEST (Finnerty and Boyd, 1984; 1987), which uses a best fit equation to the 20 kbar data of Lindsley and Dixon (1976). According to Finnerty and Boyd (1984) this thermometer, when used in conjunction with the MacGregor (1974) geobarometer, yields a geotherm which best fits that determined from geophysical models. As this thermometer is based on the Ca-Mg exchange reaction between diopside and enstatite, its use assumes that the diopside coexisted in equilibrium with enstatite. This is not unreasonable for the Sloan diamonds as orthopyroxenes of enstatite composition were recovered from four peridotitic diamonds. The calculated temperature using this method is 1224°C (Table 4.6).

A further estimate of equilibration temperature for the Sloan peridotitic diamonds is possible using the garnet/olivine pairs in diamonds SL 27-6 and SL A12. In the absence of clinopyroxene, the only method available for this assemblage is one based on the Fe-Mg exchange reaction and the thermometer used here is that of O'Neill and Wood (1979; 1980). Unfortunately, this thermometer requires an independent assessment of pressure, and in the absence of coexisting orthopyroxene from which such information can be obtained, a pressure must be assumed. Previous studies (e.g. Boyd et al., 1985) have assumed 50 kbar, as this is considered

a reasonable pressure for diamond formation and for comparative purposes the practice is continued here. Interestingly, the temperature calculated for the diopside in diamond SL A78 (1224°C) would lie on the diamond/graphite stability boundary at 50 kbar (Figure 4.10).

Keeping these considerations in mind, the temperatures calculated at 50 kbar for the garnet/olivine pairs in diamonds SL 27-6 and SL A12 are, respectively, 1294°C and 1374°C (Table 4.6). However, they may be too high since, at 50 kbar, they plot well within the graphite stability field (Figure 4.10). This suggests that either the O'Neill and Wood (1979;1980) thermometer is overestimating the temperature (possibly because the garnet/olivine pairs are not in equilibrium or possibly because the thermometer isn't calibrated for such high temperatures) or, otherwise, the assumption of 50 kbar is inappropriate. The former explanation does not seem possible because according to Boyd and Finnerty (1980), the O'Neill and Wood (1979; 1980) thermometer actually underestimates temperature by $75\text{-}100^{\circ}\text{C}$ relative to the preferred method of Lindsley and Dixon (1976). This suggests that it is the assumption of 50 kbar which is not appropriate and that the garnet/olivine pairs may have equilibrated at higher pressures.

Estimates of pressure can be inferred from the compositions of the four orthopyroxenes recovered from Sloan diamonds. Unfortunately, the two methods available for this, MacGregor (1974) and Nickel and Green (1985), are not directly applicable since the former method requires an independent estimate of temperature whereas the latter requires compositional data from coexisting garnet. Assuming 1224°C is

a reasonable estimate of temperature, the barometer of MacGregor (1974), which is based on the solubility of Al_2O_3 in orthopyroxene, yields pressures from 59 - 69 kbar (Table 4.6).

If it is assumed that the orthopyroxenes coexisted with the chrome-rich pyrope inclusions, not unreasonable since both minerals coexisted in Sloan diamonds with compositionally similar olivines, a further estimate of pressure as well as temperature can be achieved, again using TEMPEST (Finnerty and Boyd, 1984; 1987) which, using an iterative procedure, solves the MacGregor (1974) barometer simultaneously with the O'Neill and Wood (1979; 1980) thermometer. By this approach, pressures ranging from 64 - 83 kbar and temperatures from 1343 - 1469 °C are obtained (Table 4.6). Applying the same procedure using the barometer of Nickel and Green (1985), a method which accounts for the effect of chrome in garnet on the ion-exchange reaction between garnet and orthopyroxene, yields lower pressures from 56 - 79 kbar and slightly lower temperatures from 1315 - 1458 °C (Table 4.6).

Finally, additional estimates of temperature and pressure can be obtained from the orthopyroxenes using the method of Boyd and Nixon (1973). This thermometer is essentially the other limb of the diopside-solvus used in Lindsley and Dixon (1976) and it is used assuming that the orthopyroxenes coexisted in equilibrium with clinopyroxene. The temperatures obtained for the four orthopyroxenes using this method range from ~1225 - 1325 °C and the corresponding pressures using MacGregor (1974) range from 62 - 73 kbar (Table 4.6). Figure 4.10 shows the range of temperatures and pressures obtained from the Sloan peridotitic inclusions in relation to the diamond/graphite stability curve (Kennedy and Kennedy, 1976),

the ZIVC peridotite solidus (Eggler and Wendlandt, 1979) as well as the 40 mW/m² conductive geotherm (Pollack and Chapman, 1977). Although based on minimal data, the temperatures and pressures for Sloan peridotitic inclusions appear to be high relative to those found for peridotitic inclusions elsewhere (Figure 4.11).

Temperature and depth estimates for the "infertile" garnet peridotites for the Group I xenoliths are similar to the inclusions in diamond and range from approximately 1100 - 1300 °C and from 50 - 70 kbar (Eggler et al., 1987).

4.4.7 Paragenesis

The paragenetic division of peridotitic inclusions (i.e. those which crystallize in the presence of olivine) is best shown on a plot of CaO vs. Cr₂O₃ for diamond associated pyrope garnets (Figure 4.12). Generally, those garnets plotting to the left of the "85% line" of Gurney (1984) belong to the dunite-harzburgite sub-paragenesis (clinopyroxene-absent) whereas garnets belonging to the lherzolitic sub-paragenesis (clinopyroxene-present) plot to the right. The garnet (13.5 wt.% CaO and 8.0 wt.% Cr₂O₃) from the single reported instance of a wehrlitic assemblage (Sobolev et al., 1970) is not plotted.

As would be expected for equilibrium assemblages, corresponding compositional trends in the associated minerals occur. For instance, olivines coexisting with the sub-calcic garnets of the dunitic-harzburgitic suite tend to be higher in forsterite ($Fo \geq 93.5$) than those found with calcium-rich dunitic-harzburgitic and lherzolitic garnets ($Fo < 93.5$). A similar relationship is noted for $Mg/(Mg+Fe) \times 100$ in coexisting

enstatites, with 94.3 as the dividing line. Possibly of more interest is the fact that garnets coexisting with chromite plot only in the chrome-rich portion of the dunitic-harzburgitic field, whereas ilmenites are known only in two diamondiferous lherzolites.

The lherzolitic character of the Sloan inclusions is indicated firstly by the occurrence of chrome-rich diopside as an inclusion. It is further evidenced by the relatively low forsterite content of the olivines and by the calcic nature of the orthopyroxenes. Finally, the Sloan chrome-rich pyrope inclusions plot in the calcium-saturated lherzolitic region of the diagram (Figure 4.12). It is considered to be significant that, in this sampling of Sloan diamonds, the minerals of the harzburgitic/dunitic suite were not found. Although this does not prove that they are absent, it does suggest that the lherzolitic suite is the predominant peridotitic paragenesis at Sloan.

4.5 ECLOGITIC INCLUSION COMPOSITION

The eclogitic minerals recovered from Sloan diamonds include pyrope almandine, omphacitic clinopyroxene, coesite, K-feldspar, kyanite, rutile and sulphide. These minerals are discussed individually and compared to similar minerals from diamonds worldwide. They also are compared to corresponding minerals in eclogite xenoliths found at the Sloan locality, especially those from the diamondiferous eclogite described by McCandless and Collins (1989) and three diamondiferous "eclogites" found in this study. Finally, thermobarometric

data based on inclusion composition as well as paragenetic information derived from coexisting phases are discussed.

4.5.1 Garnet

Pyrope-almandine was recovered from 32 diamonds and as many as eight inclusions were recovered from individual stones. The garnets range from 25 to 200 microns in maximum dimension and usually appear as transparent, pale orange crystals which most often show rounded, but sometimes flat-faced cubo-octahedral crystal morphology (see Figure 3.29). These garnets were found coexisting with omphacitic clinopyroxene (7 diamonds), sulphide (3), rutile (2), coesite (1) and, in diamond SL A57, olivine (see Table 4.5).

Compositionally, the garnets are similar to eclogitic garnets recovered from diamonds at other localities being characteristically chrome-poor ($<.15$ wt.% Cr_2O_3), titanium-rich ($.24 - .76$ wt.% TiO_2) and containing trace levels of sodium ($.12 - .28$ wt.% Na_2O). They also have a wide range in $\text{Mg}/\text{Mg}+\text{Fe}$ ($.36 - .66$) and, except for four iron-rich garnets, the increase of iron over magnesium corresponds to a broadly defined increase in calcium (Figure 4.13). The four deviant garnets belong to a distinct group of Ca-poor and Mn-rich garnets (Figure 4.14). On this basis, two groups of eclogitic garnets from Sloan diamonds, termed "Mn-poor" and "Mn-rich", are defined (Figure 4.15 and 4.16).

As a subgroup, the Mn-rich garnets show a broad increase in manganese with decreasing $\text{Mg}/\text{Mg}+\text{Fe}$ (Figure 4.17), a trend not present in the Mn-poor garnets. On the other hand, the latter show a broad increase in titanium with decreasing $\text{Mg}/\text{Mg}+\text{Fe}$ (Figure 4.18), which is not apparent for the Mn-rich

garnets. Sodium does not vary systematically with Mg/Mg+Fe within either group (Figure 4.19). Variation with chrome is not well constrained as most had chrome contents below the detection limit (Appendix VI - Table A).

The garnets from three diamonds occurred in direct contact with other phases as biminerally inclusions. A Mn-poor garnet from diamond SL 5-4 occurred in direct contact with clinopyroxene (see Figure 3.31). The most magnesian garnet (1-15), part of the Mn-rich group, occurred in direct contact with two compositionally distinct clinopyroxene inclusions (Figure 4.20). The compositions of the clinopyroxenes are described in the next section. Finally, the most grossular garnet (A22 - see Figure 4.13) also occurs as a biminerally inclusion, itself containing a spherical inclusion of relatively pure SiO_2 (Figure 4.21). Although not confirmed, this inclusion within an inclusion is inferred to be coesite as discussed in Section 4.5.3.

Five eclogitic garnets were recovered from diamond SL A46 (see Figure 3.29) and these garnets occur in two compositional groups. Analysis A46(1) (Appendix VI - Table A) is an average of analyses for three separate inclusions (which agreed within analytical error), whereas A46(2) is an average of two compositionally equivalent fragments which possibly represent two separate inclusions. Both titanium and sodium are significantly higher in the more magnesian garnets contrary to trends expected for igneous differentiation (Figures 4.18 and 4.19).

The pyrope-almandine coexisting with olivine in diamond, SL A57, is typical of the Mn-poor garnets with respect to all

the major elements determined (Figures 4.13, 4.14, 4.17 - 4.19).

When compared to garnets from Sloan eclogite xenoliths, the inclusion garnets appear to correlate closely with garnets from the iron-rich, metaluminous eclogites (Figure 4.22) and not as closely with the peraluminous eclogites (Figure 4.23). The garnets from the diamond-graphite eclogite, TP 121 (McCandless and Collins, 1989), as well as those analyzed from two diamondiferous eclogites found in this study, are relatively iron-rich and also plot with the metaluminous eclogite garnets (Figure 4.22). More importantly, the diamond eclogite garnets as well as some of the metaluminous eclogite garnets appear to be associated with the Mn-rich group of inclusion garnets (Figure 4.22). However, the Mn-content of the xenolith garnets, including those from the diamond eclogites, is not particularly high (Figure 4.24).

When considered with respect to Na content, only nine eclogite xenolith garnets (including five metaluminous, 1 peraluminous, but significantly, all three diamondiferous eclogites), have sodium contents approaching those found in inclusion garnets (Figure 4.25).

4.5.2 Clinopyroxene

The omphacitic clinopyroxenes recovered from nineteen diamonds commonly have curved crystal faces of probable cubo-octahedral crystal morphology. Some of these appear as transparent, pale-green inclusions (Figure 3.31), but more commonly appear colourless due to their small size (15 - 200 microns). These clinopyroxenes were found coexisting with

pyrope-almandine (7 diamonds), sulphide (5) and rutile (2) (Table 4.5).

Meyer and McCallum (1986) report on six clinopyroxenes recovered from Sloan diamonds and their major element compositions are listed in Table 4.7. Of these, only samples D and E, which have compositions similar to the eclogitic clinopyroxenes in question, are discussed here. The rest are more akin to the three "possibly primary" clinopyroxenes found in this study which are discussed in Section 4.6.2.

The primary eclogitic clinopyroxenes in Sloan diamonds are enriched in potassium (.10 - 1.4 wt.% K₂O) which is typical of omphacitic clinopyroxenes recovered from diamonds worldwide (Meyer, 1987). Most have Ca/Ca+Mg ratios between .49 and .53 mol.%, although these values range to as low as ~.39 mol.% (Figure 4.26). Those with low Ca/Ca+Mg ratios are depleted in aluminium (Figure 4.27).

It is useful to consider the clinopyroxene compositions with respect to theoretical end-member molecules. In this study, end members (Table 4.8) were calculated and grouped according to the method of Hatton (1978). The Sloan inclusion clinopyroxenes have low calculated proportions of Ca-Tschermaks molecule (<3%), acmite (≤5%) and pseudojadeite (generally <3%, although the highest jadeite sample with 57 mol.% jadeite yielded a calculated pseudo-jadeite content of 7.3 mol.%). The compositional variation of the clinopyroxene inclusions can be defined based on relative proportions of the major end-member molecules: diopside-hedenbergite (Ca(Mg,Fe)Si₂O₆), jadeite (NaAlSi₂O₆) and enstatite-ferrosilite ((Mg,Fe)Si₂O₆). Figure 4.28 shows that the clinopyroxene inclusions have a wide range in jadeite (18-57

mol.%) and that some of those with low jadeite are enriched in enstatite. A broad increase in TiO_2 accompanies the increase in jadeite (Figure 4.29), but no other trends with jadeite are apparent. It is significant that the low jadeite clinopyroxenes, but especially those with high enstatite, are enriched in Mn (Figure 4.30) since, as will be shown, these appear to be associated with the Mn-rich garnets.

Two clinopyroxenes having distinctly different compositions were recovered from diamond 1-15 (Appendix VI - Table B). As already mentioned, these were apparently in direct contact with the same garnet (Figure 4.20). The clinopyroxenes are Mg-rich relative to the other inclusions (Figure 4.26) corresponding to a high enstatite content (Figure 4.28). They are also distinctly enriched in titanium (Figure 4.29) and have relatively high manganese concentrations (Figure 4.30). The inclusion as a whole is essentially an inhomogeneous, bimineralic eclogite and represents a highly unusual case of disequilibrium.

When clinopyroxenes from Sloan diamonds are plotted with those from Sloan eclogite xenoliths, it is found that, like the garnets, they group more precisely with the calcium-depleted, metaluminous xenolith clinopyroxenes (Figure 4.22) and do not appear to be associated with those from peraluminous eclogite xenoliths (Figure 4.23). The potassium enrichment of the inclusion clinopyroxenes is not apparent in xenolithic clinopyroxenes except for those in three peraluminous eclogites (Figure 4.31). The clinopyroxene from diamondiferous xenolith TP 121 (McCandless and Collins, 1989) contains .08 wt.% K_2O and is relatively jadeite-rich, whereas the clinopyroxenes from diamondiferous xenolith 56-8 (this

study) contain .07 wt.% K_2O and occur at the jadeite-poor end of the range (Figure 4.28).

4.5.3 Coesite

The occurrence of coesite, found as colourless inclusions with low-order birefringence, was confirmed in one case (A11) using X-ray diffraction techniques and inferred in two other cases. One of the latter (A22) occurs as a spherical inclusion (18 microns in diameter - Figure 4.21) within the most grossular garnet recovered. The other (A55), also a spherical crystal (diameter 55 μm), coexisted with pure K-feldspar. Its surface was highly fractured, similar to coesites observed in an eclogite xenolith by Smyth (1977) and Smyth and Hatton (1977). This feature probably reflects its physical conversion to a lower pressure polymorph.

The coesites are essentially pure SiO_2 . The coesite included in garnet A22 seemingly has significant iron and calcium (Appendix VI - Table E), but the analysis almost certainly reflects a minor contribution from its garnet host considering the difficulty in analyzing such a small inclusion. The recovery of SiO_2 inclusions from five other diamonds may reflect an important contribution of coesite to the eclogitic paragenesis of Sloan diamonds, although in these cases it is possible that the mineral is not primary.

Although two quartz-bearing eclogites belonging to the metaluminous group are reported from the Schaffer locality, coesite has not been identified (Ater, 1982). However, based on paleotemperatures and assumed paleodepths, Ater et al. (1984) suggest that the quartz eclogites equilibrated in the

coesite stability field and that coesite inverted to quartz during ascent in the kimberlite.

4.5.4 K-Feldspar

Primary K-feldspar occurred as colourless inclusions in two diamonds, SL A29 and SL A55. In the latter, the mineral coexisted with coesite (Table 4.5) and is compositionally pure with no detectable sodium. The K-feldspar in diamond SL A29 has .52 wt.% Na₂O. Although these have not been investigated using X-ray diffraction techniques, the inclusions are probably a higher temperature monoclinic form, either microcline or sanidine, an inference based on the thermobarometric considerations for the eclogitic suite of inclusions in Section 4.5.8. The distinction between microcline and sanidine is based mostly on the distribution of Al and Si atoms among the tetrahedral sites (Deer et al., 1980) which has not been investigated in this study. Meyer and McCallum (1986) also found a feldspar inclusion (.63 wt.% Na₂O) in a Sloan diamond, which they call sanidine, and Prinz et al. (1975) report on a sanidine coexisting with pyrope-almandine and magnetite in a diamond from west Africa.

Ater (1982) and Ater et al. (1984) report the occurrence of "sanidine" in both the peraluminous and metaluminous varieties of Sloan eclogites.

4.5.5 Kyanite

One kyanite inclusion was recovered from diamond SL 24-5. It appeared to be colourless, probably because of its small size (130 microns). As noted for kyanite inclusions recovered

from diamonds elsewhere (see Meyer, 1987), iron (.35 wt.% FeO) is the major impurity.

Kyanite eclogites (by definition "peraluminous") are relatively common at Sloan (Ater, 1982; Ater et al., 1984).

4.5.6 Rutile

Amber to brown rutile is common in Sloan diamonds. It occurs as crystals measuring up to 165 microns in maximum dimension which display rounded, probably cubo-octahedral crystal morphology. It was found coexisting with sulphide (3 diamonds), pyrope-almandine (2) and omphacitic clinopyroxene (2) (Table 4.5), as well as with a diopsidic clinopyroxene in diamond A32 (see Section 4.6.2).

Many of the rutiles contain significant iron (up to 1.0 wt.% FeO) and aluminium (up to 2.5 wt.% Al₂O₃) which in most cases, is inhomogeneously distributed. This is attributed to alteration effected by fluids penetrating into the diamond via fractures which were commonly associated with the rutiles. The fracturing is probably a consequence of differential expansion between the rutile inclusions and their diamond host during depressurization. The rutiles show trace quantities of calcium (\leq .10 wt.% CaO) and chrome (up to .10 wt.% Cr₂O₃). The latter is low compared to chrome in rutile coexisting with garnet, clinopyroxene and coesite in an Ellendale diamond which has (.65 wt.% Cr₂O₃) (Hall and Smith, 1984). The Sloan rutile inclusions are otherwise pure with no niobium or tantalum having been detected.

The rutiles described in State Line eclogites show compositional similarities to the inclusions in diamond with

aluminium and iron being the only important minor constituents (Ater, 1982).

4.5.7 Sulphide

Based on this sampling and the visual inspection of over 22,000 other diamonds (see Section 3.10.2), sulphide is probably the most abundant primary mineral inclusion in Sloan diamonds. Sulphide inclusions invariably occur as opaque crystalline eyes within a network of internal fractures which appear as grey to brown "rosette" petals (Figure 3.28b,c). Sometimes the eye appears white which is a consequence of reflection at the inclusion-diamond interface. The rosette fracturing is apparently a result of differential expansion between the main inclusion and its diamond host. It is not certain what the rosette material actually consists of, although it has previously been assumed that it is finely disseminated sulphide material which invaded the fracture during decompression (Harris and Gurney, 1979b). This has yet to be confirmed, especially for rosetted inclusions containing transparent, silicate eyes.

Sulphide crystals, ranging from 40 to 140 microns in maximum dimension, were recovered from 23 Sloan diamonds. The normally flat-faced crystals exhibit equant to tabular habits (Figure 3.28d) which could sometimes be identified as cubo-octahedral in form. They are usually bronze to yellow in colour with a metallic luster. Sulphide was found coexisting with omphacitic clinopyroxene (6 diamonds), pyrope-almandine (3) and rutile (3) (Table 4.5). It was also recovered along with corundum, but the primary nature of corundum is in question (Section 4.6.4).

The sulphides are predominantly pyrrhotitic in composition, always with minor pentlandite exsolution accounting for the inhomogeneous nickel distribution as indicated from replicate microprobe determinations on single crystals. One inclusion is bimineralic with pyrrhotite coexisting with a copper-rich sulphide (10.0 wt.% Cu). The latter also had a significant cobalt content (0.94 wt.% Co).

For the reasons discussed in Section 4.3, all of the sulphides so far recovered from the Sloan diamonds are thought to belong to the eclogitic paragenesis. This is supported by their chemical composition which is nickel-poor relative to sulphide inclusions of the peridotitic suite (Yefimova et al., 1983).

Sulphide has not been described from either eclogitic or peridotitic xenoliths recovered from the Sloan locality.

4.5.8 Thermobarometry

The best method presently available for calculating equilibration temperatures for eclogitic mineral assemblages is that of Ellis and Green (1979) which takes into account the effect of calcium upon Fe-Mg partitioning between coexisting garnet and clinopyroxene. Pressure cannot be calculated for garnet-clinopyroxene pairs with presently available methods, but previous investigations of eclogitic inclusions in diamond have calculated temperatures assuming 50 kbar, mostly because it is a reasonable pressure with respect to diamond formation. For comparison with other studies, the practice is continued in this study.

The garnet-clinopyroxene pairs found coexisting in Sloan diamonds are plotted together in Figure 4.32. Note that the

tie lines do not cross which is generally taken to indicate an equilibrium assemblage. However, this may not be justified for Sloan eclogitic inclusions especially considering the occurrence of garnet in direct contact with two compositionally distinct clinopyroxenes in diamond SL 1-15. Both Mn-poor and Mn-rich garnets are represented and the two Mn-rich garnets are, interestingly, associated with enstatite-rich clinopyroxenes.

The temperatures, calculated at 50 kbar and assuming all iron is present as Fe^{2+} , are listed in Table 4.6. Except for those derived from diamond SL 1-15, the temperatures are considered to be plausible for a number of reasons. Firstly, the temperatures plot in the diamond stability field at 50 kbar. They also fall within the range defined by similar inclusion pairs found elsewhere (Figure 4.33). Finally, on a plot of Ca in garnet vs $\ln K_d$, and except for those derived from sample 1-15, the temperatures define a field which is similar, although at a lower temperature, to those found at other localities (Figure 4.34).

The large discrepancy between the two temperatures calculated for the two possible garnet-clinopyroxene combinations for the inhomogeneous, bimineralic eclogite inclusion from diamond SL 1-15 (Table 4.6) is not unexpected considering the compositional differences between the two clinopyroxenes. Their deviation from the other eclogitic temperatures might also have been predictable considering the compositional dissimilarities found between the two phases and the rest of their respective minerals from the Sloan diamonds.

The eclogitic inclusion temperatures are significantly higher than those calculated for most of the Sloan eclogite

xenoliths (Ater, 1982) (Figure 4.35); the single exception being the diamondiferous eclogite, TP 121 (McCandless and Collins, 1989), which has essentially the same calculated equilibration temperature as the inclusions.

4.5.9 Paragenesis

Although a number of garnet-clinopyroxene pairs in diamond have previously been reported, more specific information on their paragenesis relative to common eclogitic accessory minerals is lacking. Sobolev (1974; 1984b) attempted the division of eclogitic inclusions into specific groups based partly on accessory phase inclusions in diamond, but mostly on the occurrence of rutile, coesite, corundum and kyanite in eclogite xenoliths, especially the diamondiferous varieties (Table 4.9). The garnets and clinopyroxenes associated with these accessory minerals in diamond and diamond-eclogites reported in the literature are plotted on a Ca-Mg-Fe ternary diagram in Figure 4.36.

Although based on sparse data from diverse localities, each of which will show its own evolutionary signature, general trends are found. Garnets coexisting with rutile, although still showing a wide range in $Mg/(Mg+Fe)$, are distinctly depleted in their grossular content relative to garnets coexisting with kyanite, corundum and coesite. The latter group approaches pure grossular and, in the extreme case, belong to the rare grosspydite paragenesis as identified by Sobolev (1984a). A similar relationship is found in the clinopyroxenes as rutile coexists only with omphacites having relatively low $Ca/(Ca+Mg)$ ratios, whereas coesite, corundum and kyanite occur with omphacites having higher $Ca/(Ca+Mg)$ ratios

(Figure 4.36). A general division is evident, but a more detailed division of eclogitic inclusions must await more data. Sulphide is present throughout the spectrum of eclogitic garnet and clinopyroxene compositions.

The Sloan inclusions conform to these general trends (Figure 4.36). The two garnets, found coexisting with rutile, are relatively low in calcium and the most grossular garnet, A22, has a coesite inclusion (Figure 4.21). The omphacitic clinopyroxenes coexisting with rutile occur in the field defined for diamond and rutile-associated omphacitic clinopyroxenes elsewhere. Rutile presumably stopped crystallizing when the titanium concentration of the system fell below saturation. The generally higher titanium values in the high calcium garnets and clinopyroxenes are presumably a consequence of the increased solubility of titanium in more grossular garnet. Again, it is noted that these trends could be slightly different at each locality.

4.6 OTHER MINERAL INCLUSIONS

This section deals with inclusion minerals which for one reason or another could not be classified with respect to paragenesis and/or be confirmed as primary. The latter includes a number of possibly primary minerals of unknown paragenesis as well as possible contaminants derived during the inclusion recovery process. The composition of secondary inclusion minerals recovered in this study also are considered.

4.6.1 Zircon

Two colourless to pale brown zircon fragments which represent one inclusion were recovered from diamond SL A61. The largest fragment is elongate (70 microns in length) and displays curved crystal faces. Zircon has been described in diamonds from Brazil (Meyer and Svisero, 1975) and Zaire (Mvuemba Ntanda et al., 1982). In those cases, as well as in this study, no other minerals were found coexisting with the zircons and, therefore, its paragenesis remains uncertain.

Zircon is the mineral most frequently used for U-Th-Pb model age determinations. As an inclusion in diamond, it could provide a classic case of a closed system and should give concordant ages assuming the inclusion has sufficient U-Th contents. On this assumption, the zircon was sent to W. Compston for analysis on SHRIMP (Sensitive High Resolution Ion Microprobe), which was designed and built at the Australian National University in Canberra, A.C.T., Australia (Compston et al., 1983). Preliminary work on the Sloan zircon inclusion, (I. Williams, pers. comm., 1989) found relatively homogeneous U and Th concentrations of ~290 and ~19 ppm respectively (Figure 4.37). These levels are much higher than those found in megacryst zircons from kimberlite (Davis, 1977; Kinny et al., 1989) and the Th/U ratio (~.063) is also unusual. The age information from this unique sample is not easily forthcoming and the following is a summary of the problem as provided by I. Williams (op cit.).

The data in Figure 4.37 was produced by scanning the Pb, U and Th isotopes repeatedly at a rate of one scan every three minutes. The plot is for 14 scans on each of three areas, with the rate of sputtering being about 0.1 micron per scan.

As can be seen, U and Th remain relatively constant, but the total Pb concentration varies haphazardly between 25 - 110 ppm on less than a 0.1 micron scale. According to Williams (pers. comm., 1989), possible explanations for this include: variable Pb loss; common Pb addition; radiogenic Pb addition; or some combination of the three.

In considering this problem, Williams (op cit.) first determined whether the Pb isotope composition was constant. This was accomplished by stepping rapidly between the Pb peaks and trying to measure the isotope ratios on a time scale shorter than that of the count rate variation. He found that the Pb isotope composition varied as a function of count rate; the higher the Pb concentration, the higher the $^{207}\text{Pb}/^{206}\text{Pb}$ ratio and the lower the $^{208}\text{Pb}/^{206}\text{Pb}$ ratio. Based on this, Williams (op cit.) rejects recent variable Pb loss. He suggests that it is the high Pb concentration which is intrinsic to the zircon as it is more consistent with the measured Th/U ratio of the sample. The Th/U = 0.063 should give a $^{208}\text{Pb}/^{206}\text{Pb}$ between .02 (at 500 Ma) and .018 (at 2000 Ma), but as the calculated ratio of .015 is closer to the latter value, Williams (op cit.) suggests that the trend towards lower count rates is due to previous Pb loss.

Because of the scan-to-scan fluctuation in the $^{207}\text{Pb}/^{206}\text{Pb}$ ratios, it is not meaningful to simply plot the values on a Concordia diagram, so Williams (op cit.) estimates the best $^{207}\text{Pb}/^{206}\text{Pb}$ for each count rate and then plots these values on a Concordia plot. The result (Figure 4.38) is a diagram in which $^{206}\text{Pb}/^{238}\text{U}$ is completely model independent, but $^{207}\text{Pb}/^{235}\text{U}$ is dependent on the assumed variation in $^{207}\text{Pb}/^{206}\text{Pb}$. Based on this plot, none of the analyzed zircon

has a $^{206}\text{Pb}/^{238}\text{U}$ age of less than 500 Ma and two scans give $^{206}\text{Pb}/^{238}\text{U}$ ages of ~2000 Ma. The great majority of the $^{206}\text{Pb}/^{238}\text{U}$ ages are less than 1000 Ma. The model $^{207}\text{Pb}/^{206}\text{Pb}$ end member of .114 is equivalent to 1865 Ma.

According to Williams (pers. comm., 1989), the zircon is at least 1000 Ma old, and probably 1600 to 1865 Ma old. It has suffered strong and variable Pb loss, probably about 500 Ma ago. He rejects the possibility that the grain is about 500 Ma old, but contains inheritance, because the $^{208}\text{Pb}/^{206}\text{Pb}$ associated with high $^{207}\text{Pb}/^{206}\text{Pb}$ is most consistent with the measured Th/U ratio. Finally, the high $^{207}\text{Pb}/^{206}\text{Pb}$ is not a problem of common Pb contamination because: 1) it is associated with low $^{208}\text{Pb}/^{206}\text{Pb}$ and 2) it is not associated with high ^{204}Pb .

4.6.2 Possibly Primary Clinopyroxene

Three diopsidic clinopyroxenes recovered from Sloan diamonds SL A11, SL A28 and SL A32, which could not be confirmed as primary are discussed in this section.

Clinopyroxene A11 was documented as being associated with fractures and it therefore cannot be confirmed as primary. Although it coexisted with coesite, it is atypical of the eclogitic suite of inclusions found elsewhere being essentially devoid of the jadeite molecule (Figure 4.28) and titanium (Figure 4.29). It is not typical of peridotitic clinopyroxenes either (Figure 4.6). It may have been altered by secondary processes.

Clinopyroxene A28 is diopsidic with typically low aluminium (2.01 wt.% Al_2O_3), low sodium (.27 wt.% Na_2O) and with significant chrome (.42 wt.% Cr_2O_3). However, it is

uncharacteristically enriched in titanium and iron (1.20 wt.% TiO_2 and 7.22 wt.% FeO) and plots out of the field of chrome-rich diopside inclusions found elsewhere (Figure 4.6). It is perhaps best termed a titano-chromian augite and its paragenesis remains uncertain.

Finally, clinopyroxene A32 coexisted with rutile. Like most eclogitic minerals, the diopside is devoid of chrome, but, besides having very low jadeite composition (Figure 4.28), it has only trace amounts of titanium (Figure 4.29) and potassium. For this reason, and because it was not seen before breaking the diamond, it is of questionable origin.

Of the six clinopyroxenes reported by Meyer and McCallum (1986), three (B,C,F) have compositions roughly similar to Sloan clinopyroxene A32 (see Figures 4.27 and 4.28). Meyer and McCallum (1986) document an alteration trend in omphacitic inclusions from one diamond where, as alteration advances, calcium and iron increase at the expense of aluminium and sodium. Although inclusions B, C and F, as well as clinopyroxene A32 in this study, are depleted in iron relative to the omphacitic clinopyroxenes, their high calcium and low aluminium and sodium contents may reflect post-crystallization alteration of omphacites. The acmite inclusion, G (not plotted) coexists with inclusion F and is considered by Meyer and McCallum (1986) to be an alteration product.

4.6.3 Other Possibly Primary Inclusions

Inclusions discussed here include hornblende, ilmenite, magnetite, titano-magnetite, sphene, wollastonite and an unusual Si-Ti-K phase (Appendix VI - Table I). Although compositionally homogeneous, none of these inclusions exhibit

primary morphological characteristics. In most cases, they were documented as being associated with fractures to the diamond surface.

The hornblende is similar to one reported as secondary by Prinz et al. (1975). The ilmenite is magnesium- and chrome-rich like those described from Zairean diamonds (Mvuemba Ntanda et al., 1982), but is compositionally unique relative to the two ilmenites reported from Sloan diamonds by Meyer and McCallum (1986).

Relatively pure magnetite was recovered from Sloan diamond SL 45-6. The sample is pictured in Figure 3.28a. The mineral apparently occurs both as an inclusion as well as on the surface of the diamond. It is not certain if the included mineral was recovered and it cannot therefore be considered primary with certainty. However, Meyer and McCallum (1986) also recovered magnetite and they consider it to be primary. The titano-magnetite was associated with fractures. For this reason, and because it is compositionally unique relative to other worldwide occurrences, it also cannot be considered primary with certainty.

Sphene and wollastonite have not previously been described in diamond. Sphene is present as an accessory phase in one of the Sloan metaluminous eclogite xenoliths described by Ater (1982). The unusual Si-Ti-K mineral has not been identified.

4.6.4 Possible Contaminants

During the course of this study, green moissanite and colourless corundum fragments were found during inclusion recovery. These were initially considered to be primary

inclusions largely because inclusions consistent with being both minerals were seen in at least one diamond each before cracking and recovery. However, in both cases the visual identification was ambiguous.

Two green inclusions were noted in diamond SL A78 from which both chrome-rich diopside and moissanite were recovered. A reappraisal of the recovery notes suggests that two chrome-rich diopside crystals were recovered. Corundum fragments were found along with omphacitic clinopyroxenes in two diamonds. Both minerals can be colourless in diamond and both exhibit birefringence in polarized light. From these considerations it should be evident that it is not a certainty that the moissanite and corundum found during inclusion recovery were in fact present in the diamond.

Both moissanite and corundum are commonly used as abrasives in laboratories worldwide and the discovery of these minerals should always be considered with this in mind. Many reports of "natural" moissanite have been discredited, the SiC apparently resulting from contamination during the rock cutting and slab grinding process in the laboratory (Sobolev, 1979; Milton and Vitaliano, 1984). In this regard, it must be re-emphasized that the moissanite and corundum fragments were recovered and mounted in epoxy before being exposed to possible contaminating abrasives. The possibility of contamination previous to recovery and mounting was not immediately considered.

During diamond cracking, the thumbscrew tips in contact with the diamond (Figure 4.1) become damaged by the diamond. In fact, a number of fragments of this material (steel) were mounted as possible inclusions. According to the microprobe

analyses, these grains could be native iron, but according to other characteristics, especially morphology, they could not be considered primary inclusions. (The occurrence of native iron in Sloan diamonds was reported by Meyer and McCallum (1986)). Because of the damage, the cracker tips were periodically ground flat using one of the various grinding wheels in the departmental workshop. Before re-use, these were cleaned using ultrasonic agitation. As a check, material from these grinders was recovered and analyzed for major elements using the electron microprobe. Both moissanite (green and blue grains) and colourless corundum were identified. Both the grinder moissanite and the alleged inclusion moissanite were pure SiC. The grinder corundum composition is listed along with the alleged corundum inclusion compositions in Table 4.10. The similarity is evident.

Even with ultrasonic cleaning, it is possible that some of the grinder material would still be embedded in the cracker tips and, upon diamond cracking (an often jarring process), could have been dislodged and have fallen along with the diamond and inclusion material onto the glass slide. Based on this unhappy scenario, moissanite and corundum cannot, with confidence, be considered primary inclusions in the Sloan diamonds.

Finally, it is noted that moissanite has not been found in either xenoliths or heavy mineral concentrate from the Sloan locality. Corundum, which was colourless in thin section, was present in two eclogite xenoliths from the Schaffer kimberlite occurrence (Ater, 1982). The latter did not contain titanium or chrome.

4.6.5 Secondary Inclusions

The major secondary minerals recovered from Sloan diamonds are listed in Table 4.3. Their identification is based mostly on composition since no other work has been done on them. In most cases they probably result from alteration of primary inclusions (see Figure 3.27). Many other polyphase inclusions were also recovered. These are highly inhomogeneous, hydrated minerals which could not be identified with confidence based on microprobe analysis. Future work might consider alteration paths by noting which phases occur with which primary phases, as Meyer and McCallum (1986) have done with clinopyroxenes from Sloan diamonds.

4.7 RELATIONSHIPS

Differences in both primary and secondary physical characteristics are found between peridotitic and eclogitic diamonds.

The most convincing relationship seen in this small sample of inclusion-bearing diamonds is between diamond mass and inclusion paragenesis. The relationship is more properly exhibited for primary mass (whole crystals only) (Figure 4.39), but is also evident with respect to secondary mass which includes broken crystals (Figure 4.40). As can be seen, even before resorption, all of the peridotitic diamonds weighed less than .02 carat, whereas the eclogitic diamonds include many stones heavier than .02 carat and ranging up to .47 carat in primary mass.

Also found is a relationship between paragenesis and primary morphology. A greater proportion of the peridotitic

diamonds are twinned crystals whereas the eclogitic diamonds are mostly single crystal octahedra (Table 4.11). Diamond colour does not appear to vary significantly with paragenesis (Table 4.12).

Finally, a relationship between paragenesis and resorption morphology (Figure 4.41) was found. The relationship can also be considered with respect to percentage preservation (Table 4.13). The smaller, peridotitic diamonds are apparently better preserved relative to the eclogitic diamonds. A similar relationship was found for peridotitic and eclogitic diamonds from Argyle (Jaques et al., 1989).

4.8 DISCUSSION

At least two primary subpopulations of diamond, defined by their eclogitic and peridotitic inclusions, are present in the Sloan kimberlites. These minerals have unique compositional, thermobarometric and paragenetic qualities when compared to those from other worldwide localities. The two diamond types are further distinguished based on morphology and mass. The smaller peridotitic diamonds comprise the larger proportion of twin/aggregate crystals in the sample whereas the eclogitic diamonds, which include all of the larger stones, grew mostly as single crystal octahedra. These are interpreted as primary traits related to physico-chemical differences in the two diamond growth environments. As suggested in Section 3.12, the observed size variation could be related to growth rate and/or the duration of the growth event. Either the peridotitic diamonds grew more slowly or they grew over a shorter span of time (or both) relative to

the eclogitic diamonds. The high proportion of macles and aggregates in the peridotitic subpopulation is possibly related to increased nucleation density. As shown for the synthetic system by Wakatsuki (1984), this parameter increases with pressure and, according to inclusion thermobarometry, the peridotitic diamonds apparently crystallized at significantly higher pressures than did the eclogitic diamonds.

Crystals from both paragenetic subpopulations exhibit non-uniform resorption and/or xenolithic surface features (Section 3.9.1) which suggests that diamonds of both parageneses were derived from disaggregated xenoliths. This is consistent with the discoveries in the State Line kimberlite district of a diamond peridotite (McCallum and Egger, 1976) and a diamond-graphite eclogite (Collins, 1982), as well as the three diamondiferous "eclogites" reported in this study (Figures 3.4 - 3.6). The better preservation of the smaller, peridotitic diamonds relative to the eclogitic diamonds is unexpected since smaller diamonds should become more resorbed for similar times of resorption. The observation is obviously a consequence of reduced exposure to the resorption medium. This could be a consequence of protection within a xenolith during the resorption event. Diamonds exhibiting no resorption must have been totally shielded or, alternatively, have crystallized after the resorption event ceased as suggested for some diamonds by Haggerty (1986). At Sloan, unresorbed, sharp-edged, smooth-faced crystals occur in both paragenetic subpopulations although they are more abundant in the smaller peridotitic diamonds. It, therefore, seems likely that at Sloan such unresorbed morphologies are due to more efficient shielding

within a xenolith during resorption. Further, it would appear that peridotitic host rocks are more efficient protectors of diamond than the eclogitic host rocks. This is possibly because the peridotitic xenoliths were less susceptible to disaggregation and only fell apart later during the resorption event. Alternatively, the smaller peridotitic diamonds may more commonly be locked inside minerals rather than along grain boundaries and therefore not be subject to immediate attack after xenolith disaggregation.

The peridotitic diamonds appear to be of a deeper origin than those reported from most other localities. The occurrence of calcium-enriched orthopyroxenes is consistent with higher temperatures and the high potassium content of the chrome-rich diopside may indicate a high pressure origin as suggested for chrome-rich diopsides from Koffiefontein (Rickard et al., 1989). Ferro-periclase, which indicates a reducing environment of diamond growth, may also indicate higher pressures (Scott Smith et al., 1984).

Models concerned with the genesis of peridotitic diamonds (Harte et al., 1980; Boyd and Finnerty, 1980; Richardson et al., 1984; Schulze, 1986) are concerned only with mineral inclusions of the dunitic-harzburgitic paragenesis because of their predominance in diamonds studied worldwide. The relationship between harzburgitic minerals and those of lherzolitic affinity is not well constrained. The occurrence of two compositionally distinct peridotitic inclusion populations at Premier (Gurney et al., 1986) suggests that the more calcic peridotitic inclusions (ie. lherzolitic minerals) at that locality may be unrelated to those of the dunitic-harzburgitic suite. Recent trace element and isotopic work on

lherzolitic diopsides from Premier (Richardson, 1989) and Finsch (Smith et al., 1989b) support this inference. Both reports suggest that lherzolitic diamonds may represent a more recent peridotitic diamond crystallization event relative to diamonds of dunitic-harzburgitic affinity.

The similarity between mineral compositions of peridotitic inclusions in Sloan diamonds and the minerals from "infertile" garnet peridotites is intriguing. These rocks are believed to be residua of a major Archaean (?) melting event involving the entire lithosphere (Eggler et al., 1987), although the age is not well constrained.

Eclogitic xenoliths found in kimberlite have been divided into two groups based on textural evidence (MacGregor and Carter, 1970). McCandless and Gurney (1989) demonstrated that a chemical classification based on sodium in garnet and potassium in clinopyroxene agrees with the textural split in more than 90% of the cases. Eclogites having garnets with $>.09$ wt.% Na_2O and clinopyroxene with $>.08$ wt.% K_2O are Group I eclogites, whereas those with minerals having lower values are Group II eclogites. On this basis, both groups of eclogitic garnets and clinopyroxenes in Sloan diamonds are Group I minerals as is found for inclusions worldwide.

The relationship between eclogitic minerals in Sloan diamonds and Sloan eclogitic xenolith minerals is of interest. Rutile, quartz, sanidine and kyanite, in addition to sphene and corundum, are found as accessory minerals in Sloan eclogite xenoliths (Ater et al., 1984), but Na-rich garnets and K-rich clinopyroxenes are rare. Although six of the Sloan eclogites studied by Ater (1982) and Ater et al. (1984), including a graphite eclogite and a grospydite, have garnets

with significant sodium contents, their coexisting clinopyroxenes are devoid of potassium. This may be a result of decompression melting. However, those eclogites having clinopyroxenes with significant potassium do not have Na-rich garnets. Ater et al. (1984) do not consider any of the Sloan eclogites they studied to be Group I rocks.

Only the diamondiferous eclogite (TP 121) recovered from Sloan (Collins, 1982), which has significant sodium in its garnets as well as significant potassium in its clinopyroxenes (McCandless and Collins, 1989), can unambiguously be considered a Group I eclogite. Based on thermometric data (Figure 4.35), the diamondiferous eclogite and eclogitic inclusions from Sloan diamonds appear to be associated. The three diamondiferous xenoliths found in this study probably also belong to this association.

It is pertinent at this point to mention the disparity in abundance between the two eclogite groups at Sloan. The Group I eclogites may simply disaggregate more easily relative to the non-Group I eclogites. Alternatively, the phenomenon may simply be reflecting the ratio of Group I to Group II material at depth. In the latter case, all eclogites are subject to disaggregation and there is no need to have a special mechanism by which Group I eclogites would more easily fall apart.

The eclogitic inclusions in Sloan diamonds occur in two compositional groups. Based on coexisting minerals, the Mn-poor garnets appear to be associated with jadeite-rich omphacites, whereas enstatite-rich clinopyroxenes are associated with Mn-rich garnets (Figure 4.32). Similar Mn-rich and Mn-poor eclogitic garnets groups are present at

Finsch (Gurney et al., 1979; Smith et al., 1989b) and based on trace element and isotope analyses, Smith et al. (1989b) suggest that the two groups represent distinct crystallization events. The Sloan eclogitic inclusions, therefore, may represent two eclogitic diamond crystallization environments sampled by the Sloan kimberlite.

Based on garnet compositions (Figures 4.22 & 4.23), the diamondiferous xenoliths appear to be associated with Mn-rich inclusions. However, the clinopyroxene from one of the two diamondiferous xenoliths is significantly enriched in the jadeite molecule (Figure 4.28) similar to the clinopyroxene inclusions associated with Mn-poor garnets and this suggests that both eclogitic groups are derived from disaggregated xenoliths.

According to Sunagawa (1984), natural diamonds do not appear to have formed in metamorphic events and igneous processes have been proposed on the basis of major element inter-relationships elsewhere (see, for instance, Gurney et al., 1984a). Hatton (1978) suggested that the Group I eclogites from Roberts Victor represent cumulates which formed as a result of crystal fractionation in a magma chamber. The broad increase in titanium with decreasing $Mg/(Mg+Fe)$ for Mn-poor eclogitic garnets from Sloan diamonds (Figure 4.18) and the increase of titanium with increasing jadeite in the associated jadeite-rich clinopyroxene (Figure 4.29) may reflect igneous crystallization. Hatton (1978) argues that such broad trends may result from crystallization in a long-lived magma chamber which is periodically injected with fresh pulses of melt. It may be significant that the Mn-rich

garnets and associated enstatite-rich clinopyroxenes do not exhibit such broad trends.

Disequilibrium assemblages occur in association with both Mn-poor and Mn-rich garnets in diamonds SL A46 and SL 1-15, respectively. As already mentioned, the more magnesian garnet from diamond SL A46 is titanium and sodium enriched relative to its counterpart and, therefore, cannot be explained chemically by the successive entrapment of material in a closed-system, evolving magma. This casts doubt on the igneous interpretation. The occurrence of an inhomogeneous eclogite in diamond SL 1-15 implies relatively rapid quenching below the blocking temperature. This might occur if the diamond is injected into shallower regions of the lithosphere, before complete equilibration between the various phases was achieved.

The origin of diamondiferous Type I eclogite is a matter of debate. Most models of eclogite formation call for either the partial melting of a garnet lherzolite substrate (and subsequent high pressure crystallization of that melt), or invoke the partial melting or recrystallization of a subducted oceanic megacryst.

Kushiro and Yoder (1974) suggested that, if diamond eclogite is produced by the melting of garnet lherzolite, then the melting must occur in the presence of H₂O. However, the possibility of producing eclogite, at the temperatures and pressures where diamond is the stable phase of carbon, has yet to be proven experimentally. According to J.J. Gurney (pers. comm., 1989), most investigators involved with such experimental work do not believe that it would be possible to produce Type I eclogite by the melting of garnet lherzolite,

even in the presence of volatiles. However, until this view is backed up with experimental work, which takes into account the presence of not only H₂O, but also other volatile phases (carbon-bearing species, nitrogen-bearing species, alkalies), the possibility of at least some diamond associated eclogite having been produced by the melting of garnet lherzolite cannot be discounted. The presence of coesite as inclusions in diamond is at least consistent with such a process, since melting in H₂O drives the melt towards more silica-rich compositions (Kushiro et al., 1968). The further occurrence of Na-rich garnets, K-rich clinopyroxenes and K-feldspar in diamond suggests that alkalies may also be important as a volatile phase in the possible melting process (Wohletz and Smyth, 1984).

Jagoutz et al. (1984) have argued that Group I eclogites can form from subducted oceanic lithosphere. Hatton and Gurney (1987) argue that the Group I and II eclogites at Roberts Victor may have formed in a single event related to subduction. Smith et al. (1989) suggest, based on Nd and Sr isotopic systematics, that the anomalously Mn-rich garnet inclusions in Finsch diamonds may represent subducted, hydrothermally altered basalts. It is possible that the eclogitic diamonds at Sloan (especially those with Mn-rich garnets) crystallized from a Group I eclogite magma derived from the melting of a subducted oceanic megacryst.

It is not possible, based on the evidence discussed so far, to give preference to a subduction model over the volatile-induced melting of a garnet lherzolite for the production of a Group I eclogite magma. Both might occur and both models leave some questions unanswered. Carbon isotope

determinations (Chapter 5) on Sloan diamonds may prove to support one or the other.

The timing of eclogitic diamond formation at Sloan is not known, but it may be reflected by the inferred age of the zircon inclusion. This is arguable since the paragenesis of the zircon is not known. As discussed in Section 4.6.1, the zircon is likely to be younger than 1865 Ma. This is significantly younger than the inferred Archaean age for peridotitic diamonds in this study and no other paragenetic diamond sub-populations are so far recognized at Sloan. The inferred eclogitic age is reasonable since similar model ages for eclogitic inclusions in diamonds from other localities have been found (Table 4.1). On this basis, the eclogitic diamonds at Sloan are considered to be xenocrysts in the Devonian age kimberlite and their origin may be linked to processes related to continental accretion during the Proterozoic (Karlstrom and Houston, 1984).

5. CARBON ISOTOPE COMPOSITION OF SLOAN DIAMONDS

5.1 OVERVIEW

5.1.1 Terminology

This section summarizes the terminology used in stable isotope geochemistry as described in more detail by Friedman and O'Neil (1977) and O'Neil (1986), but here with emphasis on carbon isotopes.

Stable isotope geochemistry is the study of variations in isotope ratios of elements (especially the light elements H, C, N, O and S) in substances of geological interest. Isotope ratio mass spectrometers allow determination of the difference in isotope ratios between a sample and a standard. This difference is reported as a δ value which for a sample (x) and a standard (s) is defined as

$$\delta_X = \left[\frac{R_X - R_S}{R_S} \right] \times 1000 = \left[\frac{R_X}{R_S} - 1 \right] \times 1000$$

where, by convention, R is the ratio of the heavy (rare) isotope to the light (common) isotope. For carbon, $R = {}^{13}\text{C}/{}^{12}\text{C}$ and δ (written as $\delta^{13}\text{C}$ in this study) is usually calculated relative to the Peedee belemnite (PDB) standard. The $\delta^{13}\text{C}$ value, therefore, is the difference in ${}^{13}\text{C}/{}^{12}\text{C}$ between the sample and PDB expressed as parts per thousand or per mil (‰). A sample having a positive $\delta^{13}\text{C}$ value is enriched in

^{13}C relative to PDB whereas a negative $\delta^{13}\text{C}$ value indicates that the sample is depleted in ^{13}C relative to PDB.

Variations in isotope ratios can arise from kinetic and/or equilibrium isotope effects. Kinetic isotope effects are most significant in fast, incomplete or unidirectional processes such as evaporation, diffusion and disassociation. In such "disequilibrium" processes, fractionation between the heavy and light isotopes occurs because of their mass differences and it is the light isotope which first evaporates, diffuses or disassociates leaving the residue enriched in the heavy isotope. As the reaction stabilizes, the magnitude of the kinetic fractionation reduces to the value of equilibrium fractionation.

Equilibrium isotope fractionation occurs between two species, (A) and (B), coexisting in equilibrium where the heavy and light isotopes are exchanged disproportionately due to differences in binding energy. Such equilibrium effects are defined by the fractionation factor $\alpha = R_A/R_B$, a value which is determined by calculation, by experiment or inferred from measurements on natural samples.

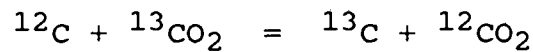
A more convenient way to express α is through the function $1000\ln\alpha$ which is the per mil fractionation between two species (A) and (B). This value is closely approximated by the Δ value where

$$\Delta_{A-B} = \delta_A - \delta_B \approx 1000\ln\alpha_{A-B}$$

These approximations of the fractionation factor are identical within the limits of analytical error for Δ 's and δ 's less

than about 10 and will be used interchangeably in this discussion.

Equilibrium isotope effects can be described according to an exchange reaction such as the one for diamond in equilibrium with carbon dioxide:



The equilibrium constant, K , for this theoretical reaction is related to α as follows:

$$K = \frac{(C^{13})(C^{12}\text{O}_2)}{(C^{12})(C^{13}\text{O}_2)} = \frac{C^{13}/C^{12}}{C^{13}\text{O}_2/C^{12}\text{O}_2} = \frac{R_C}{R_{\text{CO}_2}} \approx \alpha \text{ C-CO}_2$$

The temperature dependence of K (and therefore α) is the basis of stable isotope thermometry and fractionation curves are generated by plotting the variation of the fractionation factor with temperature. Figure 5.1 depicts fractionation curves for diamond and the various carbon-bearing species expected in the mantle from which diamond may have grown. The first named phase (i.e. diamond in this study) concentrates the heavy isotope if $1000\ln\alpha$ is positive and the light isotope if $1000\ln\alpha$ is negative. Note that except for diamond-CO₂, the fractionation factors between carbon-bearing species have not been determined for temperatures expected for diamond growth in the mantle. Note also that, although expected to be negligible, the pressure effect on α also is not known for pressures expected in the mantle.

5.1.2 Previous Work

The distribution of $\delta^{13}\text{C}$ values for diamonds from worldwide sources is shown in Figure 5.2. Most diamonds have $\delta^{13}\text{C}$ values within the range -2 to -9 ‰ (vs. PDB), with a major peak between -5 and -7 ‰, which corresponds to ranges found for other "mantle" samples including CO_2 in oceanic basalts (-1 to -9 ‰; Pineau and Javoy, 1983; Des Marais and Moore, 1984), carbonatites (-1 to -9 ‰; Deines and Gold, 1973; Pineau et al., 1973) and kimberlitic carbonates (-1 to -11 ‰; Deines and Gold, 1973; Kobelski et al., 1979; Kirkley, 1987). This range of $\delta^{13}\text{C}$ values and the average value of approximately -6 ‰ is considered by most workers to represent that of carbon in the primordial mantle.

A significant proportion of diamonds have $\delta^{13}\text{C}$ values well outside of the "primordial mantle" range (Figure 5.2) and, overall, diamonds exhibit nearly a 40 ‰ range of $\delta^{13}\text{C}$ values. The reasons for this large range are still a matter of debate. Discussion on this question has centred on the nature and the origin of the source carbon as well as on the possible mechanisms of diamond growth.

There are three basic scenarios put forth to explain this large range of $\delta^{13}\text{C}$ values. Either diamonds crystallized from primordial carbon that was indeed homogeneous having a $\delta^{13}\text{C}$ composition of approximately -6 ‰ (Javoy et al., 1986), or they crystallized from primordial carbon which was heterogeneous having a range of $\delta^{13}\text{C}$ values possibly approaching that observed for diamonds (Deines, 1980; Deines et al., 1986) or they were formed from recycled carbon likely of heterogeneous isotope composition (Koval'skiy and Cherskiy, 1972; Javoy et al., 1986). If diamonds formed from a

homogeneous source carbon, the mechanisms of diamond growth must be considered as a way of producing such a large range of $\delta^{13}\text{C}$ values.

Deines (1980) evaluated various models of diamond formation in an effort to account for the large range of $\delta^{13}\text{C}$ values observed. He noted that equilibrium fractionation factors for diamond-solid (i.e. diamond crystallization from graphite or carbonate) and diamond-melt (i.e. diamond crystallization from carbon in solution) were expected to be low at mantle temperatures and that only diamond precipitation from a vapour could produce a significant range in $\delta^{13}\text{C}$. However, the largest range he could produce from a relatively homogeneous vapour source was on the order of 15 ‰ which required diamond precipitation from CO_2 where most (i.e. ~100%) of the carbon in CO_2 is converted to diamond in a Rayleigh fractionation process. He further noted that, even if this could be achieved, diamond crystallization from CO_2 undergoing fractionation would produce a diamond population having a positively skewed distribution of $\delta^{13}\text{C}$ values and not the negatively skewed distribution observed. Although diamond crystallization from a CH_4 vapour would produce a negatively skewed distribution, the maximum range of $\delta^{13}\text{C}$ values possible is on the order of 5 ‰. From this, Deines (1980, p.943) concludes that "in all probability, carbon isotope effects (i.e. fractionation) in the diamond formation process were small and the very large range in $\delta^{13}\text{C}$ observed was probably inherited from source carbon." Based on a similarly large range of $\delta^{13}\text{C}$ values found in meteorites (Deines and Wickman, 1973), Deines (1980) suggests that the wide range in $\delta^{13}\text{C}$

values found for diamond may reflect inhomogeneities in primordial carbon.

An alternative hypothesis, propounded by Javoy et al. (1986), suggests that it would be possible to produce the full range of $\delta^{13}\text{C}$ values observed in a "global Rayleigh distillation (i.e. fractionation) process" from a relatively homogeneous CO_2 source ($\delta^{13}\text{C} = -6 \text{ ‰}$?). In their scenario, the fractionation of 4-5 ‰ (at 1000°C) between CO_2 and diamond (or CO_2 and C dissolved in the melt) could give rise, by precipitation of diamond (or by outgassing of the melt), to very large enrichments (or depletions) in the residual system. They suggest that the peaks in the worldwide diamond distribution record preferred stages of the distillation process and that the total range observed could have been produced in three or four stages. According to the modelling of Deines (1980), a set of very special circumstances would have to prevail to achieve this. Javoy et al. (1986) suggest that such circumstances may occur in the kimberlite magma.

The occurrence of individual diamonds which are internally inhomogeneous with respect to carbon isotope composition has been reported. Javoy et al. (1984) document a range of 5.8 ‰ within a small, single crystal diamond from Mbuji Mayi, Zaire. Significant variation has also been found in coated stones from Zaire (Swart et al., 1983; Boyd et al., 1987) and from Siberia (Galimov, 1984). The data of Swart et al. (1983) suggest that the cores of their diamond samples are isotopically light relative to the fibrous coats. They suggest that this relatively small variation could be a result of fractionation in a CO_2 - diamond system. Boyd et al. (1987) found that the cores of such stones can be both ^{13}C

enriched and depleted relative to the coats. They also found significantly more variation in $\delta^{13}\text{C}$ in the cores than in the coats and suggested that the core and the coat grew in different mantle environments. They suggest that inhomogeneities in the octahedral core could have resulted from fractionation during multiple growth and dissolution events during residence in the mantle. 2

Many workers (Javoy et al., 1986; Pearson et al., 1989; Kirkley and Gurney, 1989) have suggested that much of the worldwide variation in $\delta^{13}\text{C}$ can be attributed to diamond crystallization from crustal carbon reintroduced to the mantle environs via subduction.

It is now known that at least two diamond parageneses, peridotitic and eclogitic, which are believed to represent distinct crystallization environments and possibly distinct carbon sources, are present in the earth's upper mantle. Sobolev et al. (1979) noted that although both peridotitic and eclogitic diamonds have $\delta^{13}\text{C}$ values predominantly within the -2 to -9 ‰ range, only eclogitic diamonds appeared to fall outside the range. More recent investigations, notably those of Deines and co-workers (1984; 1986; 1987) on large parcels of diamonds from single localities, have confirmed that, except for a few deviant peridotitic diamonds, most of the $\delta^{13}\text{C}$ values outside of the "mantle" range, as determined on diamonds of known paragenesis, are indeed from eclogitic diamonds (Figure 5.3).

The studies of Deines et al. (1984; 1987) have been successful in delineating subgroups within the main paragenetic types (Figure 5.4). The peridotitic diamonds at Premier and the eclogitic diamonds at Roberts Victor both

display marked bimodal distributions with respect to $\delta^{13}\text{C}$ values and these correlate well with compositional differences between their associated mineral inclusions. The range of $\delta^{13}\text{C}$ values found within paragenetic subpopulations at single localities is relatively small (2-5 $^{\circ}$ / $_{\text{OO}}$) and, according to the modelling of Deines (1980), could have been produced by Rayleigh fractionation of single, relatively homogeneous carbon sources. They may alternatively reflect a slightly inhomogeneous source carbon reservoir.

As such, carbon isotopes have added a new dimension to our understanding of compositional variations in the diamond growth environments and it is obvious that defining the primary subpopulations at individual localities with respect to both inclusion paragenesis and carbon isotope composition is vital to our understanding of diamond genesis. Here, fragments from most of the Selected sample diamonds have been analyzed for carbon isotope composition. Relationships between these data, the physical characteristics of the diamonds as well as their included mineral parageneses and compositions are discussed. The resulting observations allow further discussion on the origins of the Sloan diamonds.

5.2 METHODS

Diamond fragments weighing between .02 and 5.5 mg were picked from the crush remaining from inclusion recovery. For most samples, two or more fragments were picked for replicate analyses as a preliminary check on within-diamond homogeneity. An effort was made to select both surface and internal fragments on the assumption that this would show the maximum

amount of inhomogeneity if present. Surface fragments were defined as those that exhibited either growth or resorption surface textures, whereas those identified as internal fragments did not. It is noted that this is not an ideal procedure since fragments, identified as surface fragments, may contain substantial amounts of internal diamond and those defined as internal may be near surface fragments.

The diamond "inclusion" (SL 30-1I) in diamond SL 30-1H (Figure 3.25g,h) was recovered and fragments of both the inclusion and the host were analyzed. For this sample, a surficial fragment was picked from the host on the assumption that it would have grown subsequent to any fragments chosen from the inclusion diamond. Finally, surface fragments, which appeared to be intergrown with graphite, were recovered from two of the xenolithic diamonds (SL 56-7 and SL 56-8) for analysis.

The diamond fragments were cleaned in HCl overnight, rinsed in distilled H₂O, checked for any visible impurities, dried overnight at 100 °C and, finally, weighed to the nearest .001 mg. The diamond fragments were combusted in purified oxygen following procedures similar to those described by Deines and Wickman (1973). Measured yields usually agreed within $\pm 2\%$ of the calculated yield. The CO₂ produced was analyzed using a VG Micromass 602E mass spectrometer. Results are reported as $\delta^{13}\text{C}$ (relative to PDB) with a maximum 2σ error (95% confidence limits) of approximately 0.3 ‰ as determined from replicate analyses of an in-house graphite standard. This error, therefore, accounts for mass spectrometer precision as well as possible system errors derived during CO₂ production and sample handling.

5.3 RESULTS

The results of carbon isotope determinations on the Sloan diamonds are tabulated in Appendix VII. Listed are $\delta^{13}\text{C}$ values for all fragments analyzed from each diamond, the average $\delta^{13}\text{C}$ value for each diamond and the per mil range of $\delta^{13}\text{C}$ values found within each diamond. Where both surface and internal fragments were identified, the fragment which was depleted in ^{13}C is recorded.

A large range of average $\delta^{13}\text{C}$ values, between -3.8 to -29.4 ‰, was obtained (Figure 5.5). This range nearly spans that of diamonds analyzed worldwide and, to this author's knowledge, is the largest range found to date for diamonds from a single kimberlite locality (Figure 5.6). Only diamonds analyzed from the Orapa kimberlite in Botswana (Deines et al., 1986; McCandless et al., 1989) have a range of values (-3 to -26 ‰) approaching that found in this study.

In the histogram (Figure 5.5), three major modes occur at -4, -9 and -21 ‰ and minor peaks, which may not be significant, occur at -13, -17.5, -26 and -28 ‰. Three groups are defined around the major modes (Figure 5.7). Group I is comprised of 16 diamonds having average $\delta^{13}\text{C}$ values between -3.8 and -5.9 ‰. For immediate discussion, Groups II and III are arbitrarily divided at -13 ‰. On this basis, Group II is comprised of approximately 20 diamonds with $\delta^{13}\text{C}$ values from -8.5 to -13 ‰ and Group III is comprised of over 50 diamonds with average $\delta^{13}\text{C}$ values from -13 to -29.4 ‰. In Figure 5.8, each block in the histogram is keyed to an individual diamond for reference in the ensuing discussion.

Significant variation in $\delta^{13}\text{C}$ was documented within some diamonds (Appendix VII). In Figure 5.9, the within-diamond range of $\delta^{13}\text{C}$ values as determined on two or more fragments from individual diamonds, is plotted as a vertical bar at the average $\delta^{13}\text{C}$ value of that sample on the horizontal axis. Note that the length of each bar may not represent the maximum range of carbon isotopic variation within each diamond as it is not known whether fragments representing the extreme values of $\delta^{13}\text{C}$ within each diamond were sampled. Even so, the amount of $\delta^{13}\text{C}$ variation documented within a number of the diamonds is much more than might be expected for single crystals in the size range studied (mostly < .06 carat). Similar variation has been documented within coated diamonds (Swart et al., 1983; Galimov, 1984; Boyd et al., 1987) and also within single crystal octahedra (Javoy et al., 1984). It is emphasized here that the diamonds in this study were single crystal octahedra or simple twins with no fibrous growth rims or any other obvious evidence for multistage growth histories.

The diamonds in Group I and Group II are relatively homogeneous (Figure 5.9). Only the diamonds in Group III show significant within-diamond heterogeneity. The largest within-diamond variation (4.2 ‰) occurs in sample SL-19 which also has the lowest average $\delta^{13}\text{C}$ value (-29.4 ‰). Note that this actually extends the range of $\delta^{13}\text{C}$ values found for Sloan diamonds in this study to -31.4 ‰.

In only three of the Group III diamonds, where both internal and external fragments were distinguished, did the difference in $\delta^{13}\text{C}$ exceed the 2σ error (Appendix VII). In two cases, diamonds SL A62 and SL A73, the internal fragment was isotopically light relative to the external fragment, but the

opposite was found for diamond SL A46. The diamond "inclusion" (SL 30-1I) hosted by diamond SL 30-1H (Figure 3.25g,h) was slightly ^{13}C poor relative to the host but the difference does not exceed 2σ (Appendix VII). No systematic zonation in carbon isotope composition within Sloan diamonds is apparent based on this sampling of internal and external fragments.

Not included on the plots are the $\delta^{13}\text{C}$ values found for the two xenolithic diamond surface fragments. Diamond SL 56-7, which occurred with pyrope-almandine, has a $\delta^{13}\text{C}$ value of -12.8 ‰, whereas diamond SL 56-8, which occurred with clinopyroxene, yielded a $\delta^{13}\text{C}$ value of -10.6 ‰.

5.4 RELATIONSHIPS

Relationships between the carbon isotope composition and other characteristics of the Sloan diamonds are discussed with respect to Groups I, II and III as defined in the previous section. Both between-group and within-group relationships are considered.

Differences in diamond morphology and mass are found between the three groups. The diamonds comprising Group I are predominantly twinned or aggregate crystals, whereas those in both Groups II and III are predominantly single crystal octahedra (Figure 5.10). When considered with respect to mass, the largest diamonds in the sample occur in Group II. With respect to secondary mass (Figure 5.11 and 5.12a), the diamonds in Group I do not exceed .02 carat and those in Group III do not exceed .07 carat. However, the diamonds in Group II commonly exceed .07 carat, with seven exceeding .10 carat

and ranging up to .35 carat in mass. The relationship does not change when considered with respect to primary mass (Figure 5.12b). Within Groups I, II or III there is no systematic variation of mass with $\delta^{13}\text{C}$ (Figure 5.12).

When the carbon isotope composition of each diamond is compared to mineral inclusion paragenesis (Figure 5.13), it is found that Group I is comprised entirely of peridotitic diamonds whereas most of the diamonds in Groups II and III are of eclogitic affinity. Two important exceptions are olivine-bearing diamonds, SL 11 and SL A57, having $\delta^{13}\text{C}$ values of -20.6 and -21.9 ‰ respectively (Figure 5.14). The occurrence of peridotitic inclusions in isotopically light hosts is rare, having only been reported previously for diamonds from Orapa (Deines et al., 1986) and, in one ambiguous case, at Premier (Deines et al., 1984). As discussed in Chapter 4, the olivine in diamond SL A57 coexisted with an eclogitic garnet ($\text{Mg}/\text{Mg}+\text{Fe} = .46$) and was considered an unusual case of mixed paragenesis in a single diamond. Both of the olivines in Group III diamonds are chrome-poor (below detection limit of .04 wt.% Cr_2O_3) and slightly magnesium-rich (Fo 92.7 and Fo 92.2) relative to those occurring in Group I which have significant chrome (.08-.14 wt.% Cr_2O_3) and forsterite values ranging from Fo 91.3 to 92.2.

The occurrence of clinopyroxene inclusions in the diamonds of each group are shown in Figure 5.15. Only one clinopyroxene was recovered from the peridotitic Group I diamonds and its composition is discussed in Section 4.4.4.

The omphacitic clinopyroxenes recovered from Group II diamonds are compositionally distinct relative to those found

in Group III diamonds. Those in Group II diamonds have a large range of Ca/Ca+Mg values (Figure 5.16) reflecting an enrichment in the enstatite component (Figure 5.17). They otherwise have a restricted range in jadeite content (Figure 5.17). The clinopyroxenes in Group III, on the other hand, are enriched in jadeite, but have a restricted range in Ca/Ca+Mg values (Figure 5.16) and a restricted range in the enstatite component (Figure 5.17). There is no systematic variation in clinopyroxene inclusion composition with host $\delta^{13}\text{C}$ within either Groups II or III. It may be significant that the clinopyroxene inclusions occurring in diamonds A28, A11 and A32, which were difficult to classify as to paragenesis (see Section 4.6.2), all occur in Group III diamonds (Figure 5.15). The clinopyroxene associated with xenolithic diamond SL 56-8 ($\delta^{13}\text{C} = -10.6 \text{ ‰}$) is jadeite-poor similar to the clinopyroxenes included in Group II diamonds.

The occurrence of garnet inclusions in the diamonds of each group are shown in Figure 5.18. Cr-rich pyropes were recovered from two Group I diamonds and their compositional characteristics are discussed in Section 4.4.3. It is noted that the two garnet-bearing peridotitic diamonds are ^{13}C depleted relative to the rest of the Group I diamonds.

Eclogitic garnets were recovered from 27 Group III diamonds whereas the mineral was recovered from only two of the diamonds in Group II (Figure 5.18). The two garnets occurring in Group II diamonds belong to the Mn-rich garnet group defined in Section 4.5.1 (Figure 5.19), but are distinctly Mg-rich relative to the six Mn-rich garnets from Group III diamonds (Figure 5.20). The latter and all of the Mn-poor garnets occur in Group III diamonds and both garnet

types span the Group III range of $\delta^{13}\text{C}$ values (Figure 5.18). The garnet associated with xenolithic diamond SL 56-7 ($\delta^{13}\text{C} = -12.8$ ‰) is compositionally similar (Mg- and Ca-poor) to the Mn-rich garnets in Group III diamonds, but is not significantly enriched in Mn.

Eleven of the twelve diamonds from which rutile was recovered occur in Group III (Figure 5.21) and fifteen of the 23 diamonds from which sulphide was recovered occur in the numerically smaller group of diamonds comprising Group II (Figure 5.22). However, sulphide rosettes were visually identified in fifteen other Group III diamonds (Figure 5.22) and the higher proportion of sulphides recovered from Group II diamonds is probably a consequence of their larger size.

Finally, the occurrence of the less common inclusion types within diamonds from each Group is shown in Figure 5.23. Orthopyroxene and ferro-periclase, which are classified as peridotitic in Section 4.3, occur in Group I. The diamonds releasing the silica- and alumina-rich minerals, coesite, feldspar and kyanite, all occur in Group III. The diamonds from which zircon, sphene and the Si-Ti-K phase were recovered, also occur in group III, all at approximately -20 ‰. Moissanite was recovered in association with diamonds from all three groups and corundum was recovered in association with diamonds in both Groups II and III.

Based on inclusion geothermometry, the eclogitic diamonds in both Groups II and III crystallized at approximately 1100°C (Figure 5.24). No systematic variation of equilibration temperature with $\delta^{13}\text{C}$ within Groups I, II and III is observed although it may be significant that the highest eclogitic

equilibration temperature (1116 °C) was recorded for inclusions from a Group II diamond.

5.5 MODELLING

As is discussed in Section 5.1.1, isotope ratios are subject to both kinetic and equilibrium isotope effects. Kinetic effects are not easily modelled and will not be considered here. Simple equilibrium and fractional crystallization models in both closed and open systems are considered. Within this framework, the nature of the source, including possible carbon-bearing species involved, its isotope composition and initial homogeneity are discussed. A similar procedure was followed by Deines (1980) in his attempt at modelling the worldwide distribution of diamond $\delta^{13}\text{C}$ values.

It is apparent that the diamonds in Groups I, II and III are distinct with respect to carbon composition as well as the composition of the host mantle as indicated by variations in inclusion composition. Here, only the characteristics of the carbon are considered and, for the purposes of modelling, it is assumed that each group represents a distinct carbon reservoir.

The carbon isotope characteristics of each group are summarized in Table 5.1. The demarcation of Groups II and III is problematic because of possible overlap in $\delta^{13}\text{C}$ compositions of the two possible crystallization environments. For modelling purposes, the two xenolithic diamonds, SL 56-7 and SL 56-8, which have $\delta^{13}\text{C}$ values of -12.8 and -10.6 ‰ respectively, are classified as Group II diamonds. This

classification is based largely on diamond size (both weigh ~.13 carat). Diamonds SL A68, SL A81 and SL 45-3 ($\delta^{13}\text{C} = -13.4, -12.7$ and -12.5 ‰ respectively), on the other hand, are considered to be Group III diamonds, mostly on the basis of inclusion composition.

Based on inclusion thermometry (Table 4.6), it is assumed that the peridotitic Group I diamonds crystallized at approximately 1300°C whereas the eclogitic diamonds in both Groups II and III crystallized at 1100°C . On this assumption, the equilibrium fractionation factors between diamond and possible source carbon species can be estimated by extrapolation of published values (Figure 5.1). The factors used for this modelling exercise are listed in Table 5.2. Note that, according to this extrapolation, the values for CO_2 and carbonate would be approximately the same at the temperatures being modelled, and therefore these sources are considered together.

The modelling is accomplished on the assumption that each diamond crystallized while maintaining isotopic equilibrium with its source carbon. The difference in carbon isotope composition between the crystallizing diamond and its source, therefore, is governed purely by the sign and the magnitude of the fractionation factor ($1000\ln\alpha$). On this basis, if the carbon source changes in C isotope composition, so then do the diamonds produced. It is only the distribution of $\delta^{13}\text{C}$ values (shape and range) of the diamonds crystallized which will vary depending on the particular crystallization model chosen.

Note that this modelling does not presume an origin for the carbon. In other words, the modelling is accomplished regardless of whether the carbon is primordial or recycled.

Although this modelling is simplified, a more rigorous treatment is not justified considering the limited amount of data.

5.5.1 Equilibrium Crystallization

This process can be considered qualitatively for both closed and open systems. As equilibrium crystallization proceeds in a closed system, the source would become enriched or depleted in ^{13}C depending on the species involved. For example, as diamond crystallizes from CH_4 , the diamond concentrates ^{13}C ($1000\ln\alpha_{\text{DIAMOND-CH}_4}$ is positive) and the CH_4 source reservoir becomes depleted in ^{13}C . According to the process of equilibrium crystallization, the crystallized diamonds could theoretically maintain equilibrium with the changing reservoir (i.e. the diamonds themselves also become depleted in ^{13}C with ongoing crystallization) and at 100% crystallization, the distribution of $\delta^{13}\text{C}$ values for the diamond should be the same as that of the original CH_4 source. If the Sloan diamonds in Groups I, II and/or III crystallized under such conditions, their sources must have had the same carbon isotope compositions (ranges and distribution shapes) as observed in the diamonds (Figure 5.7).

An open system is here envisaged as a reservoir of carbon which is continuously replenished and, therefore, would maintain its initial carbon isotope composition during diamond crystallization. The diamonds produced from such a reservoir would have the same range and distribution shape as the source. However, because the source does not change composition and because the diamonds remain in equilibrium

with the source, their carbon isotope composition will be offset from that of the source as required by the sign and magnitude of the fractionation factor. This model is illustrated for the Sloan diamonds in Figure 5.25. Based on the extrapolated fractionation factors, possible CH₄ and graphite sources would have been slightly ¹³C depleted for crystallization at 1100 and 1300 °C, whereas possible CO₂ and carbonate sources would have been ¹³C enriched relative to the diamonds. Note that similar offsets would occur for the various species involved in closed system equilibrium crystallization if 100% crystallization was not attained. In general, if the Sloan diamonds in Groups I, II and/or III crystallized by equilibrium crystallization, then the carbon sources must have been at least as inhomogeneous as their observed ranges.

5.5.2 Fractional Crystallization

Here is considered the possibility of producing the carbon isotope ranges and distribution shapes observed for the diamonds in Groups I, II and III by simple Rayleigh fractionation (Rayleigh, 1896) from homogeneous sources. In this model, diamond crystallizes and is removed from the source. As diamond crystallizes, the residue (and therefore the next crystallizing diamond) becomes continuously enriched or depleted in ¹³C to a greater or lesser degree depending on the magnitude and sign of the fractionation factor.

The following expression (Taylor and Epstein, 1963) describes the change in the carbon isotopic composition of the residue as diamond crystallizes and is removed:

$$\delta^{13}\text{C}_{\text{RESIDUE}} = [(\delta^{13}\text{C}_{\text{INITIAL}} + 1000) f^{\frac{\Delta}{1000}}] - 1000$$

Δ = fractionation factor
(product - residue)
 $\approx 1000 \ln \alpha$

f = fraction of carbon remaining in residue

By way of example, for diamond crystallizing in isotopic equilibrium with CO_2 vapour at 1000°C , the fractionation factor is $1000 \ln \alpha_{\text{DIAMOND-CO}_2} \approx -4$ (i.e. diamond concentrates ^{12}C). For an assumed initial source composition of $\delta^{13}\text{C} = -6$ ‰, the first diamond (i.e. $f = 1$) would have a composition of -10 ‰. After 10% of the CO_2 has converted to diamond (i.e. $f = .9$), the residual will have a composition of -5.6 ‰ and diamond forming from this will have a composition of -9.6 ‰. As crystallization continues (i.e. $f = .8, .7$ etc.) the residue as well as the crystallizing diamond becomes more enriched in ^{13}C until all of the CO_2 converts to diamond (i.e. as f approaches 0). Note that for 100% crystallization, the resulting diamond population will have the same average $\delta^{13}\text{C}$ composition as the source CO_2 , but will have a positively skewed distribution shape. For diamond crystallizing from CH_4 , where the fractionation factor is positive, diamond concentrates ^{13}C and the final distribution would be negatively skewed. However, because the fractionation factor is expected to be of lower magnitude, the final range of $\delta^{13}\text{C}$ values produced would be smaller.

For the Sloan diamonds, initial source compositions are estimated based on: 1) the extreme $\delta^{13}\text{C}$ values observed in each group; 2) the carbon species (x) from which diamond crystallized and 3) the extrapolated fractionation factors ($1000 \ln \alpha_{\text{Diamond-x}}$) for each species (Table 5.2). For Group I,

with a range of values between -3.8 and -5.9 ‰, a progressive change in $\delta^{13}\text{C}$ starting at -3.8 ‰ must produce successively ^{13}C depleted diamonds (i.e. towards -5.9 ‰) and only carbon species x with positive $1000\ln\alpha_{\text{Diamond-x}}$ values (i.e. CH_4 or graphite) are applicable. The progression towards ^{13}C enriched values starting at -5.9 ‰ could be produced by CO_2 or carbonate sources, which have negative $1000\ln\alpha_{\text{Diamond-x}}$ values.

The model CH_4 , graphite and CO_2 (or carbonate) source compositions for Groups I, II and III are listed in Table 5.3 and the diamond distributions which would be produced by ~100% crystallization of the source in a closed system are illustrated in Figure 5.26. It should be obvious that in an open system, which is continuously replenished with carbon, such fractionation will not occur. These models will be considered further in the following discussion.

5.6 DISCUSSION

Based on the correlations between carbon isotope composition, morphology, mass and inclusion composition, at least three compositionally distinct diamond crystallization environments are represented in the Sloan kimberlite occurrence (Table 5.4). The extent to which they represent distinct diamond crystallization events and/or carbon reservoirs is a matter for debate.

The peridotitic diamonds comprising Group I are distinctly enriched in ^{13}C relative to other Sloan diamonds, including two olivine-bearing diamonds in Group III. The differences in chrome and forsterite content between the

olivines in the two groups is notable. Based on these differences, but especially on host diamond $\delta^{13}\text{C}$ values, it is unlikely that the olivine-bearing diamonds in Group III crystallized in the peridotitic environment represented by Group I diamonds. Whether they represent a separate crystallization environment within Group III is not known. The coexisting olivine and eclogitic garnet in diamond SL A57 may represent a mixed paragenesis or, alternatively, may represent a case of disequilibrium.

The carbon isotope data on eclogitic diamonds supports the inference, based on garnet and clinopyroxene inclusion compositions (see Section 4.8), that at least two compositionally distinct eclogitic diamond crystallization environments were sampled by the Sloan kimberlites (Table 5.4). However, the exact relationship between the eclogitic diamonds in Group II and those found in Group III is difficult to ascertain.

In general, the relatively ^{13}C enriched Group II eclogitic diamonds appear to have grown in a Mg-rich environment relative to most of the Group III eclogitic diamonds as reflected by included garnet and clinopyroxene compositions. The ^{13}C depleted Group III diamonds, on the other hand, may represent more than one eclogitic crystallization environment. The bulk of the Group III diamonds appear to have grown in a relatively Mn-poor and Ca-rich environment as reflected by included garnet and clinopyroxene compositions. The more common occurrence of rutile inclusions in these diamonds suggests that the environment was also relatively enriched in titanium. Based on included garnet compositions, a small but significant

proportion of the Group III diamonds must have grown in a relatively Ca-poor, but extremely Mn-rich environment. It may be significant that these Mn-rich garnets were not found coexisting with either clinopyroxene or rutile. The compositional similarity between the Mn-rich garnets in Group III diamonds and the two garnets in Group II diamonds suggests that they may be related which further suggests that there may be significant overlap with respect to $\delta^{13}\text{C}$ composition between the two inferred eclogitic crystallization environments.

Based on diamond size, Groups II and III are distinct. As has been previously suggested, the larger Group II diamonds may have grown more rapidly or over a longer period of time relative to the Group III diamonds.

The three xenolithic diamonds found in this study appear to belong to Group II based on carbon isotope composition and size. The jadeite-poor character of the clinopyroxene associated with diamond SL 56-8 is consistent with the diamond's Group II carbon isotope character. However, the clinopyroxenes from diamond eclogite, TP 121 (McCandless and Collins, 1989), are jadeite-rich and more akin to the clinopyroxenes included in Group III diamonds. Based on clinopyroxene compositions, the diamonds from both Groups II and III may have been associated with xenoliths. This is supported by the occurrence of xenolithic surface features on diamonds from both groups. However, this inference must be confirmed by determining the $\delta^{13}\text{C}$ composition of diamonds from TP 121.

Finally, the difference in internal $\delta^{13}\text{C}$ homogeneity between the two groups provides further support for distinct

crystallization environments. Only the diamonds in Group III, including those associated with both Mn-rich and Mn-poor garnets, show significant within-diamond heterogeneity. There appears to be a general increase in inhomogeneity towards lighter $\delta^{13}\text{C}$ values. Whether this trend is real cannot be confirmed on available evidence, but the extreme variability within Group III diamonds appears to reflect some aspect of the Group III crystallization environment which differs from the environments in which Group II (and Group I) diamonds formed. The group of diamonds with $\delta^{13}\text{C}$ values lying between -26 and -29 ‰ (Figure 5.9) may represent a fourth eclogitic diamond subpopulation, but these diamonds are not distinguished by other characteristics.

The fact that $\delta^{13}\text{C}$ variation, within individual diamonds from all three groups, does not mirror within-group variation may be significant. It suggests that the diamonds grew either from regionally inhomogeneous but locally more homogeneous carbon sources, or that they crystallized and were removed from a fractionating carbon source. In this respect, it is useful to consider the results of the various diamond crystallization models presented in Section 5.5.

It is emphasized that the models considered are ideal cases which may not correspond to the natural systems. It seems unlikely that diamonds would grow and maintain isotopic equilibrium with a continuously changing source as is envisaged for the closed system, equilibrium crystallization model. Diamond crystallization in a closed system is more likely to be represented by a Rayleigh fractionation model. However, the occurrence of a totally closed system, in general, seems unlikely. Most plausible is the open system

model where the carbon source is continually replenished, as might be envisaged for a degassing earth or for metasomatic fluids flushing through the mantle.

As already stated, if the Sloan diamonds formed by equilibrium crystallization in a closed system, then the observed diamond $\delta^{13}\text{C}$ compositions (average $\delta^{13}\text{C}$, range and distribution shape) would reflect, exactly, those of their carbon sources, assuming 100% crystallization. If the Sloan diamonds crystallized in an open system, then similarly heterogeneous sources would be required, but the source compositions would be enriched or depleted in ^{13}C relative to those observed in the diamonds, depending on the species from which diamond crystallized (Figure 5.25).

Possibly of more interest, is whether the observed distributions can be produced from homogeneous sources. According to the modelling, the small range of $\delta^{13}\text{C}$ values observed for the Group I diamonds (2.1 ‰) and the slightly larger range observed for Group II (4.3 ‰) could have been produced by Rayleigh fractionation of homogeneous CH_4 or CO_2 /carbonate sources, but probably not from homogeneous graphite (Figure 5.26). However, the high temperatures (and correspondingly small fractionation factors) require that a large fraction (~100%) of the source carbon be converted to diamond. It therefore seems more plausible that the ranges observed in Group I and II diamonds are a reflection of minor source heterogeneity.

All of the possible sources modelled for Group I diamonds have $\delta^{13}\text{C}$ compositions in the range inferred for primordial carbon (-2 to -9 ‰). A relatively reduced crystallization environment for Group I diamonds is suggested by the

occurrence of ferro-periclase as an inclusion and further by the possibility that chrome in olivine is present as Cr^{2+} . It is therefore suggested that the source carbon was also relatively reduced, possibly occurring as CH_4 .

The negatively skewed distribution observed for the Group II diamonds is closely reproduced by the Rayleigh fractionation model with a CH_4 source (Figure 5.26). This suggests that a relatively homogeneous CH_4 source ($\delta^{13}\text{C} \sim -9.3$) may have produced the Group II diamonds. Such a source may represent a mixing of the Group I and Group III carbon sources. It is notable that the Group II diamonds could also have been produced in an open system from primordial carbon. The carbon source having a primordial signature may have been $\text{CO}_2/\text{Carbonate}$ (Figure 5.25). According to the model, this source for Group II diamonds would have had a range of $\delta^{13}\text{C}$ values between -5.5 and -9.8 ‰ (average ~ -7 ‰). Such a source might possibly represent the slightly ^{13}C depleted carbon remaining after the crystallization of ^{13}C enriched, Group I diamonds.

Based on the modelling, Group III diamonds were almost certainly not produced by fractional crystallization from a single, isotopically homogeneous carbon source (Figure 5.26). This can be said for diamonds associated with both Mn-poor and Mn-rich garnets, since the diamonds hosting both types of garnet span the range of $\delta^{13}\text{C}$ values of Group III (Figure 5.18). The apparent lack of systematic zonation in single, inhomogeneous diamonds also suggests that the diamonds were not produced in a simple fractionating system. The large range of $\delta^{13}\text{C}$ values observed in Group III diamonds probably reflects an extremely heterogeneous carbon source. The same

can be said for the carbon source represented by Group II diamonds if the overlap with Group III is significant.

It has been suggested by others (e.g. Javoy et al., 1986), that such extremely ^{13}C depleted diamonds may represent recycled carbon. The Mn-rich garnet inclusions in Group III diamonds, as mentioned in Section 4.8, are compositionally similar to those at Finsch which were postulated by Smith et al. (1989b) to have a subducted origin. Based on these observations, it is suggested that the Group III diamonds were most likely formed from subducted material.

6. SUMMARY AND CONCLUSIONS

The study of diamonds from the Sloan kimberlite occurrence of the Colorado-Wyoming State Line kimberlite district, has provided information which is pertinent to deciphering the processes responsible for their growth, as well as the events experienced by the diamonds subsequent to growth. This has been accomplished by considering physical characteristics, mineral inclusion composition, carbon isotope composition and relationships between these parameters.

The characterization of the Sloan diamonds was accomplished on three samples of the total test production parcel provided for study. Two relatively large samples, termed the Sieved and the Representative samples, were investigated in order to document the overall physical character of the Sloan diamonds. A smaller sample of inclusion-bearing diamonds, termed the Selected sample, was also described and, subsequently, investigated for mineral inclusion composition and carbon isotope composition.

Physical characteristics were described using a diamond description scheme which recognizes both primary and secondary characteristics. The characteristics described are crystal state, crystal regularity, morphology, mass/size, colour, surface features and inclusion content.

Over 50% of the Sloan diamonds are broken crystals and this feature was found to vary with respect to diamond size

and diamond colour. Larger crystals appear to be more susceptible to breakage relative to small crystals, and brown diamonds are apparently more prone to breakage relative to grey crystals.

With respect to crystal regularity, the large proportion of diamonds in the sample are distorted as is found at most localities worldwide.

The diamonds were characterized with respect to both primary and secondary (resorption) morphology. Regarding primary morphology, the parcel consists mostly of single crystal octahedra, a significant proportion of simple aggregates or twins, and minor proportions of polycrystalline aggregates, cubo-octahedra or cube diamonds. It was found that the proportion of single crystal forms relative to twinned/aggregate forms varies with diamond colour. A higher proportion of twinned/aggregate forms occur in the grey diamond subsample relative to the brown diamond subsample.

The resorption morphologies were described according to a classification system devised by Robinson (pers. comm., 1984), which recognizes transitional forms resulting from the conversion of an octahedron to a tetrahexahedroid (Figure 3.12). On this basis, the Sloan diamonds, as a whole, are approximately equally distributed over the range of morphologies. However, when considered by kimberlite phase, a higher proportion of Category 1 diamonds occur in the Sloan 1 and Dyke kimberlite bodies relative to the Sloan 2 kimberlite body. The better preservation of Sloan 2 diamonds is possibly due to their size since, as will be discussed, the Sloan 2 diamonds tend to be larger than the Sloan 1 and Dyke diamonds and, in general, the proportion of each individual crystal

lost upon resorption is found to decrease with increasing size (i.e. larger crystals are better preserved).

The Sloan diamonds are small with most (~ 75%) weighing <.02 carat. The largest diamond recovered from Sloan weighs 1.24 carat (Shaver, 1988). Robinson's resorption morphology classification method allows a semi-quantitative calculation of primary mass. When the primary mass of the Sloan diamonds is calculated, it is found that approximately 25% of the Sloan diamond population mass was lost during resorption. A semi-quantitative calculation of primary mass for individual crystals suggests that few diamonds at Sloan exceeded two carats prior to resorption. As mentioned previously, the Sloan 2 kimberlite body had a higher proportion of larger crystals relative to the Sloan 1 and Dyke bodies. This is not due to better preservation, since the trend is also apparent for primary mass.

The predominant diamond colour observed is brown, but significant proportions of grey and colourless diamonds were found. Only minor proportions of yellow, amber, green and pink diamonds are present. The proportion of grey diamonds increases at the expense of brown diamonds with increasing diamond size, a feature which may relate to impurity content.

Surface features are divided into three categories: xenolithic, deformation and "other". Approximately 20% of the Sloan diamonds display xenolithic surface features, suggesting that they were derived from the disaggregation of xenoliths. Many of these features appear to be growth features (intergrowth pits, serrate laminae, knob-like asperities, associated graphite). Other xenolithic features (etch channels, non-uniform resorption) suggest that the diamonds

were partially protected during the resorption event. Only about 2% of the diamonds exhibit lamination lines, a feature indicative of plastic deformation. This is low compared to diamond populations at other localities (Robinson et al., 1989). The more common occurrence of lamination lines on brown diamonds reported elsewhere is not apparent for the Sloan diamonds. Included in the "other" category are resorption features which suggest that the Sloan diamonds experienced high-temperature (>900 °C) resorption, possibly by oxidation in the presence of fluids rich in H_2O or CO_2 . Perhaps the most interesting observation with respect to surface features is the more common occurrence of corrosion sculpture on diamonds from the Sloan 2 kimberlite body relative to those from the Sloan 1 and Dyke kimberlite bodies. This is believed to have resulted from slower cooling of the kimberlite magma as might have occurred in a "blind" diatreme which, as suggested by McCallum (1976), is what the Sloan 2 kimberlite body represents.

Finally, based on this visual assessment, the predominant primary inclusion mineral in Sloan diamonds is believed to be sulphide. A small proportion ($<5\%$) of the diamonds had discernible transparent primary inclusions which, based largely on colour, occur in the two paragenetic groups, peridotitic and eclogitic, found at all localities investigated worldwide. Based on the visual assessment of 2000 diamonds, however, the relative proportions in which these two paragenetic diamond types occur cannot be ascertained.

Both peridotitic and eclogitic inclusions were recovered from the Sloan diamonds. Eclogitic minerals include sulphide,

pyrope-almandine, omphacitic clinopyroxene, rutile, coesite, K-feldspar, kyanite and probably zircon. The peridotitic minerals are olivine, orthopyroxene, Cr-rich pyrope, Cr-rich diopside and ferro-periclase. At Sloan, the eclogitic minerals predominate with an E/(E+P) ratio = .78. This is believed to be a good approximation of their relative abundances, as sampled by the kimberlite, since sulphides are included in the calculation and diamonds over the whole size range were studied.

A high proportion of the peridotitic diamonds are twinned/aggregate crystals, whereas the eclogitic diamonds are mostly single-crystal octahedra. It is speculated that the peridotitic diamonds crystallized under conditions of higher nucleation density relative to the eclogitic diamonds. In addition, all of the peridotitic diamonds weigh under .02 carat, whereas most of the eclogitic diamonds are heavier than .02 carat and range up to .35 carat. It is suggested that the larger eclogitic diamonds either grew over a longer period or at a faster rate relative to the smaller peridotitic diamonds. Based on this sample of 100 inclusion-bearing diamonds, the peridotitic diamonds are less resorbed relative to eclogitic diamonds. This is unexpected since, in general, larger diamonds tend to be better preserved.

The peridotitic inclusions are calcium-enriched and belong to the lherzolitic sub-paragenesis. They appear to have equilibrated at higher temperatures (1224-1469 °C) and higher pressures (56-83 kbar) relative to peridotitic inclusions investigated elsewhere. They are compositionally similar to minerals in "infertile" garnet peridotite xenoliths from Sloan, as well as to the diamondiferous peridotite from

the Schaffer locality. These peridotites are believed to be the residua from an Archaean melting event (Eggler et al., 1987). The compositional link between these xenoliths and the peridotitic inclusions suggests an ancient age for the peridotitic diamonds.

The eclogitic inclusion minerals are compositionally typical of those found in diamonds from most localities. The inclusion minerals, those from the diamond-graphite eclogite described by McCandless and Collins (1989), as well as those from the three diamondiferous eclogites found in this study, are Group I eclogite minerals as chemically defined by significant sodium in the garnets and potassium in the clinopyroxenes (McCandless and Gurney, 1989). No other Group I eclogite material has been reported from any of the State Line kimberlites. The unique equilibration temperatures of diamond-associated Group I eclogite material relative to non-Group I eclogite xenoliths from Sloan suggests that the two eclogitic types may be unrelated to each other.

The eclogitic garnet inclusions occur in two compositional groups, termed "Mn-rich" and "Mn-poor". The Mn-rich garnets are relatively Ca-poor and are associated with relatively jadeite-poor, enstatite enriched clinopyroxenes. The Mn-poor garnets are Ca-rich and show a broad increase in titanium with decreasing Mg/Mg+Fe. The omphacitic clinopyroxenes associated with these garnets are jadeite-rich and show a broad increase in titanium with increasing jadeite. These are interpreted as representing an igneous trend. The two groups of eclogitic minerals are interpreted as representing at least two eclogitic diamond crystallization environments.

The time of some eclogitic diamond formation is possibly Proterozoic as inferred from U-Th-Pb isotope determinations on a zircon inclusion of unconfirmed, but likely eclogitic, paragenesis. This would imply that at least some of the eclogitic diamonds are xenocrysts in the Devonian age kimberlites. It further implies that some eclogitic diamond formation may have occurred in response to processes related to continental accretion, which was occurring in the region during the Proterozoic.

The carbon isotope compositions of selected Sloan diamonds were determined. A large range in average $\delta^{13}\text{C}$ values between -4 and -29 ‰ (versus PDB) was obtained. This range nearly spans that of diamonds analyzed worldwide and, to this author's knowledge, is the largest range found to date for diamonds from a single kimberlite locality.

Major modes occur at -4, -9 and -21 ‰ and three groups are defined around these modes: -4 to -6 ‰ (Group I); -8 to -13 ‰ (Group II); and -13 to -29 ‰ (Group III).

Group I is comprised entirely of peridotitic diamonds whereas most of the diamonds in Group II and Group III are of eclogitic affinity. Two important exceptions are olivine-bearing diamonds having $\delta^{13}\text{C}$ values of -20.6 and -21.9 ‰. In the latter, the olivine coexisted with an eclogitic garnet ($\text{Mg}/\text{Mg}+\text{Fe} = .46$). The olivines in Group III diamonds are relatively chrome-poor and slightly Mg-rich relative to those occurring in Group I. It is considered unlikely that the olivine-bearing diamonds in Group III crystallized in the peridotitic environment represented by Group I diamonds.

The differences in carbon isotope composition found between the eclogitic diamonds in Groups II and III is

reflected by differences in mass and inclusion composition. The largest diamonds all occur in Group II. Those in Group III do not exceed .06 carat, whereas most of those in Group II do, with seven exceeding .10 carat and ranging up to .35 carat.

The Mn-poor garnets (as defined previously) and associated jadeite-rich clinopyroxenes occur exclusively in the ^{13}C depleted, Group III diamonds. The Mn-rich garnets occur in both Groups II and III, but those in Group II are significantly more magnesian than those in Group III diamonds. The jadeite-poor and enstatite-rich clinopyroxenes are apparently associated only with the more magnesian garnets in Group II diamonds.

Finally, significant variation in $\delta^{13}\text{C}$ (as much as 4.2 ‰) was documented within single diamonds. Only in Group III diamonds did the variation exceed analytical error. There appears to be a general increase in inhomogeneity with decreasing $\delta^{13}\text{C}$, but this trend cannot be confirmed on available evidence.

Groups I, II and III are interpreted as representing at least three primary diamond subpopulations which formed in compositionally distinct environments beneath North America. Based on carbon isotope modelling, it is shown that the range of $\delta^{13}\text{C}$ values for Groups I and II, could conceivably have been produced in a closed system by fractional crystallization of relatively homogeneous sources. However, this would have occurred only if nearly 100% of the source carbon had been converted to diamond and this is considered to be an unlikely scenario. It is therefore suggested that the ranges, though relatively small, are more a reflection of source

heterogeneity. Furthermore, the diamonds in both Groups I and II could have been produced from carbon sources having $\delta^{13}\text{C}$ compositions within the range inferred for primordial carbon (i.e. -2 to -9 ‰). Alternatively, the Group II diamonds could have been produced from a slightly more ^{13}C depleted carbon source of ~ -9 ‰, which could conceivably represent a mixture of the Group I and Group III carbon sources. The Group III diamonds were probably produced from a relatively heterogeneous carbon source and are believed to represent a strong case for recycled carbon.

ACKNOWLEDGEMENTS

It is a pleasure to add this written word of appreciation and thanks to all those persons who provided scientific, technical and/or moral support towards the completion of this thesis.

Perhaps the most deserving is John Gurney, who has provided me with a most enjoyable and stimulating thesis project; who has provided and/or arranged financial support for my sustenance and for various excursions including a trip to Sloan and one to Australia for the Fourth International Kimberlite Conference; and who's knowledge and expertise in diamond research and in mantle research in general was invaluable. To John and his family, Dot, Jean, James and the twins, Kim and Leigh, who together have served as one of my surrogate families since my arrival in Cape Town, I wish to express my deepest appreciation.

The diamonds and partial support were provided, initially on the impetus of Hugo Dummett, by Superior Oil Company Minerals Division (subsequently Long Lac Mineral Exploration (Texas), Inc.). The personnel at Long Lac, Mike Waldman, Ken Shaver, John Carlson, Steve Marsh, Karen Hilton and Dale Kentgen are thanked for providing much needed and helpful assistance during the course of this project, especially during my visits to their offices in Fort Collins. Mal McCallum, Tia, Greg and Ellie took me into their home on both visits to Long Lac and I hope to join them again sometime for

a sopapilla and cerveza at one of the many Mexican restaurants in Fort Collins.

Derek Robinson and the Anglo American Research Laboratory kindly allowed the use of his resorption morphology classification scheme and provided helpful discussions during the course of this project. My colleagues in the Kimberlite Research Group were always available for discussion. Rory Moore, with whom I spent long hours in the "Mantle Room" during the diamond cracking and inclusion recovery portion of this project, was a constant source of knowledge and evolved humour during these past years. His family, Jill, Jessica, Sophie and Ned, have also provided a home away from home. Stuart Hill is thanked for his input into the diamond and inclusion description schemes and Melissa Kirkley for her helpful discussions on carbon isotopes.

Jenny Hops is thanked for putting up with constant interruptions as my office-mate for most of the duration of this thesis. She, more than once, provided key insight which aided in solving dilemmas encountered during the course of this study. In the final rush, Jenny was there and there is no doubt that she should be an author on this thesis.

Helpful discussions were provided by many others, notably Torsten Vennemann, Tom McCandless, Craig Smith, Mal McCallum, Steve Richardson, Jeff Harris, Leon "The Dog" Daniels and Anton le Roex. Anton, Sue, Craig, Tanya and Nikki (who was born when this thesis began) also provided me with a home away from home.

Technical support was provided on a number of fronts. Bruce Cairns built the diamond cracker and both he and Eric Bryce often came to the rescue with technical assistance.

David Wilson, Henry Hendricks and Robert Oliver provided technical assistance for the mounting and polishing of the micron-sized mineral inclusions.

Klaus Schultes and Dane Gerneke provided instruction and technical assistance on the SEM and Charlie Basson worked especially diligently in the final hours to produce the SEM photographic plates included in this thesis.

Professor Toggs Pienaar, of the University of Stellenbosch, did XRD determinations on a number of micron-sized inclusions. Tom McCandless, with the help of Bruce Cairns, built the diamond combustion line and provided instruction on its use. John Lanham, who maintains the Archaeometry stable isotope mass spectrometer, was always available, even after hours, for consultation. Roddy Sauls, Susan Sayers and Anne Westoby drafted a large proportion of the figures in this thesis. Lynn O'Neill, Susie Wisdom, Patrick Sieas, Nadima Ebrahim, Dieneke van der Heyde, Brian Hoal and many others also are thanked for their inspiration and support.

A special message of appreciation is due to Ruth Elsie May Mennie who put considerable effort into this thesis on both technical and personal fronts. She, over all others, will be especially pleased to hear that this thesis is finally completed. Thank you, Ruth.

Finally, my family must be mentioned. The weekly letters from home have become essential to my wellbeing. Their support and understanding over the years has never faltered and, even though I was far away, I knew that their thoughts were always with me.

REFERENCES

- ATER P.C. 1982. Petrology and geochemistry of eclogite xenoliths from Colorado-Wyoming kimberlites. MSc thesis (unpublished), Colorado State University, Fort Collins.
- ATER P.C., EGGLER D.H. and McCALLUM M.E. 1984. Petrology and geochemistry of mantle eclogite xenoliths from Colorado-Wyoming kimberlites: recycled ocean crust? In: Kornprobst J. ed., Kimberlites II: The Mantle and Crust-Mantle Relationships. Elsevier Science Publishing Co, Amsterdam, 309-318.
- BELL D.R. 1985. Evaluation of geothermometry and geobarometry on mantle-derived xenoliths from kimberlites. Internal report of De Beers Consolidated Mines Ltd, Kimberlite Petrology Unit, 15p.
- BIBBY D.M. 1982. Impurities in natural diamond. Chemistry and Physics of Carbon 18, 1-91.
- BOTTINGA Y. 1969a. Calculated fractionation factors for carbon and hydrogen isotope exchange in the system calcite-CO₂-graphite-methane-hydrogen and water vapour. *Geochimica et Cosmochimica Acta* 33, 49-64.
- BOTTINGA Y. 1969b. Carbon isotope fractionation between graphite, diamond and carbon dioxide. *Earth and Planetary Science Letters* 5, 301-307.
- BOVENKERK H.P. 1961. Some observations on the morphology and physical characteristics of synthetic diamond. *American Mineralogist* 46, 952-963.
- BOYD F.R. and FINNERTY A.A. 1980. Conditions of origin of natural diamonds of peridotitic affinity. *Journal of Geophysical Research* 85(B12), 6911-6918.
- BOYD F.R. and NIXON P.H. 1973. Origin of the ilmenite-silicate nodules in kimberlites from Lesotho and South Africa. In: Nixon P.H. ed., Lesotho Kimberlites, Lesotho National Development Corporation, Maseru, 254-268.
- BOYD F.R., GURNEY J.J. and RICHARDSON S.H. 1985. Evidence for a 150-200 km thick Archaean lithosphere from diamond inclusion thermobarometry. *Nature* 315, 387-389.
- BOYD S.R., MATHEY D.P., PILLINGER C.T., MILLEDGE H.J., MENDELSSOHN M.J. and SEAL M. 1987. Multiple growth events during diamond genesis: An integrated study of carbon and nitrogen isotopes and nitrogen aggregation state in coated diamonds. *Earth and Planetary Science Letters* 86, 341-353.
- BRADLEY S.D. and McCALLUM M.E. 1984. Granulite facies and related xenoliths from the Colorado-Wyoming kimberlite. In: Kornprobst J. ed., Kimberlites II: The Mantle and Crust-Mantle relationships. Elsevier Science Publishers, Amsterdam, 205-217.

- BROZEL M.R., EVANS T. and STEPHENSON R.F. 1978. Partial dissociation of nitrogen aggregates by high temperature-high pressure treatments. Proceedings of the Royal Society of London A361, 109-127.
- BRUTON E. 1970. Diamonds. N.A.G. Press, London.
- BURNS R.G. 1975. On the occurrence and stability of divalent chromium in olivines included in diamonds. Contributions to Mineralogy and Petrology 51, 213-221.
- CARDOSO P. 1980. A study of mantle inclusions in the Koffiefontein kimberlite pipe, South Africa. MSc thesis (unpublished), University of Cape Town, South Africa, 133p.
- CARLSON J.A. and MARSH S.W. 1989. Discovery of the George Creek, Colorado kimberlite dikes. 4th International Kimberlite Conference, Kimberlites and related rocks, Vol. 2, Geological Society of Australia Special Publication No. 14, 1169-1178.
- CARSWELL D.A. and GIBB F.G.F. 1980. Geothermometry of garnet lherzolite nodules with special reference to those from the kimberlites of northern Lesotho. Contributions to Mineralogy and Petrology 74, 403-416.
- CARSWELL D.A. and GIBB F.G.F. 1987. Evaluation of mineral thermometers and barometers applicable to garnet lherzolite assemblages. Contributions to Mineralogy and Petrology 95, 499-511.
- CHRENKO R.M. 1971. Boron content and profiles in large laboratory diamonds. Nature 229, 165-167.
- CHRENKO R.M., TUFT R.E. and STRONG H.M. 1977. Transformation of the state of nitrogen in diamond. Nature 270, 141-144.
- CHRONIC J., McCALLUM M.E., FERRIS C.S.(Jr) and EGGLEER D.H. 1969. Lower Paleozoic rocks in diatremes, southern Wyoming and northern Colorado. Geological Society of America Bulletin 80, 149-156.
- COES L. 1953. A new dense crystalline silica. Science 118, 131-152.
- COLLINS D.S. 1982. Diamond collecting in northern Colorado. The Mineralogical Record 13, 205-208.
- COMPSTON W., WILLIAMS I.S. and MEYER C. 1983. U-Pb geochronology of zircons from breccia 73217 using a sensitive high mass-resolution ion microprobe. Journal of Geophysical Research, Supplement 89, B525-B534.
- CONDIE K.C. 1982. Plate tectonics model for Proterozoic continental accretion in the southwestern United States. Geology 10, 37-42.

- DAVIS G.L. 1977. The ages and uranium contents of zircons from kimberlites and associated rocks. Carnegie Institution of Washington, Yearbook 76, 631-635.
- DEER W.A., HOWIE R.A. and ZUSSMAN J. 1980. An introduction to rock forming minerals. Longman Group Limited, London.
- DEINES P. 1980. The carbon isotopic composition of diamonds: relationship to diamond shape, color, occurrence and vapor composition. *Geochimica et Cosmochimica Acta* 44, 943-961.
- DEINES P. and GOLD D.P. 1973. The isotopic composition of carbonatite and kimberlite carbonates and their bearing on the isotopic composition of deep-seated carbon. *Geochimica et Cosmochimica Acta* 37, 1709-1733.
- DEINES P. and WICKMAN F.E. 1973. The isotopic composition of 'graphitic' carbon from iron meteorites and some remarks on the troilitic sulfur of iron meteorites. *Geochimica et Cosmochimica Acta* 37, 1295-1319.
- DEINES P., GURNEY J.J. and HARRIS J.W. 1984. Associated chemical and carbon isotopic composition variations in diamonds from Finsch and Premier kimberlite, South Africa. *Geochimica et Cosmochimica Acta* 48, 325-342.
- DEINES P., HARRIS J.W. and GURNEY J.J. 1986. On the existence of ^{13}C depleted carbon in the mantle; evidence from diamond studies. 4th International Kimberlite Conference Extended Abstracts, Geological Society of Australia Abstracts Series No. 16, 383-385.
- DEINES P., HARRIS J.W. and GURNEY J.J. 1987. Carbon isotopic composition, nitrogen content and inclusion composition of diamonds from Roberts Victor kimberlite, South Africa: Evidence for ^{13}C depletion in the mantle. *Geochimica et Cosmochimica Acta* 51, 1227-1243.
- DES MARAIS D.J. and MOORE J.G. 1984. Carbon and its isotopes in mid-oceanic basaltic glasses. *Earth and Planetary Science Letters* 69, 43-57.
- EGGLER D.H. and McCALLUM M.E. 1973. Ultramafic nodules from Colorado-Wyoming kimberlite pipes. Carnegie Institution of Washington, Yearbook 72, 446-449.
- EGGLER D.H. and WENDLANDT R.F. 1979. Experimental studies of the relationship between kimberlite magmas and partial melting of peridotite. In: Boyd F.R. and Meyer H.O.A. eds., Kimberlites, Diatremes and Diamonds: Their Geology, Petrology and Geochemistry. American Geophysical Union, Washington, 330-338.

- EGGLER D.H., McCALLUM M.E. and SMITH C.B. 1979. Megacryst assemblages in kimberlite from northern Colorado and southern Wyoming: petrology, geothermometry-barometry and areal distribution. In: Boyd F.R. and Meyer H.O.A. eds., The Mantle Sample: Inclusions in Kimberlites and Other Volcanics. American Geophysical Union, Washington, 213-226.
- EGGLER D.H., McCALLUM M.E. and KIRKLEY M.B. 1987. Kimberlite transported nodules from Colorado-Wyoming: A record of enrichment of shallow portions of an infertile lithosphere. Geological Society of America Special Paper 215, 77-90.
- ELLIS D.J. and GREEN D.H. 1979. An experimental study of the effect of Ca upon garnet-clinopyroxene Fe-Mg exchange equilibria. Contributions to Mineralogy and Petrology 71, 13-22.
- EVANS T. 1976. Diamonds. Contemporary Physics 17, 45-70.
- EVANS T. 1978. In Diamond Research 1978. Industrial Diamond Information Bureau London, 17p.
- EVANS T. and QI Z. 1982. The kinetics of the aggregation of nitrogen atoms in diamond. Proceedings of the Royal Society of London A381, 159-178.
- EVANS T. and SAUTER D.H. 1961. Etching of diamond surfaces with gases. Philosophical Magazine 6, 429-440.
- FINNERTY A.A. and BOYD F.R. 1984. Evaluation of thermobarometers for garnet peridotites. Geochimica et Cosmochimica Acta 48, 15-27.
- FINNERTY A.A. and BOYD F.R. 1987. Thermobarometry for garnet peridotites: basis for the determination of thermal and compositional structure of the upper mantle. In: Nixon P.H. ed., Mantle Xenoliths. John Wiley & Sons, Chichester, England, 381-402.
- FRANK F.C. and PUTTICK K.E. 1958. Etch pits and trigons on diamond. Philosophical Magazine 3, 1273-1279.
- FRIEDMAN I. and O'NEIL J.R. 1977. Compilation of stable isotope fractionation factors of geochemical interest. In: Fleischer M. ed., Data of Geochemistry, U.S. Geological Survey Professional Paper 440-KK.
- GALIMOV E.M. 1984. Variations in isotopic composition of diamonds and inferences for diamond genesis conditions. Geokhimiya 8, 1091-1118.
- GOLD D.P. 1984. A diamond exploration philosophy for the 1980's. Pennsylvania State University, Earth and Mineral Sciences Report, 53(4), 37-42.

- GURNEY J.J. 1984. A correlation between garnets and diamonds in kimberlites. In: Glover J.E. and Harris P.G. eds., Kimberlite Occurrence and Origin: A basis for conceptual models in exploration. Geology Dept & University Extension, University of Western Australia, Publication No. 8, 143-166.
- GURNEY J.J. 1989. Diamonds. 4th International Kimberlite Conference. Kimberlites and related rocks Vol. 2, Geological Society of Australia Special Publication No. 14, 935-965.
- GURNEY J.J., HARRIS J.W. and RICKARD R.S. 1979. Silicate and oxide inclusions in diamonds from the Finsch kimberlite pipe. In: Boyd F.R. and Meyer H.O.A. eds., Kimberlites, Diatremes and Diamonds: Their Geology, Petrology and Geochemistry. American Geophysical Union, Washington, 1-15.
- GURNEY J.J., HARRIS J.W. and RICKARD R.S. 1984a. Silicate and oxide inclusions in diamonds from the Orapa mine, Botswana. In: Kornprobst J. ed., Kimberlites II: The Mantle and Crust-Mantle Relationships. Elsevier Science Publishing Co, Amsterdam, 3-9.
- GURNEY J.J., HARRIS J.W. and RICKARD R.S. 1984b. Minerals associated with diamonds from the Roberts Victor mine. In: Kornprobst J. ed., Kimberlites II: The Mantle and Crust-Mantle Relationships. Elsevier Science Publishing Co, Amsterdam, 25-32.
- GURNEY J.J., HARRIS J.W., RICKARD R.S. and MOORE R.O. 1986. Inclusions in Premier mine diamonds. Transactions of the Geological Society of South Africa 88(2), 301-310.
- HAGGERTY S.E. 1986. Diamond genesis in a multiply-constrained model. Nature 320, 34-38.
- HALL A.E. and SMITH C.B. 1984. Lamproite diamonds - are they different? In: Glover J.E. and Harris P.G. eds., Kimberlite Occurrence and Origin: A basis for conceptual models in exploration. Geology Dept & University Extension, University of Western Australia, Publication No. 8, 167-212.
- HARRIS J.W. 1968. The recognition of diamond inclusions. Part 1: Syngenetic mineral inclusions. Part 2: Epigenetic mineral inclusions. Industrial Diamond Review 28, 402-410; 458-461.
- HARRIS J.W. 1975. The etching of diamond in CO₂, H₂O and kimberlite. Cambridge, Kimberlite Symposium, unpaginated.
- HARRIS J.W. 1987. Recent physical, chemical, and isotopic research of diamond. In: Nixon P.H. ed., Mantle Xenoliths. John Wiley & Sons, Chichester, England, 477-500.

- HARRIS J.W. and GURNEY J.J. 1979a. Inclusions in diamond. In: Field J.E. ed., The Properties of Diamond. Academic Press, London, 555-591.
- HARRIS J.W. and GURNEY J.J. 1979b. A study of the mineralogy and chemistry of sulphide inclusions in diamonds. Abstract, Kimberlite Symposium II, Cambridge, England.
- HARRIS J.W. and VANCE E.R. 1974. Studies of the reaction between diamond and heated kimberlite. *Contributions to Mineralogy and Petrology* 47, 237-244.
- HARRIS J.W., HAWTHORNE J.B., OOSTERVELD M.M. and WEHMEYER E. 1975. A classification scheme for diamond and a comparative study of South African diamond characteristics. *Physics and Chemistry of the Earth* 9, 765-783.
- HARRIS J.W., HAWTHORNE J.B. and OOSTERVELD M.M. 1979. Regional and local variations in the characteristics of diamonds from some southern African kimberlites. In: Boyd F.R. and Meyer H.O.A. eds., Kimberlites, Diatremes and Diamonds: Their Geology, Petrology and Geochemistry. American Geophysical Union, Washington, 27-41.
- HARRIS J.W., HAWTHORNE J.B. and OOSTERVELD M.M. 1984. A comparison of diamond characteristics from the De Beers Pool mines, Kimberley, South Africa. *Annales Scientifiques L'Universite de Clermont-Ferrand* II 74, 1-13.
- HARRIS J.W., HAWTHORNE J.B. and OOSTERVELD M.M. 1986. A comparison of characteristics of diamonds from the Orapa and Jwaneng kimberlite pipes in Botswana. 4th International Kimberlite Conference. Geological Society of Australia Abstract Series No. 16, 395-397.
- HARTE B., GURNEY J.J. and HARRIS J.W. 1980. The formation of peridotitic suite inclusions in diamonds. *Contributions to Mineralogy and Petrology* 72, 181-190.
- HATTON C.J. 1978. The geochemistry and origin of xenoliths from the Roberts Victor mine. PhD thesis (unpublished), University of Cape Town, South Africa. 179p.
- HATTON C.J. and GURNEY J.J. 1987. Roberts Victor eclogites and their relation to the mantle. In: Nixon P.H. ed., Mantle Xenoliths. John Wiley and Sons, Chichester, 453-464.
- HAUSEL W.D., McCALLUM M.E. and ROBERTS J.T. 1985. The geology, diamond testing procedures, and economic potential of the Colorado-Wyoming kimberlite province - a review. Geological Survey of Wyoming Report of Investigations 31, 1-22.
- HENOC J., HEINRICH K.F.J. and MYKLEBUST R.L. 1973. A rigorous correction procedure for quantitative electron probe microanalysis (COR 2). U.S. Bureau of Standards Technical Note 769, U.S. Government Printing Office, Washington D.C.

- HERVIG R.L., SMITH J.V., STEELE I.M., GURNEY J.J., MEYER H.O.A. and HARRIS J.W. 1980. Diamonds: Minor elements in silicate inclusions: Pressure-temperature implications. *Journal of Geophysical Research* 85, 6919-6929.
- HILL S.J. 1989. A study of the diamonds and xenoliths from the Star kimberlite, Orange Free State, South Africa. MSc thesis (unpublished), University of Cape Town, South Africa. 187p.
- JAGOUTZ E., DAWSON J.B., HOERNES S., SPETTEL B. and WANKE H. 1984. Anorthositic oceanic crust in the Archaean Earth. Abstract. 15th Lunar and Planetary Science Conference, Houston.
- JAQUES A.L., HALL A.E., SHERATON J.W., SMITH C.B. SUN S.-S., DREW R.M., FOUDOULIS C. and ELLINGSEN K. 1989. Composition of crystalline inclusions and C-isotopic composition of Argyle and Ellendale diamonds. 4th International Kimberlite Conference. Kimberlites and Related Rocks, Vol. 2, Geological Society of Australia Special Publication No. 14, 966-979.
- JAVOY M., PINEAU F. and DEMAIFFE D. 1984. Nitrogen and carbon isotopic composition in the diamonds of Mbuji Mayi (Zaire). *Earth and Planetary Science Letters* 68, 399-412.
- JAVOY M., PINEAU F. and DELORME H. 1986. Carbon and nitrogen isotopes in the mantle. *Chemical Geology* 57, 41-62.
- KAISER W. and BOND W.L. 1959. Nitrogen, a major impurity in common Type I diamond. *Physical Review* 115, 847-863.
- KARLSTROM K.E. and HOUSTON R.S. 1984. The Cheyenne belt: analysis of a Proterozoic suture in southern Wyoming. *Precambrian Research* 25, 415-446.
- KENNEDY C.S. and KENNEDY G.C. 1976. The equilibrium boundary between graphite and diamond. *Journal of Geophysical Research* 81, 2467-2470.
- KENNEDY G.C. and NORDLIE B.E. 1968. The genesis of diamond deposits. *Economic Geology* 63, 495-503.
- KINNY P.D., COMPSTON W., BRISTOW J.W. and WILLIAMS I.S. 1989. Archaean mantle xenocrysts in a Permian kimberlite: two generations of kimberlitic zircon in Jwaneng DK2, southern Botswana. 4th International Kimberlite Conference. Kimberlites and Related Rocks, Vol. 2, Geological Society of Australia Special Publication No. 14, 833-842.
- KIRKLEY M.B. 1980. Peridotite xenoliths in Colorado-Wyoming kimberlites. MSc thesis (unpublished), Colorado State University, Fort Collins.
- KIRKLEY M.B. 1987. Aspects of the geochemistry of kimberlite carbonates. PhD thesis (unpublished), University of Cape Town, South Africa, 282p.

- KIRKLEY M.B. and GURNEY J.J. 1989. Carbon isotope modelling of biogenic origins for carbon in eclogitic diamonds. Workshop on Diamonds: Extended Abstracts, 28th International Geological Congress, Washington D.C., 40-43.
- KOBELSKI B.J., GOLD D.P. and DEINES P. 1979. Variations in stable isotope compositions for carbon and oxygen in some South African and Lesothan kimberlites. In: Boyd F.R. and Meyer H.O.A. eds., Kimberlites, Diatremes and Diamonds: Their Geology, Petrology and Geochemistry. American Geophysical Union, Washington DC, 252-271.
- KOVAL'SKIY V.V. and CHERSKIY N.V. 1972. The carbon isotope composition of diamonds. *Geologiya i geofizika* 9, 10-15. (In Russian).
- KUSHIRO I. and YODER H.S. (Jr). 1974. Formation of eclogite from garnet lherzolite: liquidus relations in a portion of the system $MgSiO_3$ - $CaSiO_3$ - Al_2O_3 at high pressures. Carnegie Institution of Washington, Yearbook 73, 266-269.
- KUSHIRO I., SYONO Y. and AKIMOTO S. 1968. Melting of a peridotite nodule at high pressures and high water pressures. *Journal of Geophysical Research* 73, 6023-6029.
- LANG A.R. 1979. Internal Structure. In: Field J.E. ed., The Properties of Diamond. Academic Press, London, 425-469.
- LARSON E.E. and AMINI M.H. 1981. Fission-track dating of the Green Mountain kimberlite diatreme near Boulder, Colorado. *The Mountain Geologist* 18(1), 19-22.
- LIGHTOWLERS E.C. and COLLINS A.T. 1975. Boron measurements in natural semiconducting diamond. Abstract, Kimberlite Symposium, Cambridge, England.
- LIGHTOWLERS E.C. and DEANE P.J. 1964. Measurement of nitrogen concentration in diamond by photon activation analysis and optical absorption. *Diamond Research 1964*; Industrial Diamond Information Bureau, London, 21-25.
- LINCOLN J.A. 1983. Schaffer-Aultman kimberlite complex, Albany County, Wyoming. Genesis of Rocky Mountain Ore Deposits, Denver Region Exploration Society Symposium, 71-77.
- LINDSLEY D.H. and DIXON S.A. 1976. Diopside-enstatite equilibria at 850°C to 1400°C, 5 to 35 kb. *American Journal of Science* 276, 1285-1301.
- LOUBSER J.H.N. and WRIGHT A.C.J. 1973. Discussion of the Endor and E.S.R. spectra of diamonds with the N3 optical system. *Diamond Research 1973*; Industrial Diamond Information Bureau, London, 16-20.
- MacGREGOR I.D. 1974. The system MgO - Al_2O_3 - SiO_2 : Solubility of Al_2O_3 in enstatite for spinel and garnet peridotite compositions. *American Mineralogist* 59, 110-119.

- MacGREGOR I.D. and CARTER J.L. 1970. The chemistry of clinopyroxenes and garnets of eclogite and peridotite xenoliths from the Roberts Victor mine, South Africa. *Physics of the Earth and Planetary Interiors* 3, 391-397.
- MAO H.K., BELL P.M. and YAGI T. 1979. Iron-magnesium fractionation model for the earth. *Carnegie Institution of Washington, Yearbook* 78, 621-626.
- MCCALLUM M.E. 1976. An emplacement model to explain contrasting mineral assemblages in adjacent kimberlite pipes. *Journal of Geology* 84, 673-684.
- MCCALLUM M.E. and EGGLER D.H. 1971. Mineralogy of the Sloan diatreme, a kimberlite pipe in northern Larimer county, Colorado. *American Mineralogist* 56, 1735-1749.
- MCCALLUM M.E. and EGGLER D.H. 1976. Diamonds in an upper mantle peridotite nodule from kimberlite in southern Wyoming. *Science* 192, 253-256.
- MCCALLUM M.E., EGGLER D.H. and BURNS L.K. 1975. Kimberlitic diatremes in northern Colorado and southern Wyoming. *Physics and Chemistry of the Earth* 9, 149-161.
- MCCALLUM M.E., EGGLER D.H., COOPERSMITH H.G., SMITH C.B. and MABARAK C.D. 1977. Field guide to the Colorado-Wyoming State Line district. 2nd International Kimberlite Conference Guidebook, Colorado State University Department of Earth Resources, Fort Collins.
- MCCALLUM M.E., MABARAK C.D. and COOPERSMITH H.G. 1979. Diamonds from kimberlites in the Colorado-Wyoming State Line district. In: Boyd F.R. and Meyer H.O.A. eds., Kimberlites, Diatremes and Diamonds: Their Geology, Petrology and Geochemistry. American Geophysical Union, Washington, 42-58.
- MCCANDLESS T.E. and COLLINS D.S. 1989. A diamond-graphite eclogite from the Sloan 2 kimberlite, Colorado, USA. 4th International Kimberlite Conference. *Kimberlites and Related Rocks Vol. 2*, Geological Society of Australia Special Publication No. 14, 1063-1069.
- MCCANDLESS T.E. and GURNEY J.J. 1989. Sodium in garnet and potassium in clinopyroxene: Criteria for classifying mantle eclogites. 4th International Kimberlite Conference. *Kimberlites and Related Rocks Vol. 2*, Geological Society of Australia Special Publication No. 14, 827-832.
- MCCANDLESS T.E., KIRKLEY M.B., ROBINSON D.N., GURNEY J.J., GRIFFIN W.L., COUSENS D.R. and BOYD F.R. 1989. Some initial observations on polycrystalline diamonds mainly from Orapa. Workshop on Diamonds: Extended Abstracts, 28th International Geological Congress, Washington D.C., 47-51.
- MEYER H.O.A. 1968. Chrome pyrope: an inclusion in natural diamond. *Science* 160, 1446-1447.

- MEYER H.O.A. 1987. Inclusions in diamond. In: Nixon P.H. ed., Mantle Xenoliths. John Wiley and Sons, Chichester, England, 501-522.
- MEYER H.O.A. and BOYD F.R. 1969. Mineral inclusions in diamonds. Carnegie Institution of Washington, Yearbook 67, 130-135.
- MEYER H.O.A. and McCALLUM M.E. 1986. Mineral inclusions in diamonds from the Sloan kimberlites, Colorado. *Journal of Geology* 94, 600-612.
- MEYER H.O.A. and SVISERO D.P. 1975. Mineral inclusions in Brazilian diamonds. *Physics and Chemistry of the Earth* 9, 785-795.
- MEYER H.O.A. and TSAI H.- M. 1976. The nature and significance of mineral inclusions in natural diamond: A review. *Minerals Science and Engineering* 8, 242-261.
- MILASHEV V.A. 1965. Petrochemistry of the kimberlites of Yakutia and characteristics of their diamond mineralization. Nedra publication, Leningrad.
- MILTON C. and VITALIANO D. 1984. Moissanite, SiC, a non-existent mineral (Abstract). XXVII International Geological Congress, Moscow.
- MISER D. and ROSS C.S. 1922. Diamond-bearing peridotite in Pike county, Arkansas. *U.S. Geological Survey Bulletin* 735, 279-322.
- MITCHELL R.S. and GIARDINI A.A. 1953. Oriented olivine inclusions in diamond. *American Mineralogist* 38, 136-138.
- MOORE R.O. and GURNEY J.J. 1985. Pyroxene solid solution in garnets included in diamond. *Nature* 318, 553-555.
- MOORE R.O. and GURNEY J.J. 1989. Mineral inclusions in diamond from the Monastery kimberlite, South Africa. 4th International Kimberlite Conference. Kimberlites and Related Rocks Vol. 2, Geological Society of Australia Special Publication No. 14, 1029-1041.
- MOORE R.O., OTTER M.L., RICKARD R.S., HARRIS J.W. and GURNEY J.J. 1986. The occurrence of moissanite and ferro-periclase as inclusions in diamond. 4th International Kimberlite Conference, Extended Abstracts, Geological Society of Australia Abstracts Series No. 16, 409-411.
- MVUEMBA NTANDA F., MOREAU J. and MEYER H.O.A. 1982. Particularites des inclusions cristallines primaires des diamants du Kasai, Zaire. *Canadian Mineralogist* 20, 217-230.
- NAESAR C.W. and McCALLUM M.E. 1977. Fission-track dating of kimberlitic zircons. Extended Abstracts, 2nd International Kimberlite Conference, Santa Fe.

- NAVON O., HUTCHEON I.D., ROSSMAN G.R. and WASSERBURG G.J. 1988. Mantle-derived fluids in diamond micro-inclusions. *Nature* 335, 784-789.
- NEWTON M.G., MELTON C.E. and GIARDINI A.A. 1977. Mineral inclusions in an Arkansas diamond. *American Mineralogist* 62, 583-586.
- NICKEL K.G. and GREEN D.H. 1985. Empirical geothermobarometry for garnet peridotites and implications for the nature of the lithosphere, kimberlites and diamonds. *Earth and Planetary Science Letters* 73, 158-170.
- O'NEIL J.R. 1986. Theoretical and experimental aspects of isotopic fractionation. *Mineralogical Society of America, Reviews in Mineralogy* 16, 1-40.
- O'NEILL H.St.C. and WOOD B.J. 1979. An experimental study of Fe-Mg partitioning between garnet and olivine and its calibration as a geothermometer. *Contributions to Mineralogy and Petrology* 70, 59-70.
- O'NEILL H.St.C. and WOOD B.J. 1980. An experimental study of Fe-Mg partitioning between garnet and olivine and its calibration as a geothermometer: Corrections. *Contributions to Mineralogy and Petrology* 72, 337.
- ORLOV Y.L. 1973. Mineralogy of the Diamond. Izdatel'stvo Nauka, Translated from Russian by J.Wiley & Sons, New York.
- OZIMA M., ZASHU S. and NITOH O. 1983. $^3\text{He}/^4\text{He}$ ratio, noble gas abundance and K-Ar dating of diamonds - An attempt to search for the records of early terrestrial history. *Geochimica et Cosmochimica Acta* 47, 2217-2224.
- PEARSON D.G., DAVIES G.R., NIXON P.H. and MILLEDGE H.J. 1989. Graphitized diamonds from a peridotite massif in Morocco and implications for anomalous diamond occurrences. *Nature* 338, 60-62.
- PETERMAN Z.E., HEDGE C.E. and BRADDOCK W.A. 1968. Age of Precambrian events in the northeastern Front Range, Colorado. *Journal of Geophysical Research* 73(6), 2277-2296.
- PHAAL C. 1965. Surface studies of diamond. *Industrial Diamond Review* 25, 486-489; 591-595.
- PINEAU F. and JAVOY M. 1983. Carbon isotopes and concentrations in mid-oceanic ridge basalts. *Earth and Planetary Science Letters* 62, 239-257.
- PINEAU F., JAVOY M. and ALLEGRE C.J. 1973. Etude systematique des isotopes de l'oxygene, du carbone et du strontium dans les carbonatites. *Geochimica et Cosmochimica Acta* 37, 2363-2377.

- POLLACK H.N. and CHAPMAN D.S. 1977. On the regional variation of heat flow, geotherms and lithospheric thickness. *Tectonophysics* 38, 279-296.
- PRINZ M., MANSON D.V., HLAVA P.F. and KEIL K. 1975. Inclusions in diamonds: garnet lherzolite and eclogite assemblages. *Physics and Chemistry of the Earth* 9, 797-815.
- RAYLEIGH J.W.S. 1896. Theoretical considerations respecting the separation of gases by diffusion and similar processes. *Philosophical Magazine* 42, 493-498.
- RICHARDSON S.H. 1986. Latter-day origin of diamonds of eclogitic paragenesis. *Nature* 322, 623-626.
- RICHARDSON S.H. 1989. Radiogenic isotope studies of diamond inclusions. Workshop on Diamonds: Extended Abstracts, 28th International Geological Congress, Washington D.C., 87-90.
- RICHARDSON S.H., GURNEY J.J., ERLANK A.J. and HARRIS J.W. 1984. Origin of diamonds in old enriched mantle. *Nature* 310, 198-202.
- RICKARD R.S., HARRIS J.W., GURNEY J.J. and CARDOSO P. 1989. Mineral inclusions in diamonds from Koffiefontein mine. 4th International Kimberlite Conference: Kimberlites and Related Rocks Vol.2, Geological Society of Australia Special Publication No. 14, 1054-1062.
- ROBERTSON R., FOX J.J. and MARTIN, A.E. 1934. Two types of diamond. *Philosophical Transactions of the Royal Society of London* A232, 463-538.
- ROBINSON D.N. 1978. The characteristics of natural diamond and their interpretation. *Minerals Science and Engineering* 10, 55-72.
- ROBINSON D.N. 1979a. Surface textures and other features of diamonds. PhD thesis (unpublished), University of Cape Town, South Africa, 221p.
- ROBINSON D.N. 1979b. Diamond and graphite in eclogite xenoliths from kimberlite. In: Boyd F.R. and Meyer H.O.A. eds., The Mantle Sample: Inclusions in Kimberlites and Other Volcanics. American Geophysical Union, Washington, 50-58.
- ROBINSON D.N., GURNEY J.J. and SHEE S.R. 1984. Diamond eclogite and graphite eclogite xenoliths from Orapa, Botswana. In: Kornprobst J. ed., Kimberlites II: The Mantle and Crust-Mantle Relationships. Elsevier Science Publishing Co, Amsterdam, 11-24.
- ROBINSON D.N., SCOTT J.A., VAN NIEKERK A. and ANDERSON V.G. 1989. The sequence of events reflected in the diamonds of some southern African kimberlites. 4th International Kimberlite Conference. Kimberlites and Related Rocks Vol. 2, Geological Society of Australia Special Publication No. 14, 980-990.

- SCHULZE D.J. 1986. Calcium anomalies in the mantle and a subducted metaserpentinite origin for diamonds. *Nature* 319, 483-485.
- SCOTT SMITH B.H. and SKINNER E.M.W. 1984. A new look at Prairie Creek, Arkansas. In: Kornprobst J. ed., Kimberlites I: Kimberlites and Related Rocks. Elsevier, 255-284.
- SCOTT SMITH B.H., DANCHIN R.V., HARRIS J.W. and STRACKE K.J. 1984. Kimberlites near Orroroo, South Australia. In: Kornprobst J. ed., Kimberlites I: Kimberlites and Related Rocks. Elsevier, 121-142.
- SHAVER K.C. 1988. Exploration of the Sloan Range complex: a diamondiferous kimberlite prospect in northern Colorado. *Mining Engineering*, January 1988, 45-48.
- SHEPPARD S.M.F. and SCHWARCZ H.P. 1970. Fractionation of carbon and oxygen isotopes and magnesium between metamorphic calcite and dolomite. *Contributions to Mineralogy and Petrology* 26, 161-198.
- SKINNER E.M.W., SMITH C.B., BRISTOW J.W., SCOTT SMITH B.H. and DAWSON J.B. 1985. Proterozoic kimberlites and lamproites and a preliminary age for the Argyle lamproite pipe, Western Australia. *Transactions of the Geological Society of South Africa* 88, 335-340.
- SMITH C.B. 1979. Rb-Sr mica ages of various kimberlites. Abstract, Kimberlite Symposium II, Cambridge, England.
- SMITH C.B. 1983. Pb, Sr and Nd isotopic evidence for sources of southern African Cretaceous kimberlites. *Nature* 304, 51-54.
- SMITH C.B., McCALLUM M.E., COOPERSMITH H.G. and EGGLER D.H. 1979. Petrochemistry and structure of kimberlites in the Front Range and Laramie Range, Colorado-Wyoming. In: Boyd F.R. and Meyer H.O.A. eds., Kimberlites, Diatremes, and Diamonds: Their Geology, Petrology and Geochemistry. American Geophysical Union, Washington, 178-189
- SMITH C.B., GURNEY J.J., HARRIS J.W., ROBINSON D.N., SHEE S.R. and JAGOUTZ E. 1989a. Sr and Nd isotopic systematics of diamond-bearing eclogite xenoliths and eclogitic inclusions in diamond from southern Africa. 4th International Kimberlite Conference. *Kimberlites and Related Rocks Vol. 2*, Geological Society of Australia Special Publication No. 14, 853-863.
- SMITH C.B., GURNEY J.J., HARRIS J.W., OTTER M.L., KIRKLEY M.B. and JAGOUTZ E. 1989b. Nd and Sr isotope systematics of large eclogite and lherzolite paragenesis single diamonds, Finsch and Kimberley Pool. Workshop on Diamonds: Extended Abstracts, 28th International Geological Congress, Washington D.C., 102-104.
- SMYTH J.R. 1977. Quartz pseudomorphs after coesite. *American Mineralogist* 62, 828-830.

- SMYTH J.R. and HATTON C.J. 1977. A coesite-sanidine grosspydrite from the Roberts Victor kimberlite. *Earth and Planetary Science Letters* 34, 284-290.
- SOBOLEV N.V. 1974. Deep-Seated Inclusions in Kimberlites and the Problem of the Composition of the Upper Mantle. Translated from Russian by D.A. Brown (1977). In: Boyd F.R. ed., American Geophysical Union, Washington D.C.
- SOBOLEV N.V. 1984a. Crystalline inclusions in diamonds from New South Wales, Australia. In: Glover J.E. and Harris P.G. eds., Kimberlite Occurrence and Origin: A basis for conceptual models in exploration. Geology Dept & University Extension Publication No. 8, University of Western Australia, 213-226.
- SOBOLEV N.V. 1984b. Kimberlites of the Siberian Platform: Their geological and mineralogical features. In: Glover J.E. and Harris P.G. eds., Kimberlite Occurrence and Origin: A basis for conceptual models in exploration. Geology Dept & University Extension Publication No. 8, University of Western Australia, 275-287.
- SOBOLEV N.V., BARTOSHINSKIY Z.V., YEFIMOVA E.S., LAVRENT'YEV Y.G. and POSPELOVA L.N. 1970. Olivine-garnet-chrome diopside assemblage from Yakutian diamond. *Doklady Akademii Nauk SSSR* 192(6), 1349-1353.
- SOBOLEV N.V., BOTKUNOV A.I., LAVRENT'YEV Yu.G. and USOVA L.V. 1976a. New data on the compositions of minerals coexisting with diamonds from the Mir kimberlite, Yakutia. *Geologiya i Geofizika* 12, 3-15.
- SOBOLEV N.V., YEFIMOVA E.S., KOPTIL V.I., LAVRENT'YEV Yu.G. and SOBOLEV V.S. 1976b. First find of inclusions of the coesite paragenesis (coesite, garnet and omphacite) in Yakutian diamonds. (In Russian). *Doklady Akademii Nauk SSSR* 230, 1442-1444.
- SOBOLEV N.V., GALIMOV E.M., IVANOVSKAYA I.N. and YEFIMOVA E.S. 1979. Isotope composition of carbon of diamonds containing crystalline inclusions. *Doklady Akademii Nauk SSSR* 249, 1217-1220.
- SOBOLEV V.S. 1979. New danger of misinformation as the result of contamination of samples by accidental minerals and technical products. *Zapiski Vsisoyuznogo Mineralogicheskogo Obshchestva* 108(6), 691-695.
- SUNAGAWA I. 1984. Morphology of natural and synthetic diamond crystals. In: Sunagawa I. ed., Materials Science of the Earth's Interior. Terra Scientific Publishing Co, Tokyo, 303-330.
- SWART P.K., PILLINGER C.T., MILLEDGE H.J. and SEAL M. 1983. Carbon isotopic variation within individual diamonds. *Nature* 303, 793-795.

- TAYLOR H.P. and EPSTEIN S. 1963. O^{18}/O^{16} ratios in rocks and coexisting minerals of the Skaergaard intrusion, East Greenland. *Journal of Petrology* 4, 51-74.
- URUSOVSKAYA A.A. and ORLOV Y.L. 1964. Nature of the plastic deformation of diamond crystals. *Doklady Akademii Nauk SSSR* 154 (5), 112-115.
- VANCE E.R., HARRIS J.W. and MILLEDGE H.J. 1973. Possible origins of alpha-damage in diamonds from kimberlite and alluvial sources. *Mineralogical Magazine* 39, 349-360.
- WAKATSUKI M. 1984. Synthesis researches of diamond. In: Sunagawa I. ed., Materials Science of the Earth's Interior. Terra Scientific Publishing Co, Tokyo, 351-374.
- WHITELOCK T.K. 1973. Morphology of the Kao diamonds. In: Nixon P.H. ed., Lesotho Kimberlites. Lesotho National Development Corporation, Maseru, 128-140.
- WOHLETZ K.H. and SMYTH J.R. 1984. Origin of a Roberts Victor sanidine-coesite grosspydite. In: Kornprobst J. ed., Kimberlites II: The Mantle and Crust-Mantle Relationships. Elsevier Science Publishing Co, Amsterdam, 33-42.
- YAGI T., BELL P.M. and MAO H.K. 1979. Phase relations in the system MgO-FeO-SiO₂ between 150 and 700 kbar at 1000°C. *Carnegie Institution of Washington Yearbook* 78, 614-618.
- YEFIMOVA E.S., SOBOLEV N.V. and POSPELOVA L.N. 1983. Sulphide inclusions in diamond and specific features of their parageneses. *Zapiski Vsesoyuznogo Mineralogicheskogo Obshchestva* 112, 300-310.